# DRY BENEFICIATION OF COAL USING AN AIR DENSE-MEDIUM FLUIDISED BED SEPARATOR

**Simon Kretzschmar**

In fulfillment of the requirements for Master of Science in Chemical Engineering, Faculty of Engineering, University of KwaZulu-Natal

As the candidate's Supervisor I agree/do not agree to the submission of this thesis

Dr J. Pocock

Signature:

Supervisor: Dr J Pocock

Date of Submission: 05 / 01 / 2010

# DECLARATION

I, Simon Kretzschmar, declare that

(i) The research reported in this thesis, except where otherwise indicated, is my original work.

(ii) This thesis has not been submitted for any degree or examination at any other university.

(iii) This thesis does not contain other persons' data, pictures, graphs or other information, unless specifically acknowledged as being sourced from other persons.

(iv) This thesis does not contain other persons' writing, unless specifically acknowledged as being sourced from other researchers. Where other written sources have been quoted, then:

a) their words have been re-written but the general information attributed to them has been referenced;

b) where their exact words have been used, their writing has been placed inside quotation marks, and referenced.

(v) Where I have reproduced a publication of which I am an author, co-author or editor, I have indicated in detail which part of the publication was actually written by myself alone and have fully referenced such publications.

(vi) This thesis does not contain text, graphics or tables copied and pasted from the Internet, unless specifically acknowledged, and the source being detailed in the thesis and in the References sections.

Signed:

05 / 01 / 2010

# ACKNOWLEDGEMENTS

This research was made possible by a financial grant from the CSIR in association with Coaltech 2020. I would like to thank my Supervisor Dr J Pocock and Co-Supervisor Prof B K Loveday of the Mineral Processing Research Group at the University of KwaZulu-Natal for their invaluable guidance and assistance.

Simon Kretzschmar

06/07/2009

# ABSTRACT

Key Words: Dry Beneficiation, Coal, Fluidised Bed, Separation.

The mining of coal in arid regions has led to calls for research in to the field of dry beneficiation, not only for its lower water but also for its lower operating and plant costs. This dissertation describes coal beneficiation using a dense medium fluidised bed separator developed at the University of KwaZulu-Natal. The dense medium used being naturally occurring magnetite, a titanium mining by-product from the Richards Bay region of South Africa.

Initial semi-batch tests were conducted using density tracers followed by batch separation of discard coal which was in a size fraction of 1.5 to 3.5cm. These semi batch tests allowed for the characterisation of the bed and the design and construction of a novel separator.

The separation was optimised and tests on the equipment using high ash discard coal under semi batch operational parameters yielded a separation inefficiency (Ep) of 0.0458 at a split density of 1996 kg/m$^3$. The 2.5kg batches of coal were fed into the separator and allowed to separate over a period of 9 minutes. The coal entered at an average ash content of 60.06%. 39.75% of the coal reported to the floats with a final average ash content of 28.47%. The remaining 60.75% of the coal reported to the sinks with a final ash content of 80.90%. Continuous operation at a raw coal feed flow rate of 18 kg/hr yielded an Ep of 0.0462 at a separation density of 1996 kg/m$^3$. The coal was fed into the separator at an average ash content of 60.06%. 39.67% of the coal reported to the floats with a final average ash content of 24.61%. The remaining 60.33% of the coal reported to the sinks with a final ash content of 76.41%. The experimental data illustrated that dry separation could be just as efficient as corresponding wet methods (where Ep values of 0.05 are usually obtained).

# TABLE OF CONTENTS

# LIST OF FIGURES

# LIST OF TABLES

# 1 INTRODUCTION

## 1.1. COAL BENEFICIATION

Coal beneficiation offers a considerable number of commercial and environmental benefits. It has the duel benefit of increasing both the quality and thus value of the coal, but also of allowing the potential exploitation of coals that would be unrecoverable due to commercial or environmental limitations.

Low ash coals are not only more efficient in terms of combustion, but also result in reduced sulphur dioxide (which originates from both the organic sulphur and contained sulphides in the coal) and particulate emissions. These lower emission levels are environmentally desirable. A further benefit of the removal of ash is the reduction of transportation costs (per gigajoule) which would be due to reduction in the cost of carrying moist coal.

In the choice of beneficiation techniques, wet coal beneficiation processes are the most popular; this is due to historically higher separation efficiency and operating capacity: (Cleaner Coal Technology Programme, 2001). Two main separating principles predominate:

- Separation based upon the difference in the relative density of the coal and waste shale; pure coal has a relative density of approximately 1.3 and associated shale commonly has a relative density of greater than 2.2. Examples of processes are dense medium separation and jig washing.

- Separation based upon the difference in surface properties of the material. Coal is hydrophobic, while shale is usually hydrophilic. An example of a process utilising this type of separation would be froth flotation.

The wet processing of coal, through dense medium separation or jigs, however requires significant amounts of water. These can be in the region of 200 litres per tonne of coal processed. (Donnelly J., 1999)

### 1.2. ENVIRONMENTAL CONSIDERATIONS

A significant portion of the world's coal fields are located in water scarce arid regions (Figure 1). Conflict is beginning to develop in these areas as industry, agriculture and the local populations compete with each other for the water resources. This conflict can only be exacerbated as coal reserves dwindle and the move to develop mines in these areas intensifies. South Africa's situation is no exception, the majority of the country`s future principle reserves situated in its northern regions in the Waterberg deposits (Figure 2). (Keaton Energy, 2003)

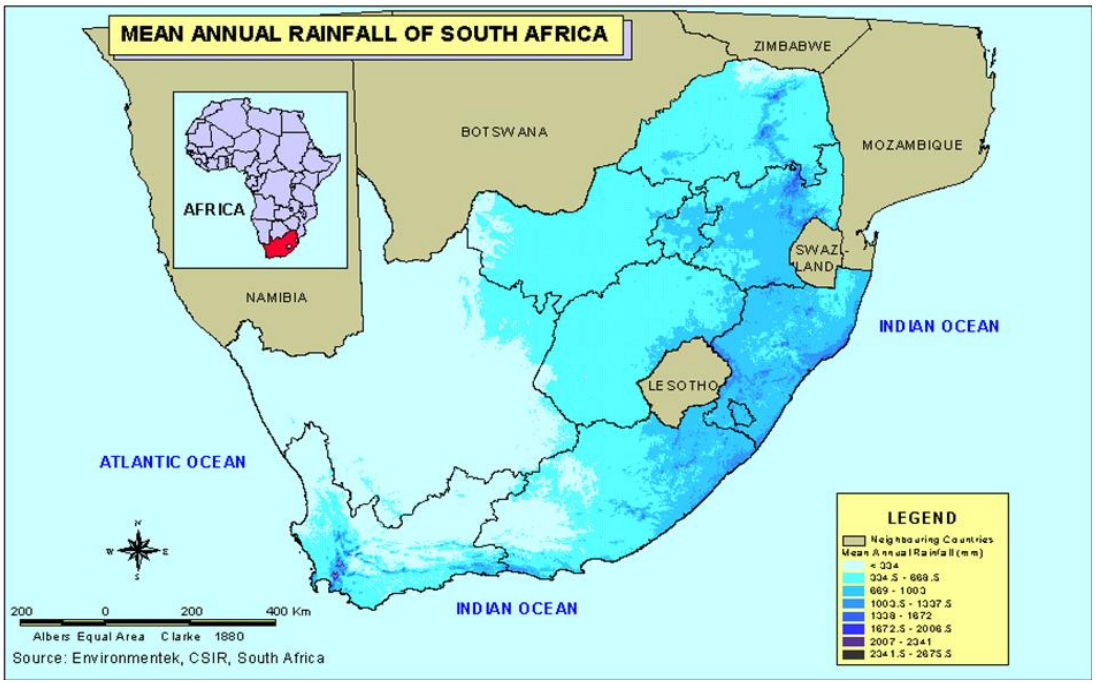


Figure 1: Mean Annual Rainfall of South Africa (Department of Environmental Affairs and Tourism, 2008)

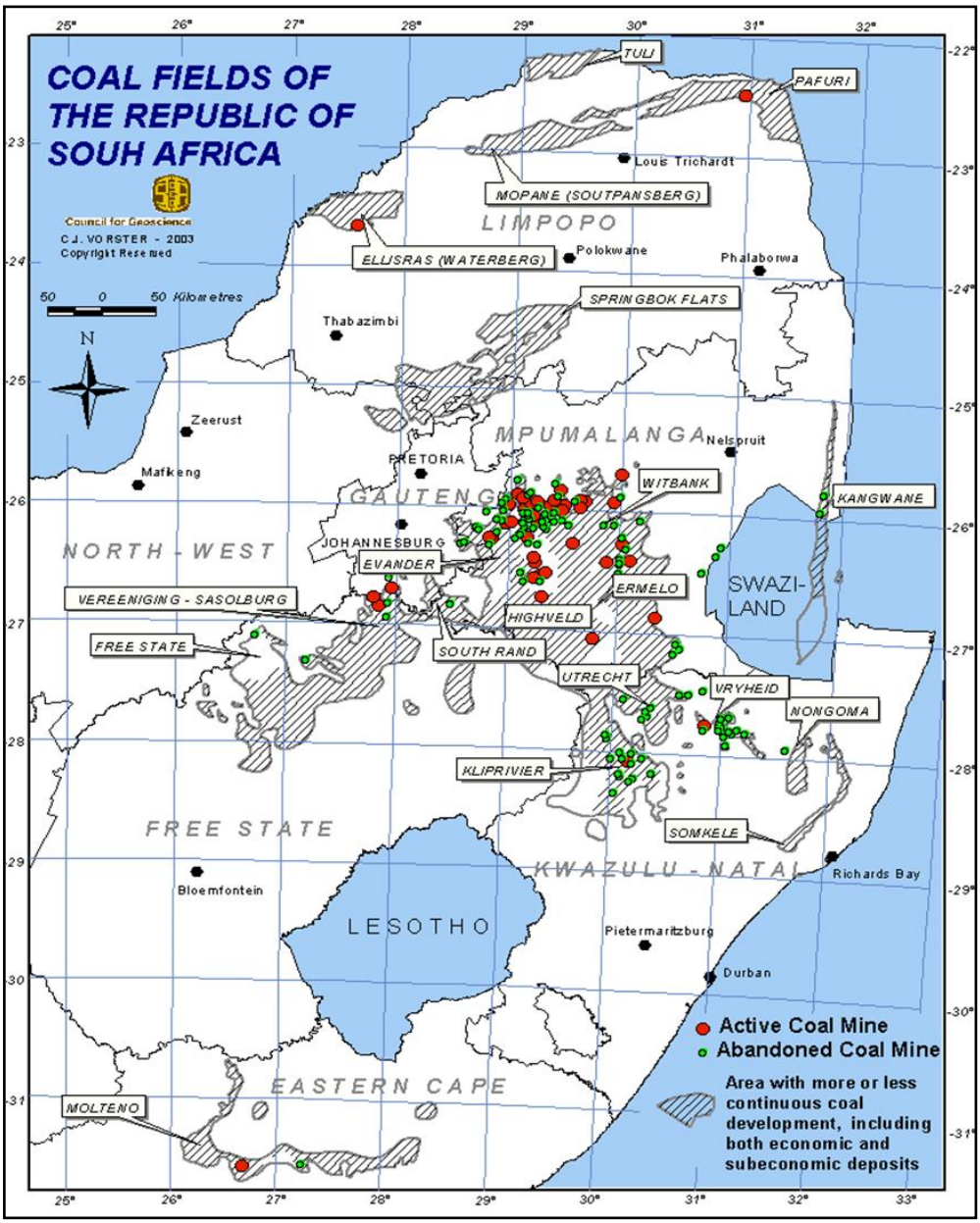


Figure 2: Coal Fields of the Republic of South Africa (Council for Geoscience, 2008)

These deposits, which extend into southern Botswana, are in an area of arid climate conditions, thus the traditional wet separation processes which have largely been employed in the coal separation industry are unsuitable. The competition for water is not the only issue as the effluent water from the coal preparation is generally saline and can be acidic (Donnelly J., 1999).

A recent article published in the *South African Financial Mail* regarding the water crisis in South Africa only serves to highlight that the situation is reaching a critical level. According to the report, South Africa, which is 30th on the list of the worlds' driest countries, is suffering major effects due to the pollution of her main rivers and water supplies. One of the main sources of contamination is effluent from mining operations. In fact one of Gauteng's major water sources, the Vaal River, is showing increased pollution levels from acid mine water. Further north in Mpumalanga, the Olifants River system which runs through the coal preparation units and supports many farms in the area, is also being affected by toxic mine water (Financial Mail, 2008). These factors are of considerable worry to a country that depends on coal for not only 90% of its electricity and 30% of its petrol and diesel but also 90% of its iron and steel production. Added to this are substantial revenues from foreign exchange brought in by coal exports. (Creamer M., 2009)

Dr Andrew Turton, in his paper; *"Three Strategic Water Quality Challenges that Decision-Makers Need to Know About and How the CSIR Should Respond",* states in no uncertain terms (Turton A., 2008):

"…South Africa simply has no more surplus water and all future economic development (and thus social wellbeing) will be constrained by this one fundamental fact..."

## 1.3. DRY BENEFICIATION: AN ALTERNATIVE

Dry beneficiation has several notable advantages. The principle of these is that the elimination of the need for water obviously eliminates the need for expensive dewatering processes such as pumping, screening, filtering and centrifuging. The saline and acidic water from the wet processing would need further treatment, an additional cost as would the removal of entrained fines. Finally freight costs per gigajoule will be considerably lower due to reduction in the cost of carrying moist coal. Thus the dry coal preparation plants would experience the multiple advantages of being smaller, cheaper, and having lower operational costs.

Traditionally however the disadvantages of dry preparation have outweighed these advantages. Coal cleaned in dry processes generally have ash contents that are higher than that of coal cleaned in more efficient wet methods, and while dry processes are susceptible to feed moisture content. This issue is not experienced with wet preparation. The problem of dust formation with dry processing is always present as is the difficulty of dry screening. Dry processing equipment on average tends to have lower capacities than corresponding wet methods. These disadvantages, if recognised, may however be overcome (Donnelly J., 1999).

## 1.4. AIMS AND OBJECTIVES

At this point the primary objectives of the project became clear, they were:

- To identify a method of dry separation, that allows for accurate, high capacity separation without excessive dust formation.

- Develop laboratory scale equipment utilising this method.

- Optimise the equipment.

- Develop the equipment, such that separation can be undertaken under continuous operating conditions.

- Investigate the scale up potential of the equipment to pilot plant capacity and beyond.

## 1.5. PROJECT LOGIC FLOW

A logic flow was determined for the project to facilitate the most effective method of proceeding with the design and development of the equipment.

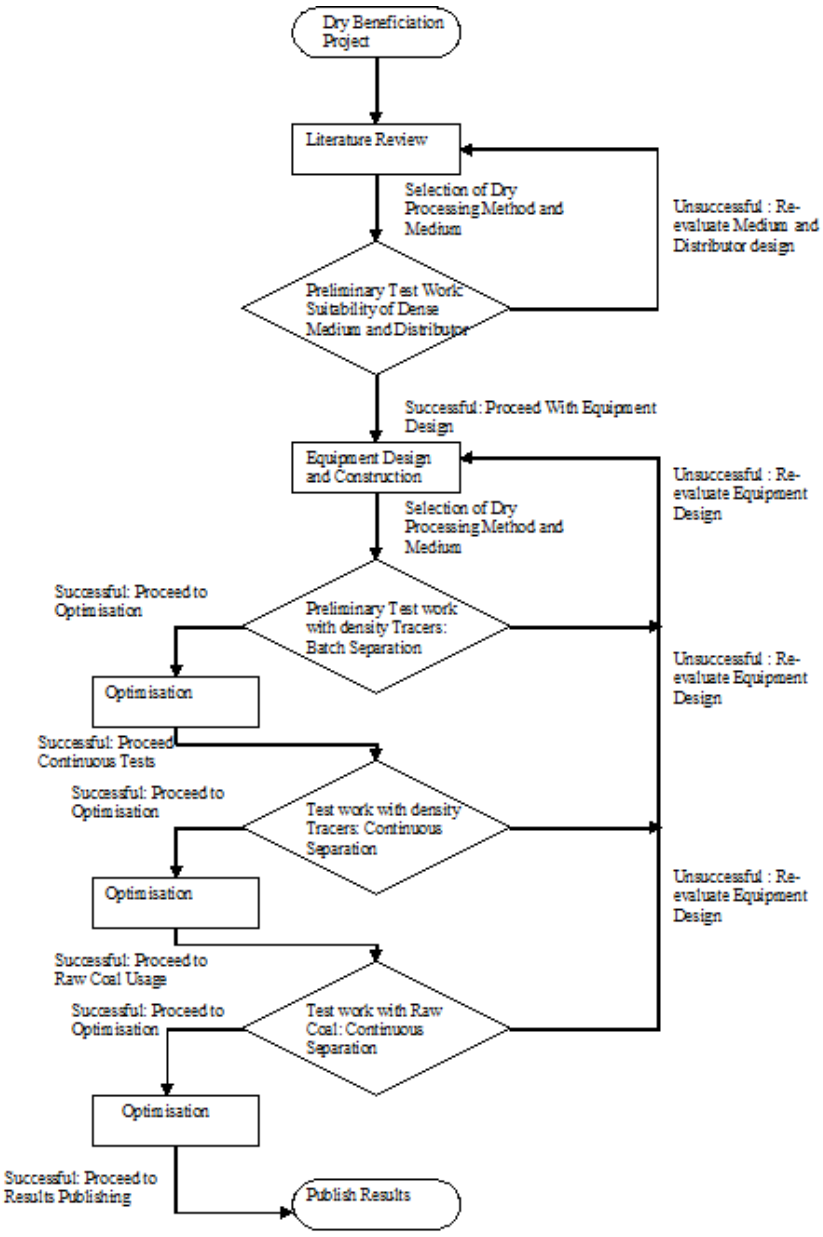


Figure 3: Project Logic Flow

# 2. LITERATURE REVIEW

## 2.1. WET COAL BENEFICIATION

Wet coal beneficiation techniques have come to represent the standard in coal beneficiation techniques; they provide a combination of accuracy of split and high capacity operation that the traditional methods of dry beneficiation could not compete with. Furthermore the moisture content of the coal is not a factor to be considered before beneficiation can take place. Techniques vary depending upon the size of the run of mine coal sent to the beneficiation process, however it is noted that the general separation inefficiency Ep for wet processing is between 0.007 (ESR International 2010) to 0.015 (Portaclone 2010).

Processing of wet coal generally follows a flowsheet typical to the one in figure 4. The coal from the mine is crushed to a top size that is acceptable through breakers, mills and crushers. From there the coal is screened into size fractions. Based upon these size fractions the coal will beneficiated according to the different methods described below.

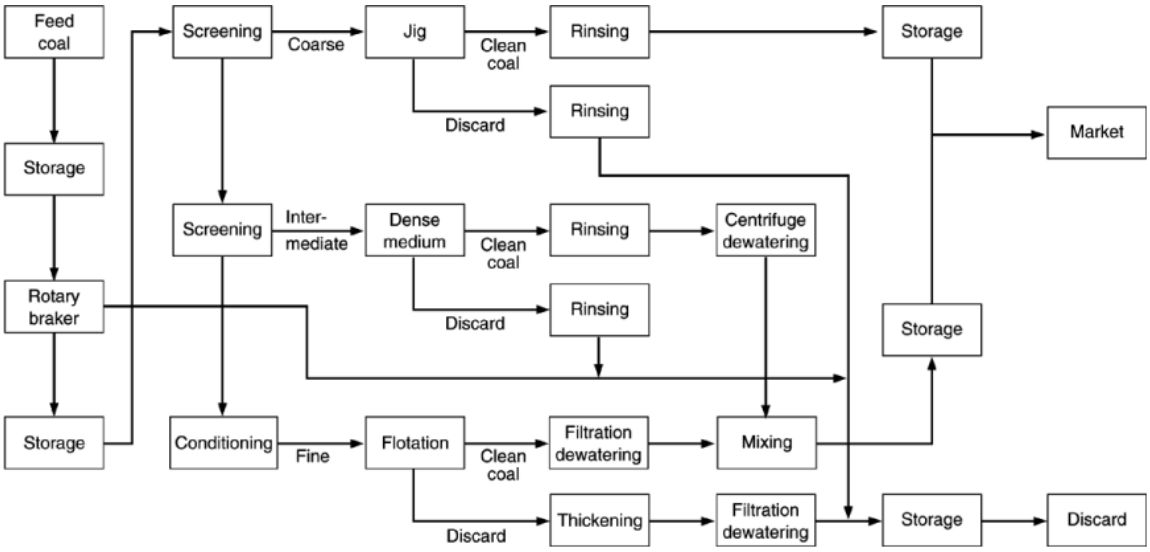


Figure 4: Coal Wet Processing Flowsheet (Chiang S.H. and Cobb J. T., 1993)

**Coarse Coal**

Two methods generally predominate, dense medium separation and jig washing. Two actions comprise the jigging operation. The first is the effect of hindered settling. This results in the lighter particle settling slower than the heavier one. The second separation process is achieved by an upward flow of water which

segregates the particles by density. By means of slurry pulses, these two actions are combined in the jig. Gravity separation utilises the settling rate of different particles in water to make a separation. Particle size, shape and density all affect the efficiency of the separation.

Dense media separation takes place in fluid media with a density between that of the light and heavy fractions that are to be separated. The separation is dependent upon density only (Metso, 2009). Dense medium separators have low separation inefficiencies generally with an Ep value in the region of 0.002 (Bateman Engineering, 2009).

The choice between these methods comes down to the unique circumstances innate to each plant. Dense medium washing provides a more accurate split, however jig washing is often perceived to be a simpler, lower cost option when accuracy of split is not paramount.

**Fine Coal (< 3000µm)**

Beneficiation of coal in this size fraction is becoming of greater importance and is usually accomplished either through spiral concentrators or teetered bed separators. These separators again achieve the split between the heavy and light fractions based on the density of the constituents.

**Ultrafine Coal (< 150µm)**

Froth flotation is still the most widely used method of beneficiation for coal of this size as density separation becomes difficult for smaller particles. This physiochemical process involves the selectivity of the attachment of air bubbles to the organic coal particles and not the not the surrounding non-organic minerals. The coal is made hydrophobic by the addition of a surfactant and an oil is used as an agglomeration agent to allow easy removal of the froth. (Davydov M.V. 2008)

The coal that has undergone the flotation separation commonly has unacceptable amounts of water and thermal drying is usually used to reduce this moisture content.

After the coal has been processed the treatment of the water used for the beneficiation becomes a focus, and the main disadvantage of wet coal beneficiation comes to the fore. After the coal has been processed the larger fraction products and rejects from the jigs and dense medium separators are rinsed. The slurries from the fine coal processing still need to undergo filtering and other dewatering processes such as settling ponds (Chiang S.H. and Cobb J. T., 1993). The treatment of the tailings and water clarification have and still remain the most costly areas of coal beneficiation, and at the same time the most difficult to control. Whilst significant attempts are made to reduce the amount of water that is actually required 200 L of water per ton of coal are still lost through product coal moisture, disposal of the tailings and evaporation. (Donnelly J., 1999). Where the buildup of slimes in the water reaches a maximum the waste water is disposed of in tailings ponds where the evaporation of the water leaves the recovery of the ultra fines possible. (Clark K. 1997).

For these processes there is the need for a high level of control in the area of online process monitoring. A trend over recent years is now to develop simpler processes that utilise larger single separation units. This trend together with a desire for plants that are modular and allow for quick relocation are not traits generally inherent to the traditional wet coal processing operations. (Cleaner Coal Technology Programme, 2001).

## 2.2. DRY SEPARATION TECHNIQUES

### 2.2.1. History of Dry Coal Beneficiation

The first dry cleaning methods of coal involved the removal of waste by handpicking off slow moving conveyers. Over time these methods were refined into today's technologies mentioned below. Despite growth during the first half of the 20$^{th}$ century, dry beneficiation processes were abandoned. The reason for this lay in the fact that available technology restricted the feed size, capacity and coal moisture content that the separators were able to a cope with. These restrictions combined with inaccurate separation meant that the popularity of dry coal cleaning fell off dramatically compared with wet separation techniques. However in areas where water is particularly scarce, such as in regions of China, dry separation methods, mentioned below, may still be found. (Donnelly J., 1999)

### 2.2.2. Fluidised Cleaners

Fluidised bed dry cleaners, became generally viewed as the most productive means of dry separation processes. They include pneumatic oscillating tables, air jigs and dense medium fluidised bed separators. Most common of these were the oscillating air tables.

#### 2.2.2.1. Oscillating Air Tables

In the oscillating air tables the oscillation of the coal bed together with fluidising pulses of air from beneath the bed allowed vertical stratification of the coal, fractions were taken off along the length of the table through various skimmers. While the tables operated at relatively high separation inefficiencies, clean coal with an ash content of 10% and reject coal with an ash content of 70% could be achieved. Explosive dust clouds, caused by the dry coal, were usually controlled through water mist sprayers. By the 1960s however oscillating air tables had fallen out of favour, mainly due to their inability to process the high ash and high moisture coals that were being increasingly encountered. Besides deshaling operations such as selective crushing dry beneficiation was virtually non-existent. (Donnelly J., 1999)

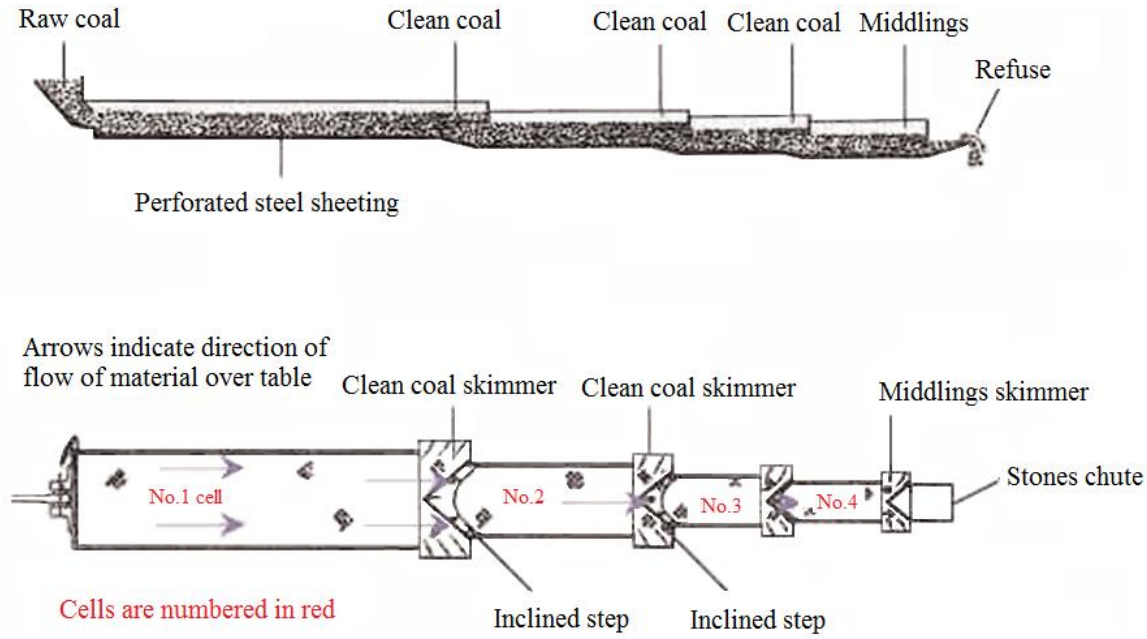


Figure 5: Diagrammatic View of Oscillatory Air Table (Donnelly J., 1999)

#### 2.2.2.2. Air Jigs

In a jig, an eccentric drive located at the feedbox head serves to impart an up or down motion to the jigging box. This motion is controlled by a fixed fulcrum located at the discharge end of the box. The fulcrum decreases the motion of the box from a maximum to minimum in the direction of feed to discharge. In addition to this a pulsating air current is applied through an air distributor screen located on the base of the jigging box. The pulse is applied during the downward stroke of the beds jig in order to fluidise the contents of the bed. The resulting stratification of the bed occurs with the high density material settling to its base and the lower density coal rising to the surface. The high density rejects are discharged by means of an adjustable toothed roller while the clean coal is removed via a chute. Due to significant dust formation such equipment is generally fitted with an extraction system.

While still on a decline air jigs are still found in some areas. An example of an air jig dry separation process is the FGX series compound dry cleaning machine. This is a series of machines that have found growing popularity over recent years, with a maximum capacity of 480tph, an efficiency of 90% and the ability to process coal with a surface moisture of up to 9% these machines are a step in the positive

direction especially considering the investment costs are up to a tenth that of that of similar capacity wet plants (Tangshan Shenzhou Machinery Co., Ltd, 2009). Yet still, the potential use of such machines is limited by their operating capacities and separating efficiencies which relative to wet processes remain low. In spite of extraction systems and dust enclosures the problem of dust generation still remains. Most dry separators require narrow bands of coal sizes and this in itself requires significant work to achieve. Despite continued investigations the best achievable separation inefficiencies by pneumatic equipment are in the region of 0.3 (Industrial Technologies Program 2006). Higher efficiency in the fluidised bed separation has been achieved using dense media separation.

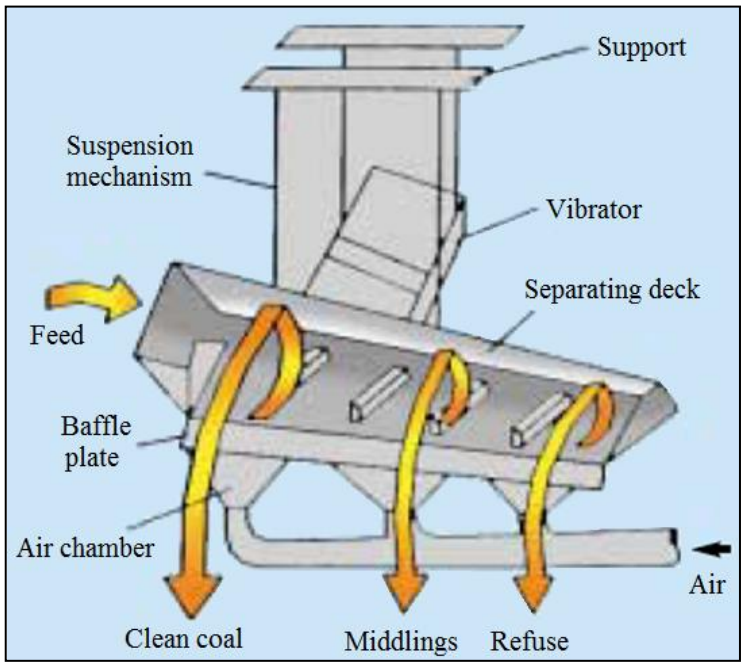


Figure 6: FGX Cleaner Schematic (Tangshan Shenzhou Machinery Co., Ltd, 2009)

#### 2.2.2.3. Other Methods

Before the investigation into the dense medium beds is undertaken it is worthwhile to look at several other points to note in the modern world of dry separation.

The advantage of the reduced size of the dry coal processing units compared with their wet counterparts has been noted especially with regards to the potential to have mobile processing units that can operate near the extraction point of the mining operation (Industrial Technologies Program 2006).

The magnetic properties of the raw coal also lead themselves to exploitation in dry separation methods. The organic coal is diamagnetic and the pyrite in the coal is paramagnetic, with weakly magnetic

constituents in the ash also predominant. The most well known examples are High Gradient Magnetic Separation (HGMS) (Chiang S.H. and Cobb J. T. 1993) and triboelectric separation (see figure 7) (Qing-ru C. and Hai-feng W. 2006).

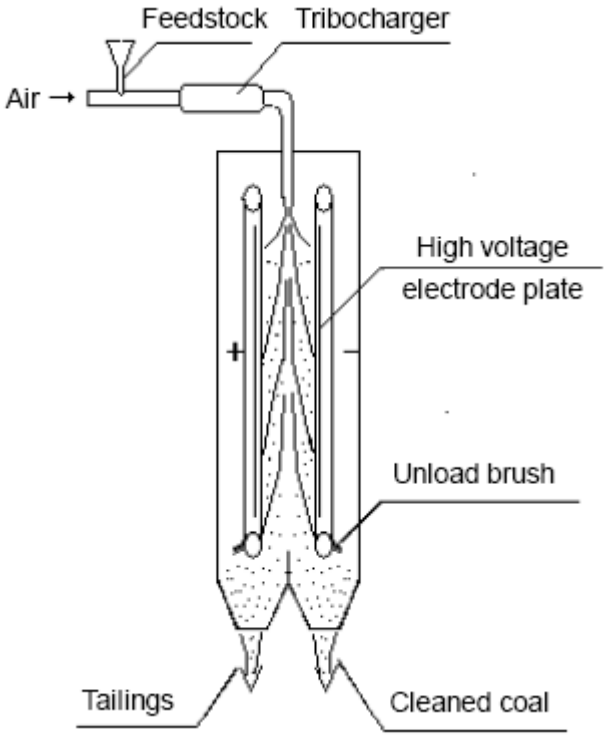


Figure 7: Triboelectric Separator (Qing-ru C. and Hai-feng W. 2006)

Whilst these processes are able to achieve high ash reduction down to 8% with yields of nearly 80%, the coal does need to be pulverized to a significant degree prior to processing (0.043mm). These applications are mainly used in the factory boilers and iron smelting blast furnaces. (Qing-ru C. and Hai-feng W. 2006)

#### 2.2.2.4. Dense Medium Fluidised Beds

The medium (similar to that of a magnetite medium in a wet plant) is an air-solids mixture. Then mixture provides a medium that is stable and of uniform density. Materials of higher density (such as ash) sink,

while lower density coal floats. This provides a quick efficient separation. The schematic of the separator is shown in Figure 8.

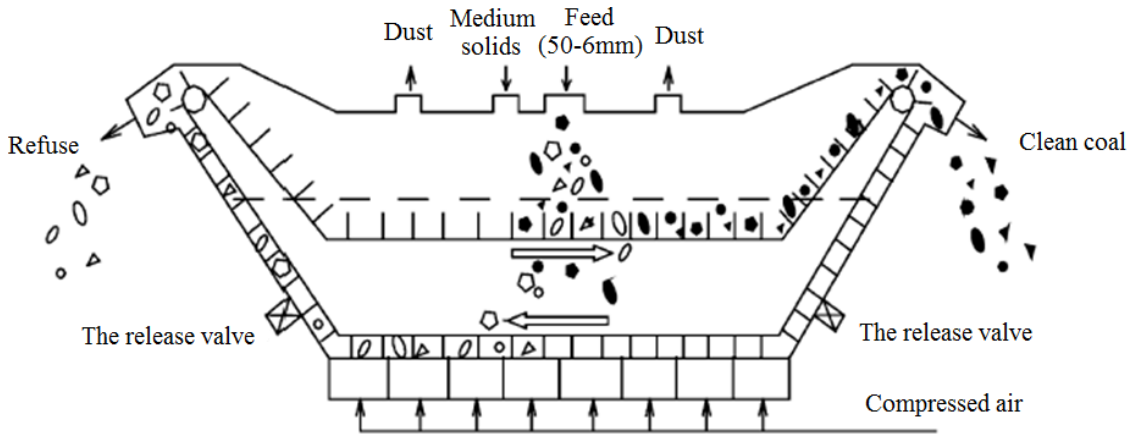


Figure 8: 50tpd Dense Medium Separator Schematic

Compared to air jigs and tables the pressure and volume of air required is lower and the smaller amount of dust produced is more easily dealt with. Separation of the sinks and floats is achieved by a push plate chain conveyor that scrapes the floats off one end of the machine whilst removing the sinks from the other. The results indicate that 6mm coal can effectively be separated at an Ep of 0.05 (where the Ep value represents the degree of inaccuracy in the split between the sinks and the floats at the separation density). A gas-solids fluidised bed with a uniform and stable density can be formed utilising a magnetite powder or a mixture of powder and fine coal. Using tight control on the fluidization and bed composition a separation density range of 1300–2200kg/$m^3$ is achievable. The advantage of this technology is that the costs associated with construction and operation are about half those for similar scaled wet processes. This is in addition to lower environmental impact (Zhenfu L. and Qingru C., 2001).

The advantage of dense medium separation is the flexibility of the design of the process. The Reflux Classifier with its parallel inclined channels that are situated above a fluidized bed uses a combination of vibration and a dense medium of sand to achieve the coal beneficiation. Separation inefficiencies Ep of 0.07 have been achieved whilst realizing a reduction of the ash in the products to 15% with a 80% yield. (MacPerson S.A. et al 2009)

# 3 BASIC PRINCIPLES AND CHARACTERISTICS

## 3.1. FLUIDISATION INTRODUCTION

Dry fluidisation is the levitation of a bed of solid particles by a gas. The bed, in this levitated state, exhibits fluid like behaviour (as shown in Figure 9). Thus it tends to establish a level and flow in response to pressure gradients that may be present in the bed (Pell M., 1990).

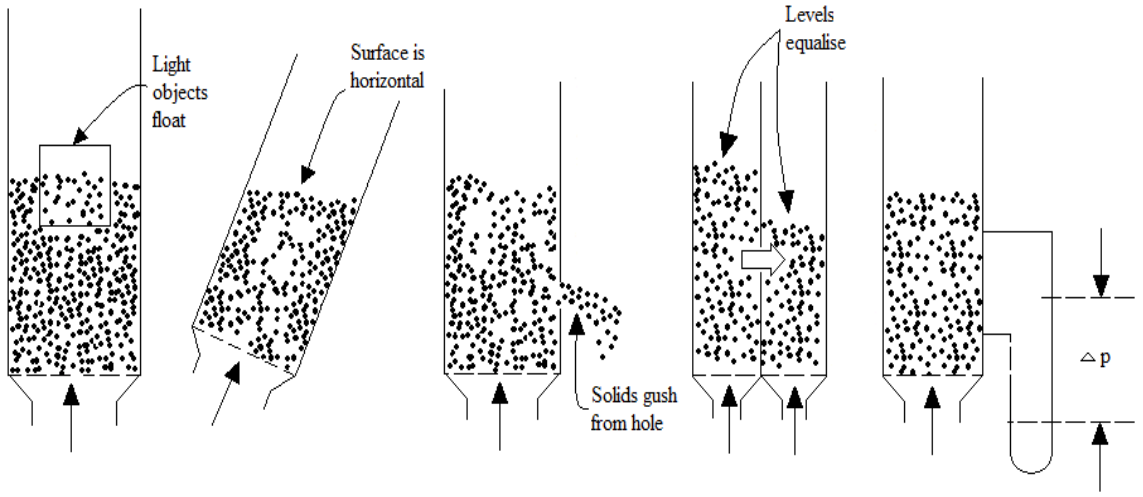


Figure 9: Pseudo Fluid Characteristics of Gas Fluidised Solids (Zhenfu L. and Qingru C., 2001)

## 3.2. PRINCIPLES OF FLUIDISATION

The principles of fluidisation and their associated properties now come into prominence as the careful fluidisation of the dense medium needs to be considered. The fluidisation regime needs to produce a dense medium that is uniform with a consistent predictable density.

### 3.2.1. General Behavior of Gas Solid Systems

Unlike liquid fluidised systems which present steady predicable behavior, the behavior of gas fluidised systems are far more complicated. Much of this complication arises from the interaction of the frictional, electrostatic and surface forces between very fine particles, which have a far greater effect than the hydrodynamic forces otherwise experienced. Coulson and Richardson (2002) describes the stages that a system experiences with an increase in gas velocity:

**Fixed Bed**

In this state, until the velocity has been increased to such a point where the pressure drop across the bed is equal to the weight per unit area of the particles in the bed, the particles remain in contact with each other resulting in a stable bed structure. This is the point of incipient fluidisation, and is velocity that of $u_{mf}$, the minimum fluidising velocity.

**Particulate Fluidisation**

The bed now begins to expand as the velocity increases. And although the agitation experienced by the particles increases the bed maintains uniformity. This type of fluidisation is typical to liquid fluidisation. Gas solid fluidisation usually only experiences this type of fluidisation at very low velocities and in some cases not at all before bubbling begins.

**Aggregative Fluidisation**

This fluidisation, also known as bubbling fluidisation, is characterised by the formation of two separate phases, a dense phase made up mainly of solids and a discontinuous lean phase formed by the channeling of the gaseous fluid phase through the particles.

**Turbulent Fluidisation**

This is a chaotic region in which the bubbles coalesce and their identity is lost.

**Fast Fluidisation**

This condition generally lies outside the realm of true fluidisation and represents the stage where there is transport of the particles vertically upwards.

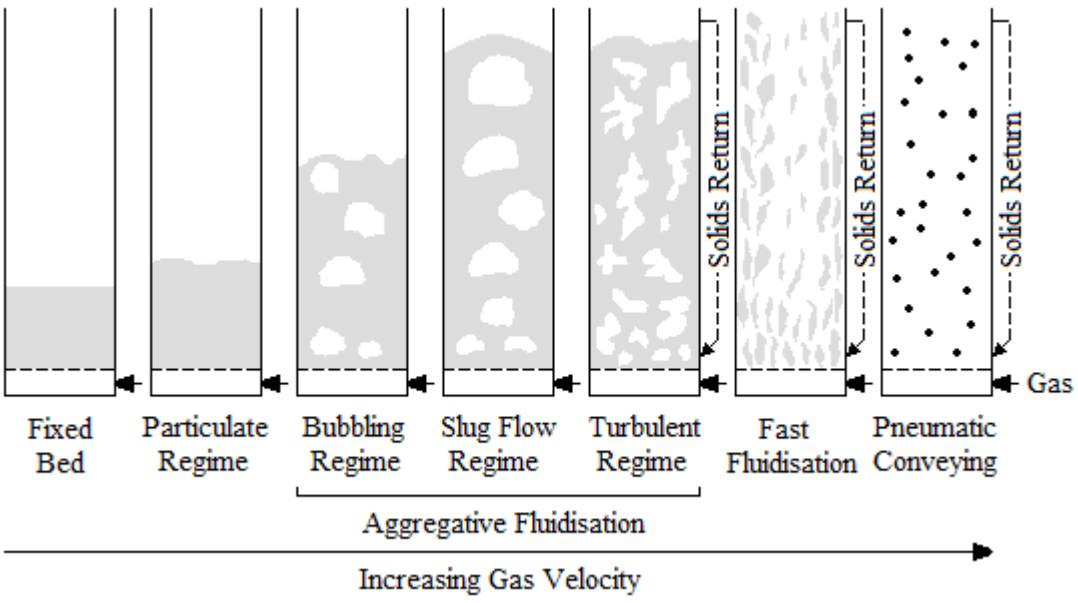


Figure 10: Fluidisation Regimes (Adapted from Perry R.H. and Green D., 1998, *Perry's Chemical Engineer's Handbook*)

The processes of feedstock variation and attrition usually result in a mixture of particle sizes in a fluidised bed. A mixed size bed fluidises more "smoothly" than a closely sized one. The smaller particles fit between than larger ones and act as ball bearings or a lubricant to make flow easier. A range of particle sizes spanning an order of magnitude is reasonable. (Pell M., 1990)

### 3.2.2. Categorisation of Solids

The properties of the particles determine the ease with which fine particles can be fluidised. Whilst the nature of the fluidisation for a particular group of particles is exactly predictable it is possible to view trends in the fluidisation. Geldart (Geldart D., 1973) classified particles into four groups. Coulson and Richardson (2002) provide Table 1 below, grouping the particles and Pell (1990) provides their location in a particle density size chart shown in Figure 11.

| | **Typical Particle Size(μm)** | **Fluidisation Characteristics** |
|---|---|---|
| Group A | 30-100 | Particulate expansion of the bed will take place over significant velocity range. Small particle size and low density |
| Group B | 100-800 | Bubbling occurs at velocities greater than $u_{mf}$. Most bubbles have velocities greater than interstitial gas velocity. |
| Group C | 20 | Fine cohesive powders difficult to fluidise and readily form channels. |
| Group D | 1000 | All but the largest bubbles rise at velocities less than interstitial gas velocity. Can be made to form sprouting beds. Particles large and dense. |

Table 1: Categorisation of Particles According to Fluidising Characteristics

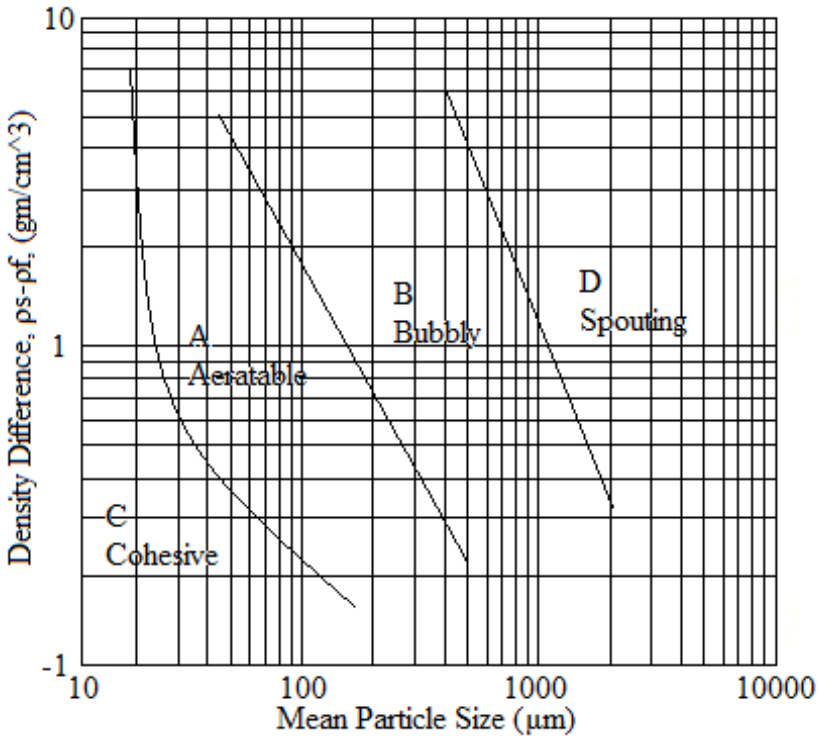


Figure 11: Geldarts Characterisation of Fluidisation Regime

### 3.2.3. Effect of Fluidising Gas Velocity on Bed Pressure Drop

The pressure drop across the bed is plotted against increasing fluidising gas velocity; a characteristic curve (Figure 12) is produced. Coulson and Richardson (2002) description is as follows.

As the gas velocity increases the bed begins to expand linearly from rest to point (A), at this point the particles within the bed become rearranged and the slope of the curve begins to decrease. As the aerodynamic drag forces begin to counter the gravitational forces the bed begins to expand as the particles move away from each other. When this aerodynamic drag equals the gravitational force the particles become suspended within the bed the pressure drop passes through its maximum at (B) and moves towards steady state conditions (C to D). No further increase in gas velocity at this point will produce a change in bed pressure drop. It should be noted that the straight line region (from rest to point A) is the packed bed region. This is where the particles do not move relative to one another and their separation is

constant. In this region the pressure drop versus velocity relationship can be described by the Ergun equation.

It may be noted that should the gas velocity be reduced at this point the characteristic double pathway (E to F) can be formed (as seen in Figure 10). This is due to the lower pressure drop typical of an expanded reformed bed resultant from settling particles. Should there be a vibration present there is a good chance that this expanded bed would not occur, as the particles are forcefully 'settled' into their original more compact state. Plotting of the pressure drop versus the fluidising velocity is usually conducted on the logarithmic curve as shown below, however it may be conducted on a semi-logarithmic or even linear depending on the nature of the system.

The minimum fluidising velocity $u_{mf}$ may now be determined by experimentally measuring these points, plotting them and then using straight line plots through the EF and CD sections to find their intersection.

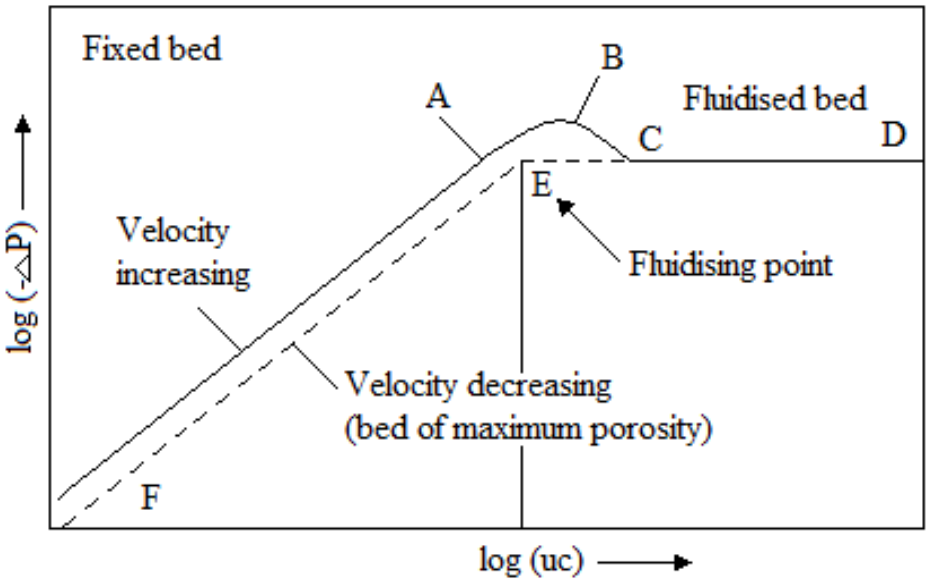


Figure 12: Pressure Drop over Fixed and Fluidised Beds (Coulson J.M. and Richardson J.F., 2002)

Where the y axis represents the the pressure drop over the bed and the x axis the superficial fluid velocity throught the bed.

### 3.3 DENSE MEDIA

In traditional wet dense media separation a suspension of dense powder in water is used to form a "Dense Liquid" (a suspension of specified density according to the volume fraction of fine solids) in which the sink-float separation process takes place. However the formation of a stable, uniform gas-solid dense medium is far more difficult and requires the careful combination of correct particle size, fluidising gas velocity and uniform air distribution. The large scale instabilities and the general heterogeneous nature of a gas-solid dense medium is in contrast to the homogeneous fluidised bed typical of a liquid-solid dense medium. These homogenous beds are a result of the higher viscosity of the fluid and similar intrinsic densities of the solids and fluid (Kunii D. and Levenspiel O., 1991). The bulk density of the gas-solid dense medium and thus the split density of the bed is a function of the density of the particles and the voidage between them (determined by the degree of fluidisation).

### 3.4. DENSE MEDIUM SEPARATORS

Archimedes' principle states (Young HD. Freedman RA., 1996):

"..When a body is completely or partially immersed in a fluid, the fluid exerts an upward force on the body equal to the weight of the fluid displaced by the body...."

In essence a body of a lower density will float on the surface of a more dense liquid, whilst bodies of higher density will sink.

Dense media separators draw on this principle and the fact that the dense medium behaves like a liquid when fluidised. The coal containing sulphur in the form of pyrites and ash is heavier than the desired high carbon coal and thus a separation density is established. With the knowledge of the separation density a fluidised bed can be created so as to separate the unwanted coal (containing more ash and sulphur) from the desired coal. (Zhenfu L. and Qingru C., 2001)

The determination of the separation inefficiency in a dense medium separator is obtained from the partition curve and is reflected by the partition coefficient. (Zhenfu L. and Qingru C., 2001)

$$Ep = \frac{\rho_{75} - \rho_{25}}{2000} \qquad (1)$$

Where the symbols $\rho_{75}$ and $\rho_{25}$ represent the densities (in kg/m$^3$) through which 75% and 25% respectively of the feed report to the underflow. This Ep value thus represents the inaccuracy of the split between the low density desired high carbon content coal and the undesired higher density high shale and ash material. Figure 13, below, shows the difference between an ideal split and a typical density separation curve. The Ep described in Equation 1 would be 0 for the ideal split as all the material above the split density reports to the underflow and all the material below reports to the overflow. The non-ideal curve shows a truer representation of what actually occurs with the effects of entrainment, particle shape, particle interaction and middlings coming into play.

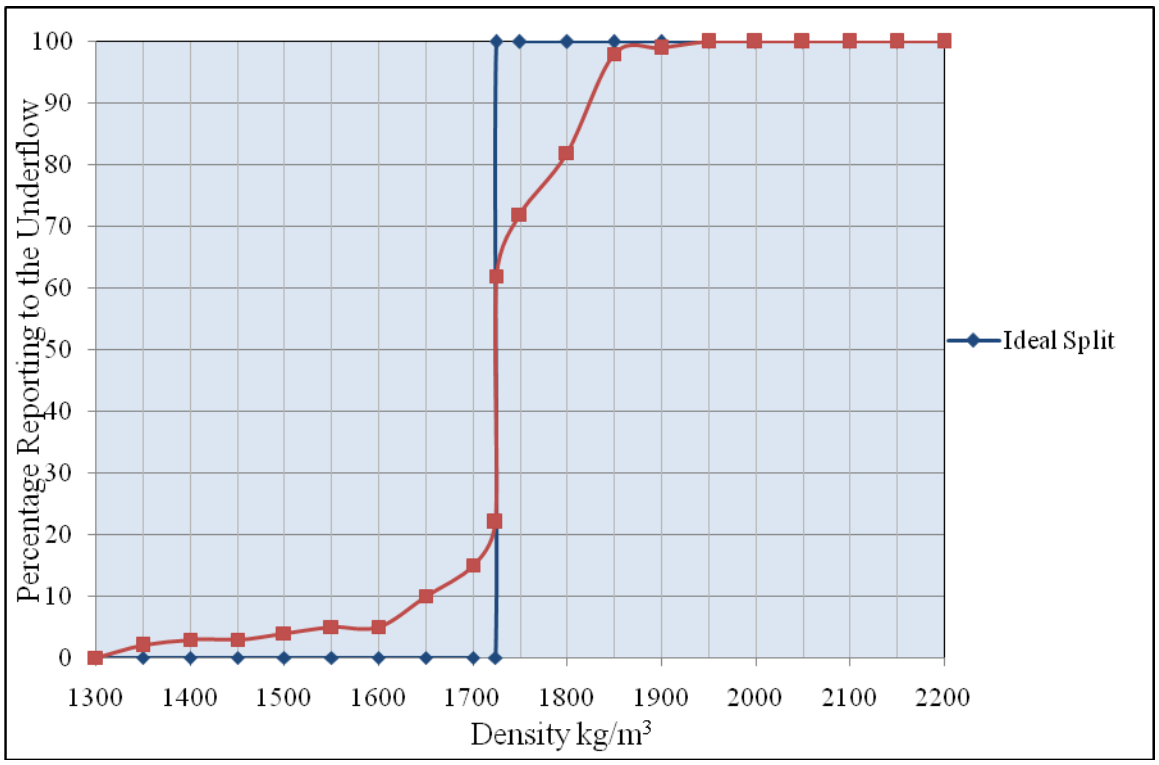


Figure 13: Figure Showing Ideal and Non-Ideal Density Splits

# 4 FLUIDISED BED DESIGN

Having considered the principles of fluidisation, careful attention now needed to be paid to the construction of the dense medium bed in which the separation would take place and within which the separator itself would be placed.

## 4.1. THE DENSE MEDIUM

The design of the dense medium fluidised beds revolves mainly around the medium to be fluidised, as the difficulty of uniform gas-solid fluidisation is notorious. The dense medium that was chosen for use was magnetite ($Fe_3O_4$). This black ferromagnetic mineral has been used in previous coal dense medium separation applications (Zhenfu L. and Qingru C., 2001) and is common to wet dense medium separations. It has a density of approximately 5150kg/m$^3$ (Excalibur Mineral Company, 2008) and a bulk density of approximately 2450kg/m$^3$ (calculated from experimental analysis of weights of known volumes).

The magnetite obtained for the dense medium was a by product of the titanium beach mining operations on the northern KwaZulu-Natal coast. This material has experienced attrition by wave action before it was deposited on the beach. This attrition produces a material that has a size spectrum that is narrow enough for uniform fluidisation, yet still includes enough fines to promote fluidisation (see Figure 14).

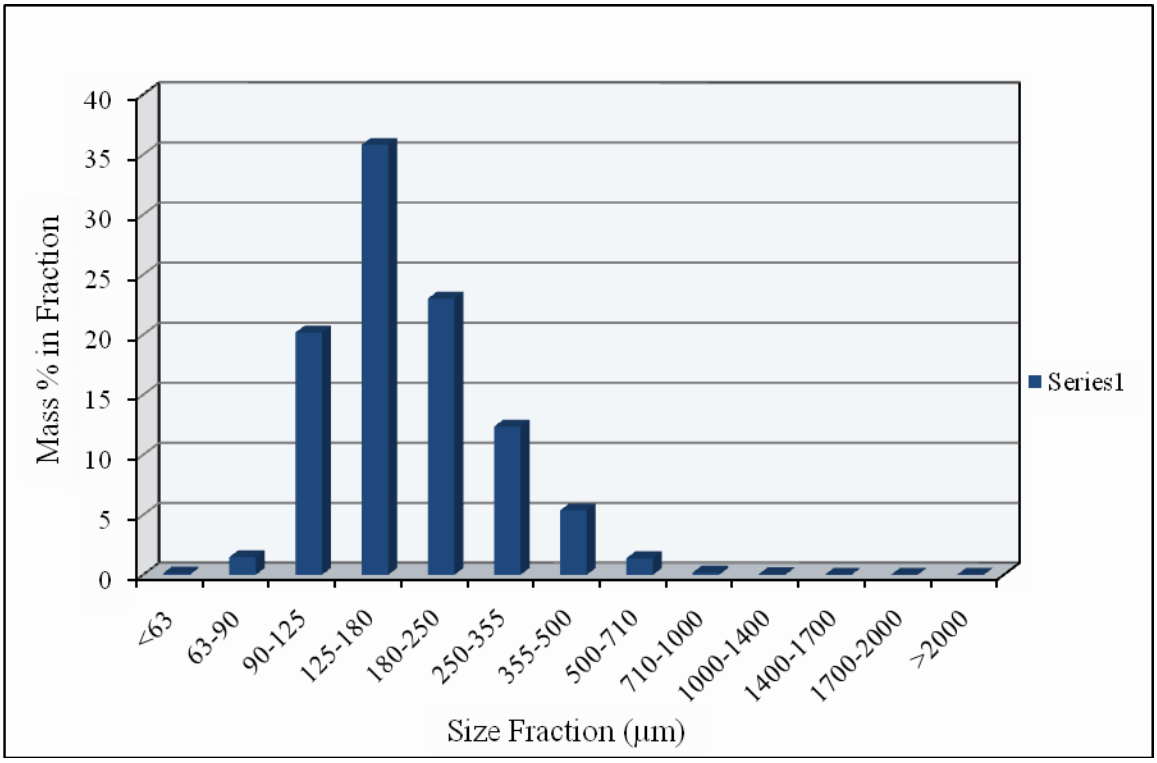


Figure 14: Size Distribution of Magnetite

The magnetite offers a bulk density that is ideal for coal beneficiation and has the added advantages of allowing magnetic recovery from the coal product.

The even fluidisation of the dense medium is of critical importance to the accuracy of the split within the bed. The most important determining factor that needs to be controlled is the air distribution into the bed of particles. The fluidisation regime of air fluidised magnetite, predicted according to Geldart's classification mentioned in the previous section, is that of a bubbly bed. These Type B particles do not form a cohesive structure that allows for uniform expansion; rather once the minimum fluidising velocity has been exceeded the formation of bubbles occurs. Poor air distribution will result in the formation of bubbles in some areas of the bed, whilst others are incompletely fluidised.

## 4.2. DESIGN OF FLUIDISED BED EQUIPMENT

### 4.2.1. Air Distributor Design

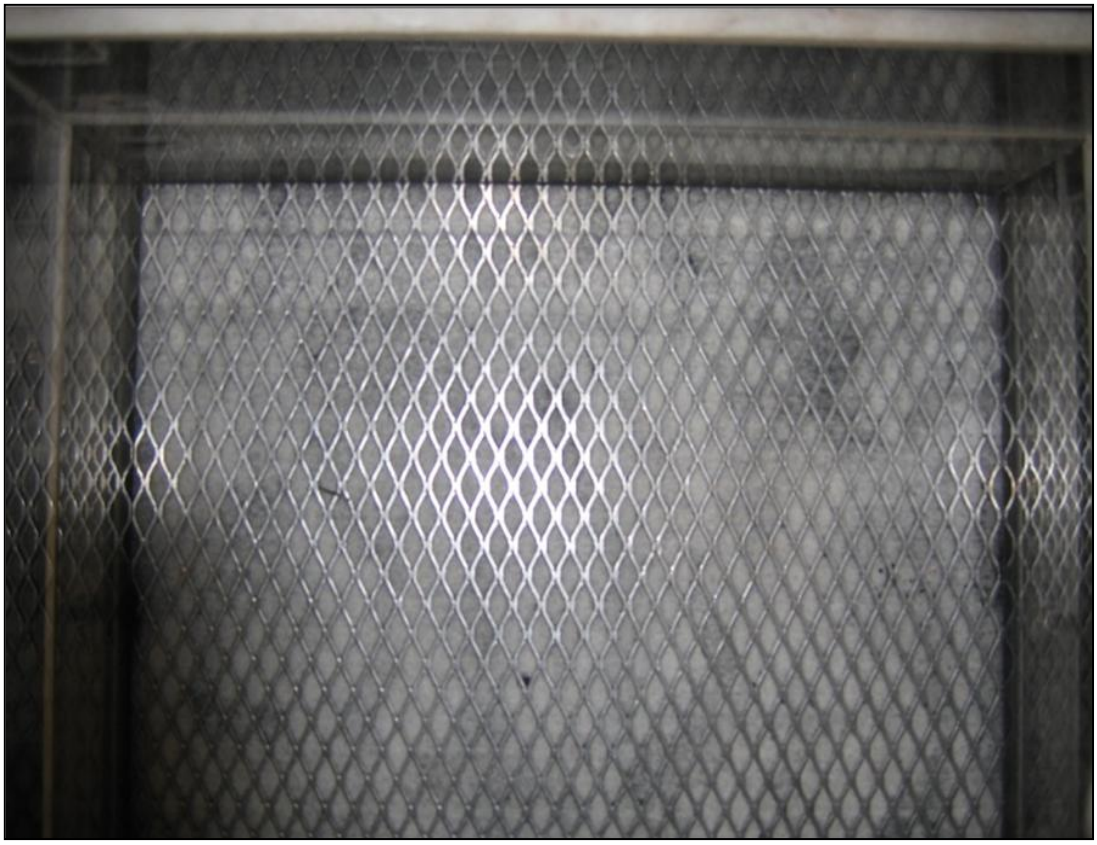

Figure 15: Overhead View of the High Pressure Distributor

The air distributor also serves the dual purpose of supporting the weight of the bed. Due to the bubbling action of the fluidised bed, there are constant small changes in the local pressure drop at the distributor. Gas inevitably tries to enter the bed in the zone of lowest pressure drop. The distributor pressure drop therefore has to be large enough to overcome the small local pressure disturbances of the bed. If the pressure drop is too small, gas will end up flowing through only some portions of the bed and establishing flow paths with high voidage and low pressure drop. At the same time, other sections would have negligible flow and remain “closed” or non-bubbling.

The above criteria are key the design of the distributor. In practice the required pressure drop is set by operating experience. For up flow the design pressure drop should be at least 30% of the bed pressure

drop, *dp*, at the minimum expected gas flow and the maximum expected bed weight (Pell M., 1990). A comfortable margin of safety is to design the grid *dp* for 100% of the bed *dp* (Coulson J.M. and Richardson J.F., 2002). This is often no strain for systems in which the gas is coming from a relatively high pressure source. The problems associated with this are that, while the gas will be well distributed, the distributor and plenum need to be designed to take these pressures. For drilled plate distributors the velocity of the gas through the holes might become high enough to cause an attrition problem (Pell M., 1990).

For the design in question it was decided to use a high pressure drop distributor considering the bubbly nature of the bed in order to ensure there was even air distribution into the bed. The distributor was constructed using filter cloth sandwiched between two stainless steel metal grids. This pressure drop was high enough to allow for uniform distribution of air whilst at the same time providing a stable structure on which the bed could rest. The metal grids prevented the ballooning of the pressure cloth either from the weight of the bed at rest or the force of the air being forced through during operation (see Figure 15 and Figure 16).

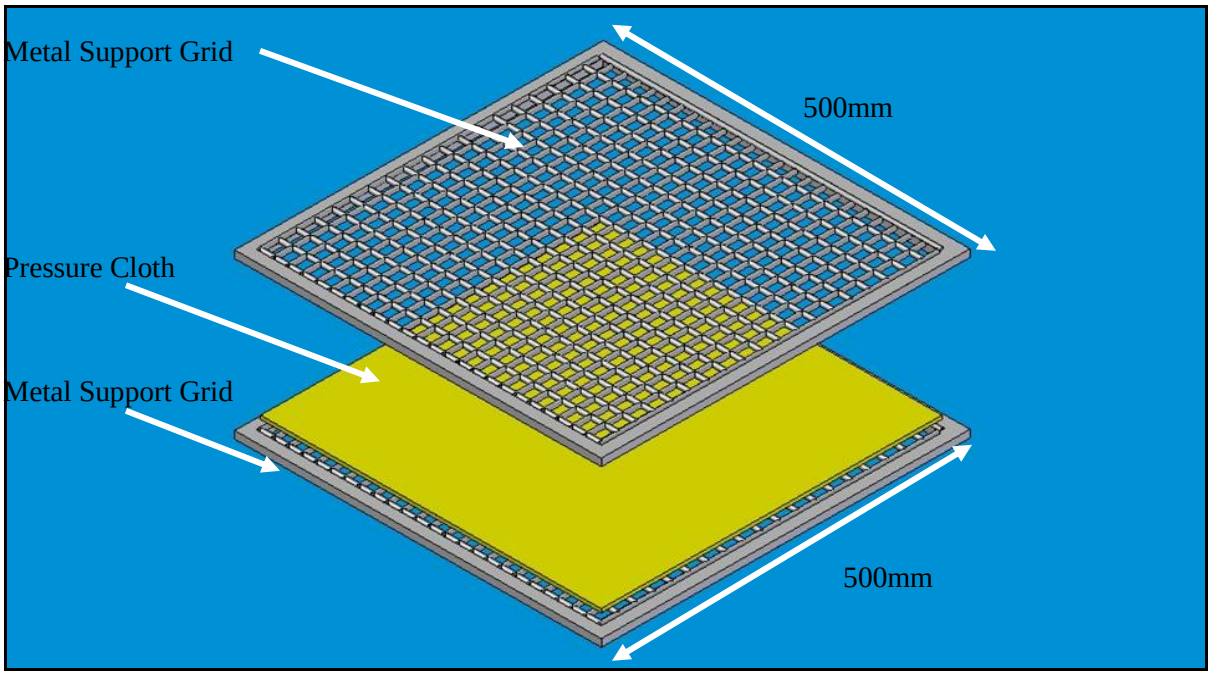


Figure 16: Schematic of the Construction of the High Pressure Drop Air Distributor

### 4.2.2. The Plenum

The design of plenum is almost of as critical importance as that of the bed itself. Correctly done it can provide additional air distribution benefits. Pell (1990) suggests the alternative plenum shapes shown below in Figure 17, (Pell M., 1990)**.** The final chosen design was based on trial and error experiments. The plenum consisted of a segregated honey comb structure Figure 18 beneath which there was a tetrahedral constriction towards the air supply flange from the blower Figure 19. The constriction allowed for good initial air distribution whilst the honey comb structure created not only a secondary air distribution zone, but also a support structure upon which the distributor could be fastened (Figure 20). Both the primary and secondary plenums were constructed from PVC plastic.

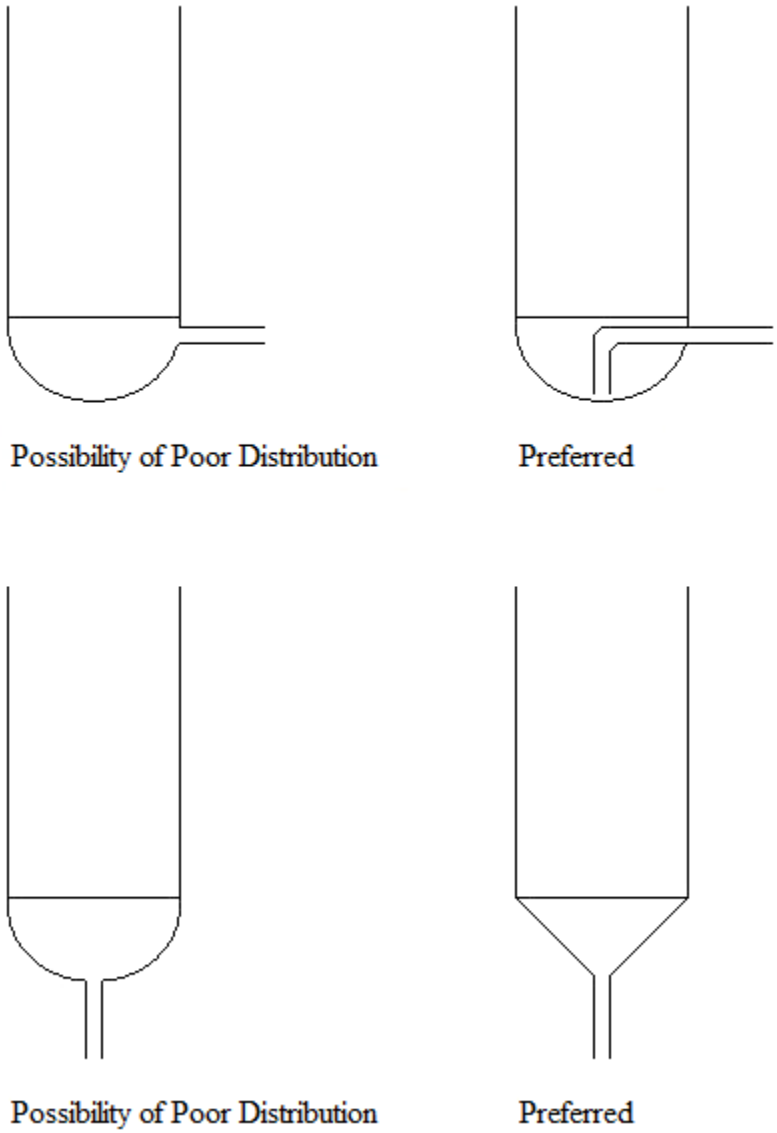


Figure 17: Possible Plenum Arrangements (Pell M., 1990)

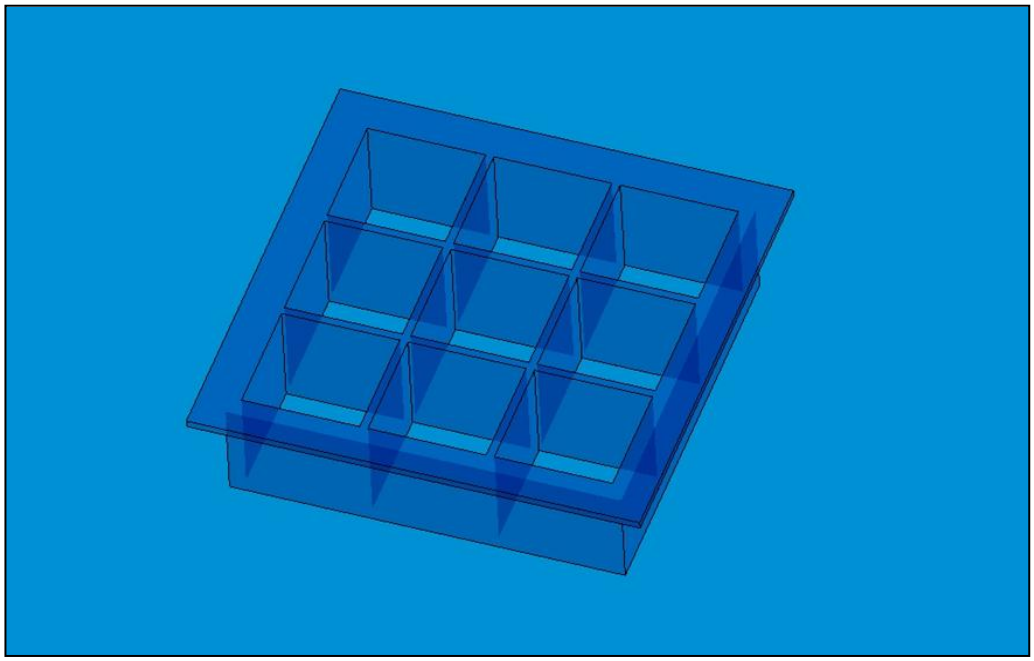

Figure 18: Schematic of Secondary Air Distributor

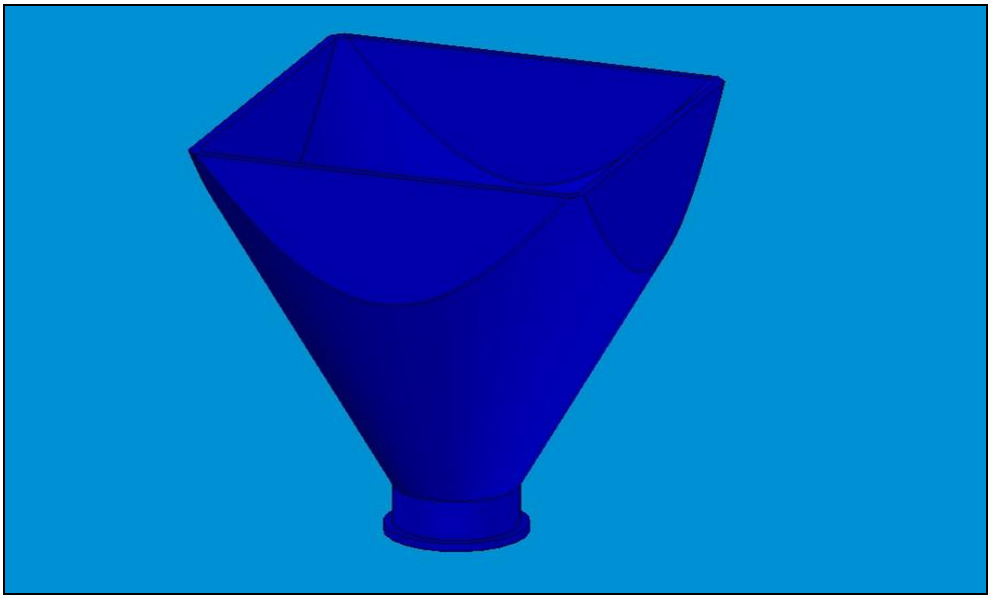

Figure 19: Schematic of Primary Air Distributor

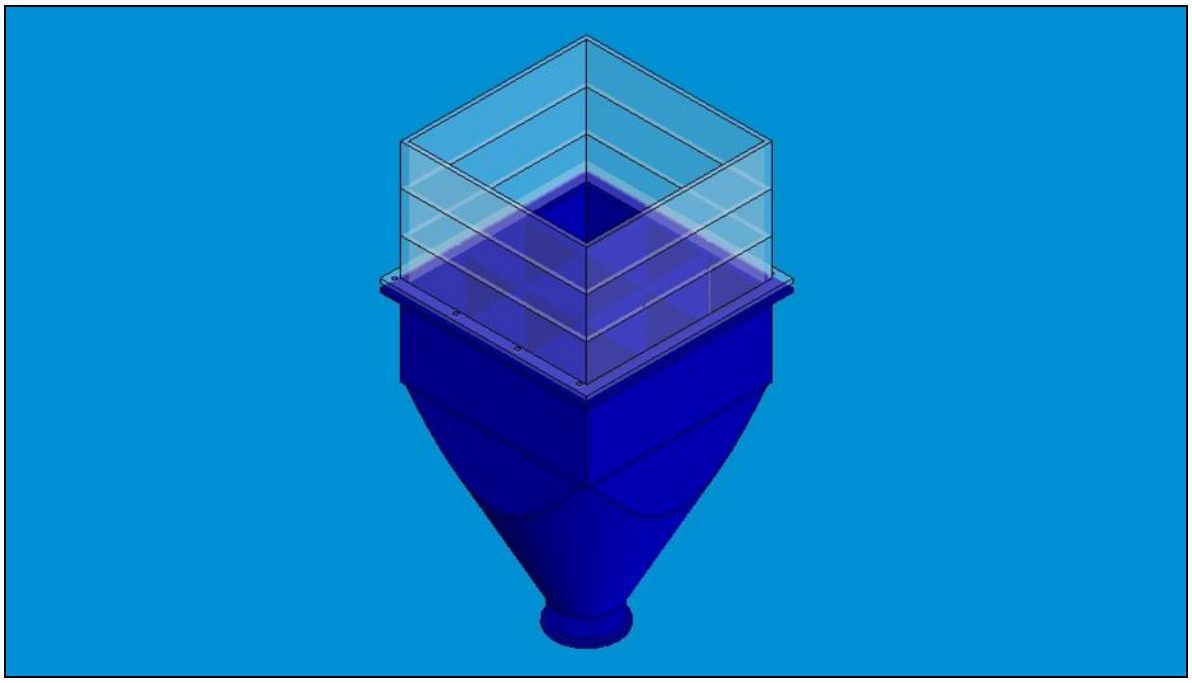

Figure 20: Assembly of the Fluidised Bed (Air Distributor Not Shown)

### 4.2.3. The Bed Walls

The fluidised beds' walls were made of interlocking sections that allowed for bed height variation from 100mm in height to 300mm in height, to allow for sufficient separation to occur. These walls were constructed from clear Perspex to allow for a degree of visual inspection of the fluidization (see Figure 21 below).

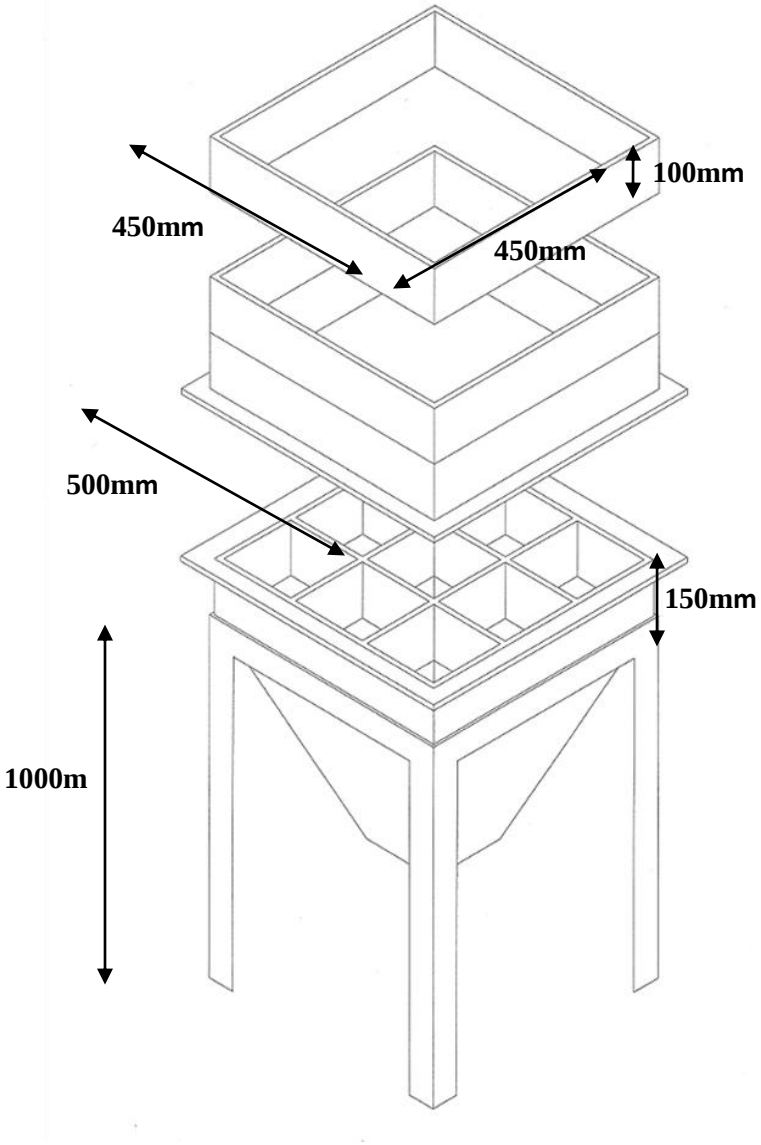


Figure 21: Exploded View of the Arrangement of the Fluidised Bed (Air Distributor Not Shown)

# 5 BED FLUIDISATION ANALYSIS

## 5.1. MAGNETITE SIZE DISTRIBUTION AND FLUIDISATION CHARACTERISTICS

Initial tests on a laboratory bed (see Figure 22) were conducted on the magnetite to analyse its fluidisation characteristics. The fluidisation characteristics allow prediction of the nature of fluidisation that the magnetite would experience in the scaled up pilot plant bed and in addition allowed the testing of the high pressure drop filter cloth.

## 5.2. FLUIDISATION CHARCTERISTICS OF MAGNETITE

The first set of fluidisation tests were conducted in the laboratory bed in Figure 1. The bed was filled with magnetite to the same depth that would be used in the pilot plant bed, namely 20cm. The bed was equipped with flow rotameters to regulate the air fed to the bed and a manometer to determine the bed pressure drop.

The effect of the distributor on the uniform fluidisation of the bed was tested. Initially a perforated plate was used; however this did not prove to be effective at all in providing uniform air distribution. The bed experienced channeling in its center, whilst at the walls dead zones were found. It was thus necessary to increase the pressure drop across the distributor to improve distribution. A substantial improvement in the air distribution was found by replacing the perforated plate with the high pressure drop distributor described previously. The results of the fluidisation would show under what conditions the magnetite would fluidise, what the nature of that fluidisation would be, its stability and the bulk density at which separation would occur.

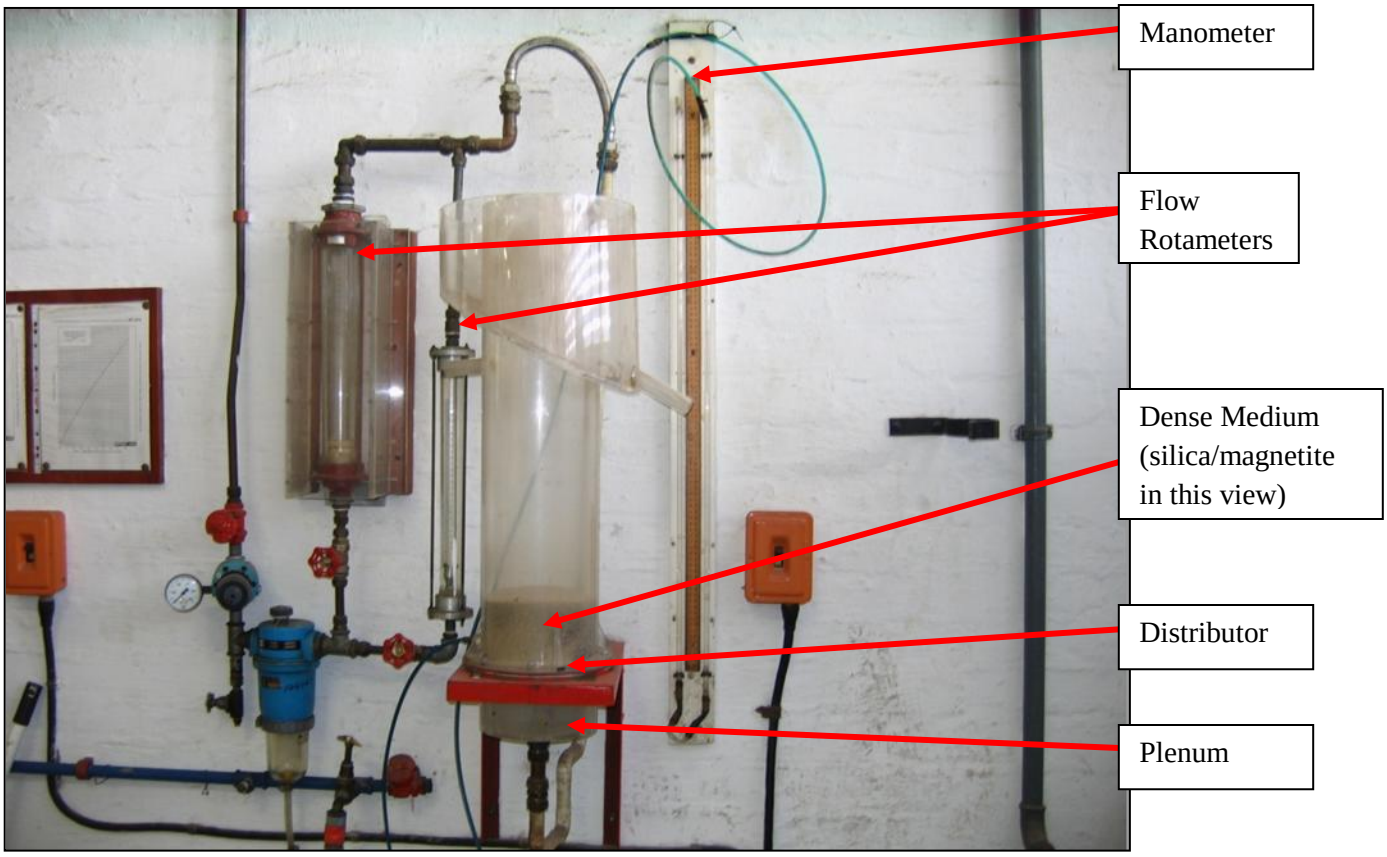


Figure 22: Laboratory Test Bed

## 5.3. FLUIDISATION CHARACTERISTIC CURVE

The characteristic fluidisation curve of the magnetite can be seen in Figure 23. This curve is typical of the fluidisation of fine particles. The gas velocity at the point of insipient fluidisation was 0.165m/s. The presence of fine particles within the bed aided fluidisation. The minimum bubbling point, as is typical of Geldart classification B particles, was experienced at 0.17m/s. The excellent distribution of air from the high pressure filter ensured that the fluidisation was uniform throughout the bed.

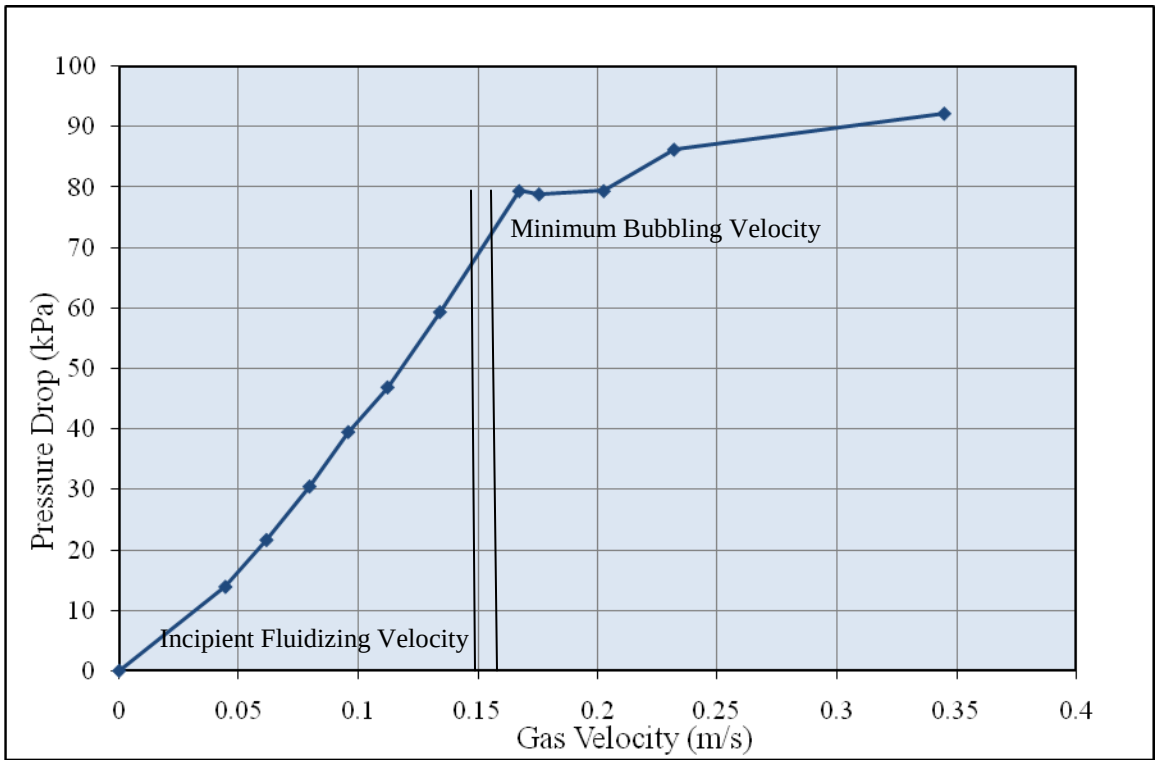


Figure 23: Magnetite Bed Characteristic Fluidisation Curve

| Gas Velocity, u (m/s) | 0.00 | 0.04 | 0.06 | 0.08 | 0.10 | 0.11 | 0.13 | 0.17 | 0.18 | 0.20 | 0.23 | 0.35 |
|---|---|---|---|---|---|---|---|---|---|---|---|---|
| Bed Pressure Drop (kPa) | 0.00 | 13.89 | 21.65 | 30.49 | 39.52 | 46.91 | 59.36 | 79.39 | 78.85 | 79.39 | 86.25 | 92.20 |
| Bed Height (cm) | 20.00 | 20.00 | 20.00 | 20.00 | 20.20 | 20.30 | 20.70 | 21.10 | 23.00 | 23.10 | 23.10 | 24.00 |
| Bed Density ($kg/m^3$) | 2200.73 | 2200.73 | 2200.73 | 2200.73 | 2173.24 | 2159.49 | 2104.51 | 2049.52 | 1788.34 | 1774.60 | 1774.60 | 1650.88 |

Table 2: Fluidisation Characteristics

## 5.4. MAGNETITE BED BULK DENSITY

The bulk density of the static bed was initially determined by observation of its volume relative to its known mass, and the resulting bulk density during fluidisation was then determined by the beds' expansion. The large drop in bed density at the superficial gas velocity of 0.17m/s was due to bubble formation. Analysis was then conducted using density tracers to determine whether the bed was fluidised enough to allow separation. Separation was limited by excessive bubbling within the bed. This excessive bubbling resulted in the bed acting more like a mixer than a separator. Effective separation was found to exist between a bulk density of 1900 and 2050kg/m$^3$.

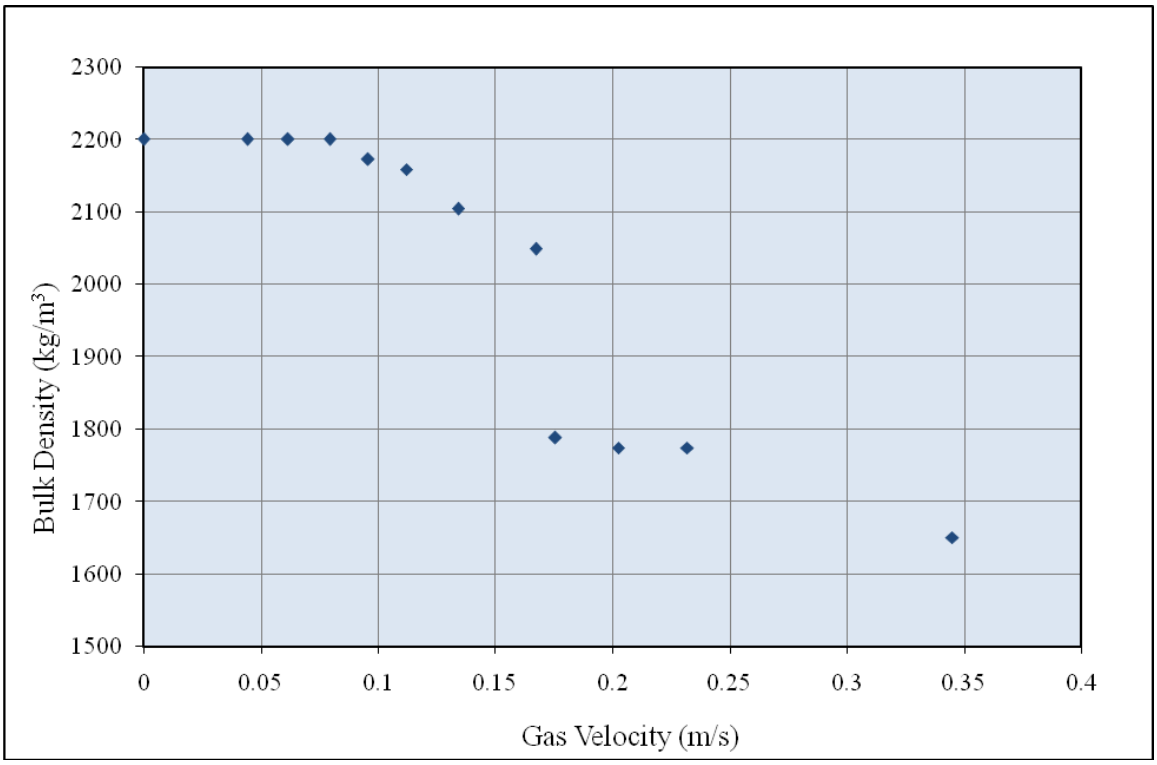


Figure 24: Magnetite Bed Bulk Density

## 5.5. INITIAL SEPARATION TESTS

### 5.5.1. Density Tracer Construction

Initial separation tests were conducted on the laboratory scale pilot plant. Density tracers were constructed to demonstrate the density split. These PVC cylinders (20mm in diameter and 20mm in length) were filled with lead and ferrosilicon in order to achieve the correct density for each fraction that they represented. The density spectrum covered by the tracers is shown in Appendix 4. Three tracers were constructed for each density fraction to reduce the possibility of entrainment errors and increase accuracy. The density spectrum of 1350 to 2850kg/m$^3$ serves to represent the mixture of coal and shale that would be received from the mine.

Figure 25: A Selection of Some of the Density Tracers Used

### 5.5.2. Batch Split Tests

The initial analysis of the pilot plant bed involved a sink-float test. The 45 density tracers (15 fractions with 3 tracers per fraction) were loaded into the bed that was operating at a superficial air velocity of 0.17m/s. The tracers were allowed 20 seconds to segregate then the air supply to the bed was stopped. This ensured that, as the tracers were being removed by hand, there would be no movement of the sinks and floats from their density fractions. The separation inefficiency of the tests can be seen below by the partition curve in Figure 26, with a split density of 2025kg/m$^3$. This split density was determined at the $\rho_{50}$. This is the point where the tracers would theoretically have a 50% probability of reporting to the sinks or floats fraction. This point would correspond to the bulk density of the bed.

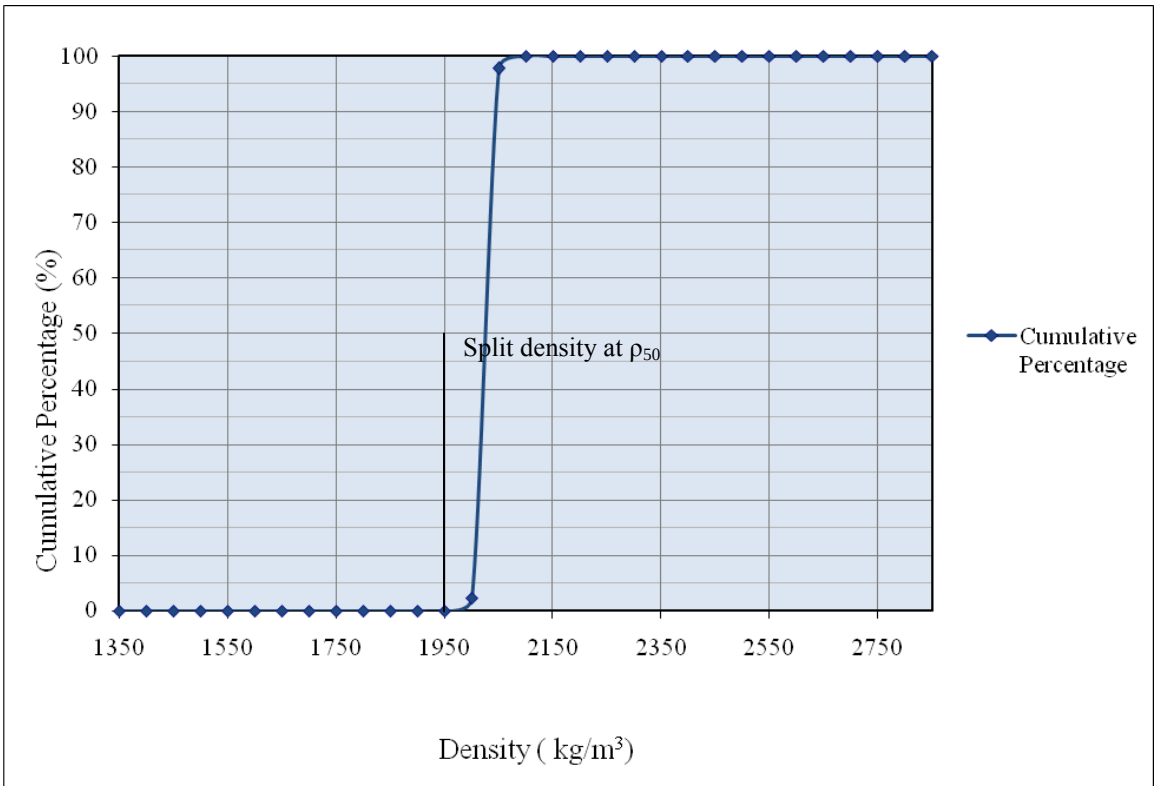


Figure 26: Partition Curve

### 5.5.3. Bulk Density Variation Within The Bed

Analysis of the density variation within the bed was then conducted. The bed was subdivided into 25 test zones. In each of these test zones a sink float test as described above was conducted to determine the local density. The sink float tests were done in preference to using hydrometers due to the effect of the bubbles within the bed on the hydrometer. The results of the density distribution can be seen in Figure 27 below. It is important to note that whilst there were observable wall effects, these were minimized through correct bed design. This resulted in a variation of approximately 4% in the bulk density of the bed.

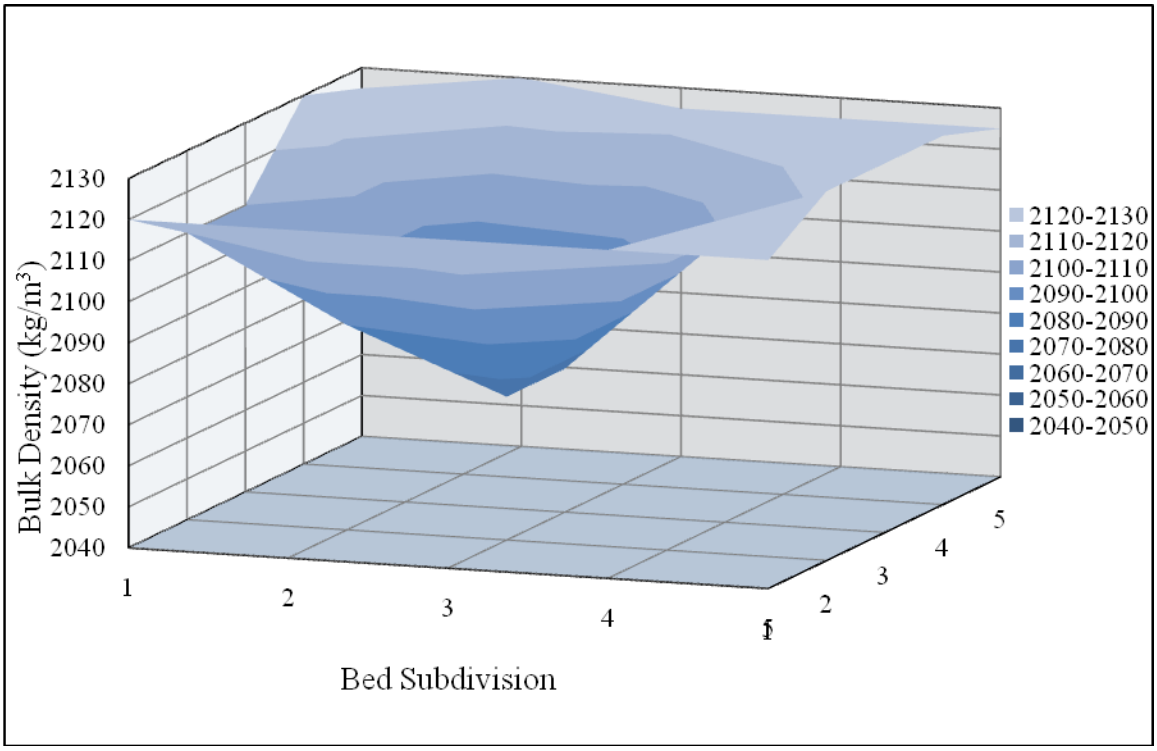


Figure 27: Bulk Density Variation within the Bed

# 6 PART 1: INITIAL CONCLUSIONS

## 6.1. FLUIDISATION OF THE DENSE MEDIUM

The fluidisation of the magnetite successfully produced a uniform medium. The presence of minor bubbling in the bed (see Figure 28) did not affect its separating capabilities. The bubbling in fact aided in separation by providing a jigging action to the bed. This liberated the lighter tracers that were entrained beneath heavier ones sinking to the bottom of the bed.

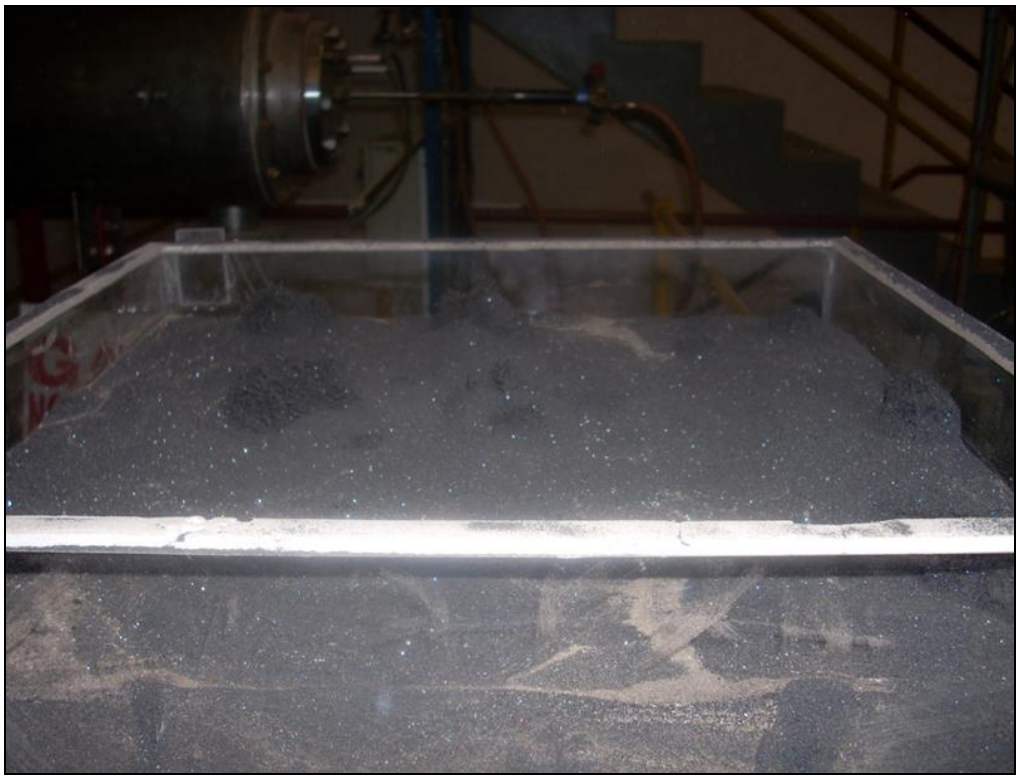

Figure 28: Bubbling in the Dense Medium Bed

The uniform air distribution below the bed provided by the segregated plenum and the high pressure drop distributor cloth ensured that there were few noticable dead zones in the bed. Due to the density and size fractions of the magnetite used there was little in the way of dust formation from the fluidisation. Any loss of magnetite from the bed came from the eruptions of the bubbles, however this was minimal.

**DENSITY SEPARATION WITHIN THE BED**

The density split separation provided by the bed was exceptionally accurate with a separation ineffiency (Ep) of 0.015 at a bulk density of 2023kg/$m^3$. In fact of the four runs conducted with the density tracers only one tracer from the floats fraction reporting to the sinks and one from the sinks reported to the floats, even so these tracers came from a density fractions immediately above and below the split density (See Figure 26 in Section 5 and Table 5 in Section 12.1 Appendix 1).

Figure 29: Density Tracers Floating on the Surface of the Dense Medium

Density tracers from the floats fraction in the fluidised bed are shown above in Figure 29. There was an increased bubbling effect in the centre of the bed caused by the presence of the sinks at the distributor. These sinks created a zone of lower pressure increasing the air flow at this point. The resultant bubbling meant that during the separation the bulk density of the bed was lower toward the centre of the bed.

This variation of bed density whilst having no effect on the actual separation would affect the efficiency of the control of the process. Thus the separator would need to ensure that there was no interaction either between the sinks or the separator itself with the distributor. It would, in addition, need to provide a mixing action within the bed that would break up the formation of large bubbles and dead zones.

# 7 SEPARATOR DESIGN AND CONSTRUCTION

## 7.1. SEPARATOR GOALS

The separation equipment must serve the following purposes:

1. Provide a mechanism for segregation and continuous removal of floats and sinks within the bed.

2. Not disrupt or adversely affect the fluidisation of the dense medium within the bed. There would need to be adequate clearance between the separator and the air distributor. Initial test work indicated that the presence of sinks in close proximity to the distributor produced excessive bubbling.

3. Provide an adequate degree of mixing that will prevent the formation of dead zones within the fluidised dense medium.

## 7.2. FINAL DESIGN CHOICES

The final separator that was designed and constructed was a rotating basket that would be partially immersed in the bed.

### 7.2.1. Outer Basket Design

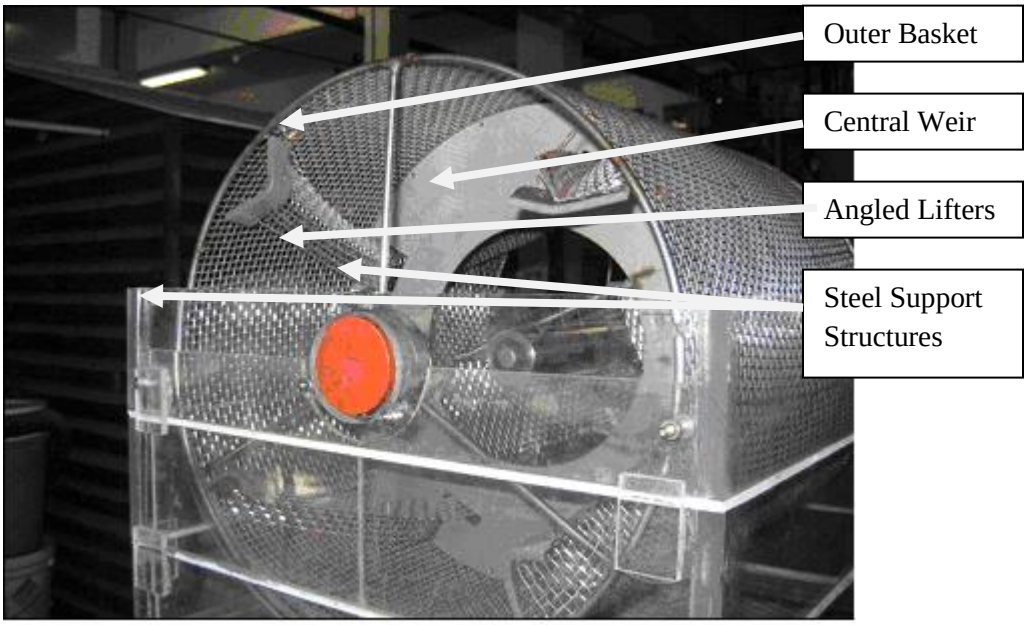


Figure 30: Rear View of the Separator with the Float Removal Chute Removed

The outer basket, 450mm long with the same diameter, was constructed of stainless steel mesh. This mesh was of 1mm diameter with 9mm gaps between the bars. The cylindrical structure of the outer basket was reinforced by 8mm steel rod (See Figure 30). The spacing was chosen after numerous experimental tests. It provided a rigid support structure that would maintain the integrity of the separator whilst allowing free flow of the fluidised magnetite. The sizing of the gaps needed to be minimal in order to prevent the density tracers and, in later tests, pieces of coal from slipping between the gaps. These particles would accumulate on the surface of the distributor, destroying the beds stability.

### 7.2.2. Separator Sub Division

The basket would be segregated into two sections by means of a solid plate weir, one for the removal of the sinks and the other for the removal of the floats. The solid weir would provide additional stability to the central section of the separator. The weir would prevent the sinks from slipping into the floats removal section while the floats could easily pass over the top.

### 7.2.3. Separator Internals

The unique internals of the separator provided a guidance mechanism to promote the segregation of the sinks and floats (see Figure 31).

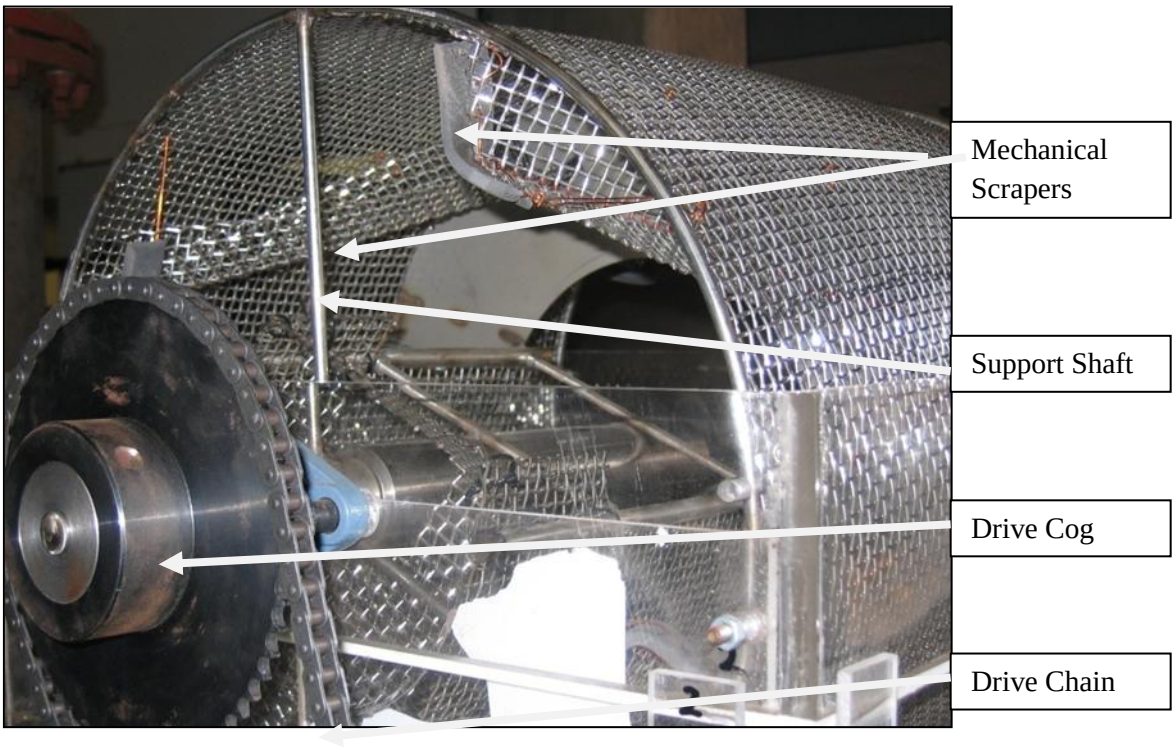


Figure 31: Front View of the Separator with Feed and Sinks Removal Chutes Removed

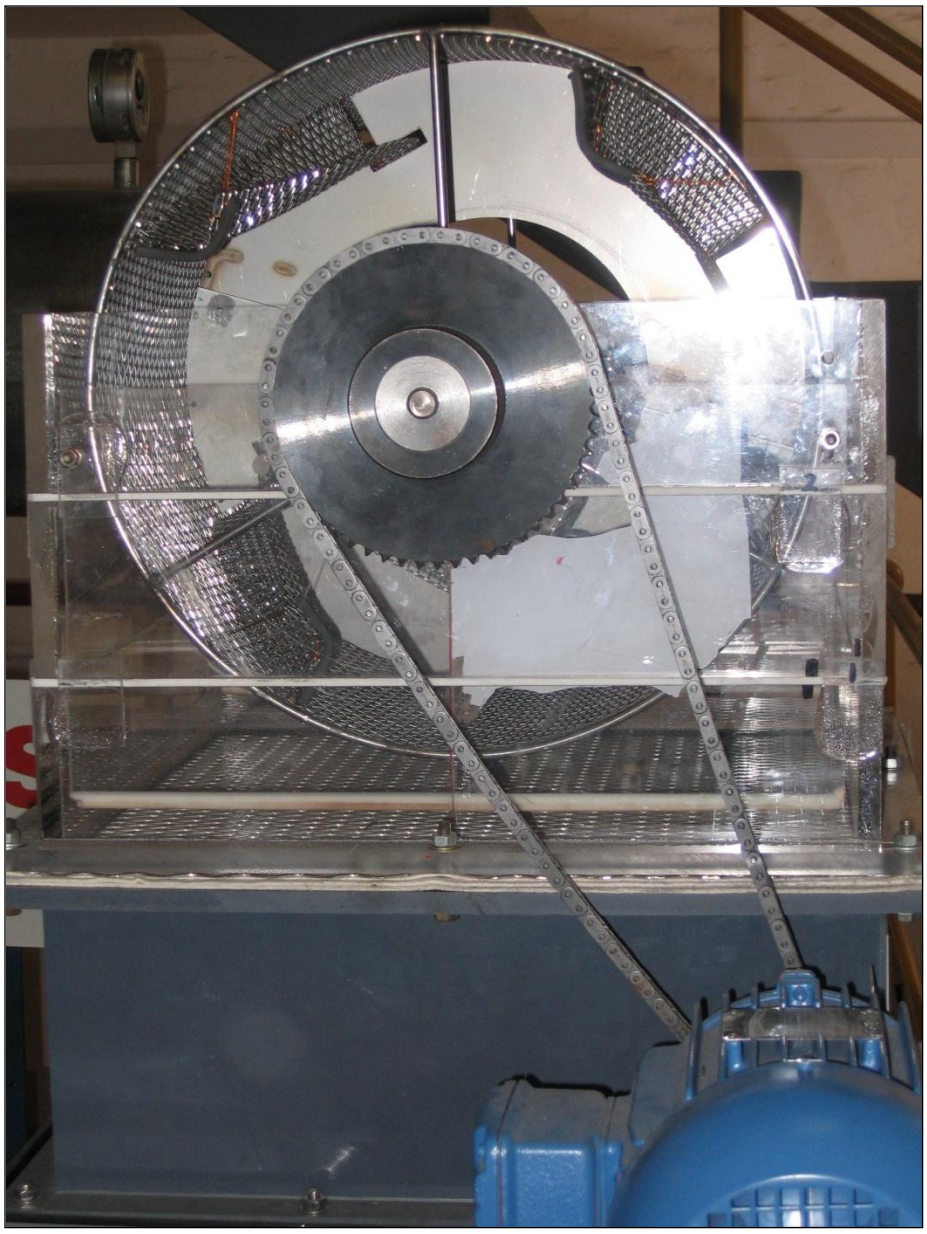

Figure 32: Front View of the Separator Bed with Feed and Sinks Removal Chutes Removed

#### 7.2.3.1. Floats Segregation Corridor

The segregation corridor in the sinks removal section was suspended from the extended drive shaft. The feed material was fed directly into this corridor. The walls extended below the surface of the fluidised dense media, thus the floats were able to move down the corridor, over the weir and into the floats removal section without being caught in the lifters in the sinks section. The sinks simply sank to be collected by the rotating lifters (see Figure 33).

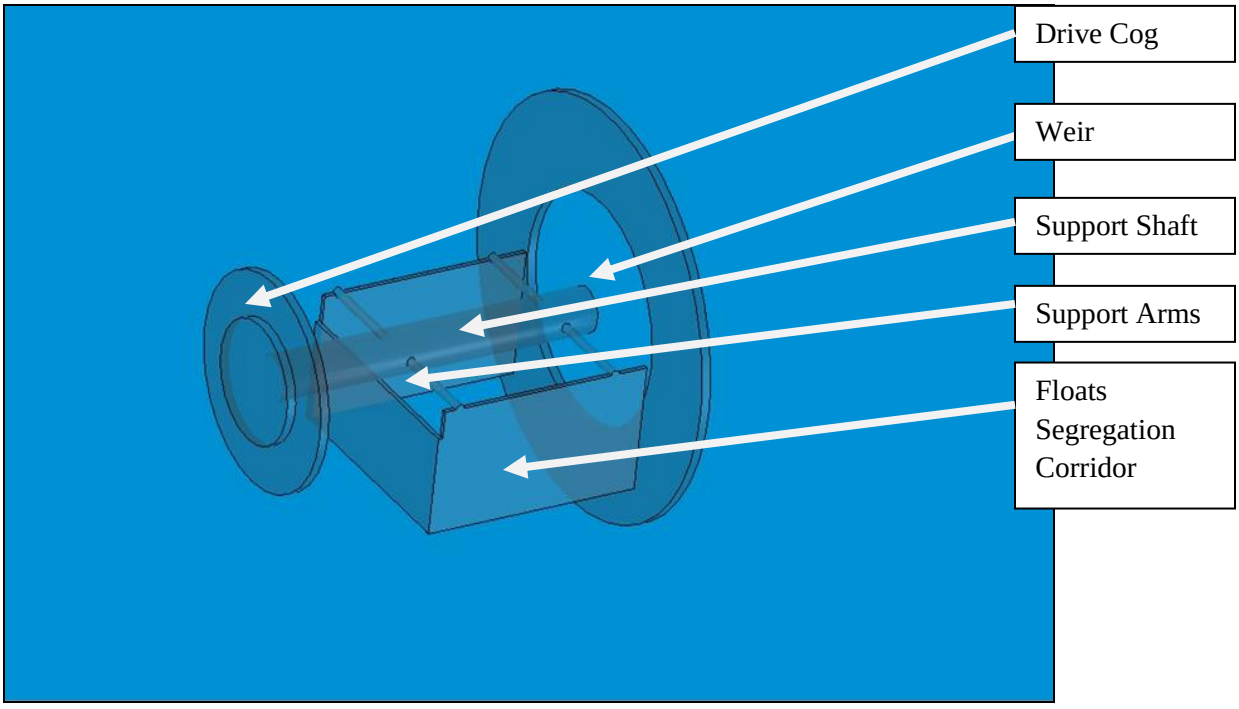


Figure 33: Representation Showing Separator Internals

#### 7.2.3.2. Mechanical Scraper

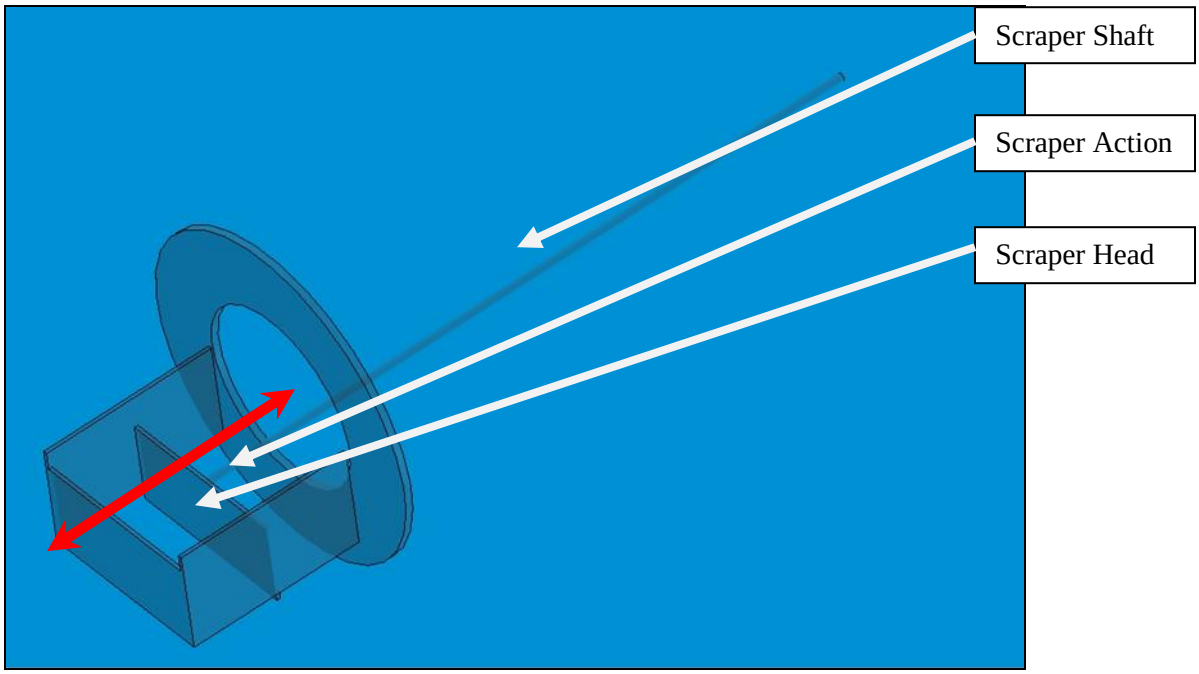


Figure 34: Diagram Showing Action of the Mechanical Scraper

The passage of the floats was aided by a mechanical scraper. The scraper was manually operated and was controlled from the floats removal side of the separator. It extended from wall to wall in the Floats Segregation Corridor and moved back and forward towards and away from the weir (see Figure 34, which was also mesh based so as to cause as little disruption to the fluidisation).

### 7.3. SEPARATION MECHANISM

- The coal was fed into the sinks removal section of the separator.

- The feed was constrained in sinks removal section so that floats were not removed with the sinks by the lifters at the separator walls.

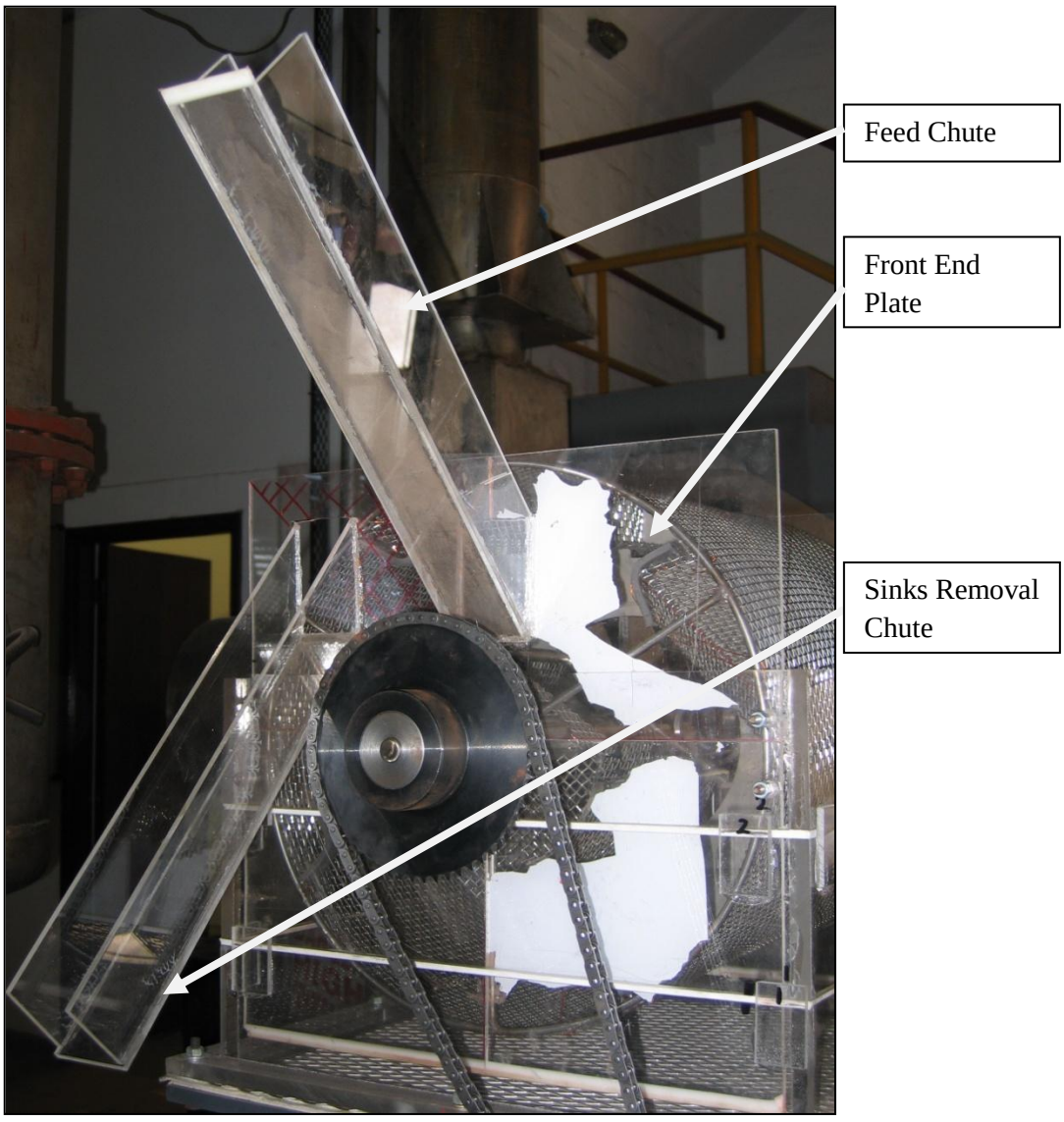


Figure 35: Front View of Separator with Feed and Sinks Removal Chutes in Place

- The sinks sank to the floor of the separator where they were scooped out by the lifters attached to the wall of the rotating basket.

- The sinks roll down the angled lifters and out of collection chutes located above the beds horizontal axis (see Figure 35).

- The floats are transported past the dividing weir to the floats collection section of the separator by means of a mechanical scraper.

- In the floats collection section the floats are dragged to the walls by means of a current induced in the bed by the motion of the separator. Once at the walls they are scooped up by angled lifters attached to the separator wall and removed via a product chute in a similar manner to that of the sinks (see Figure 36).

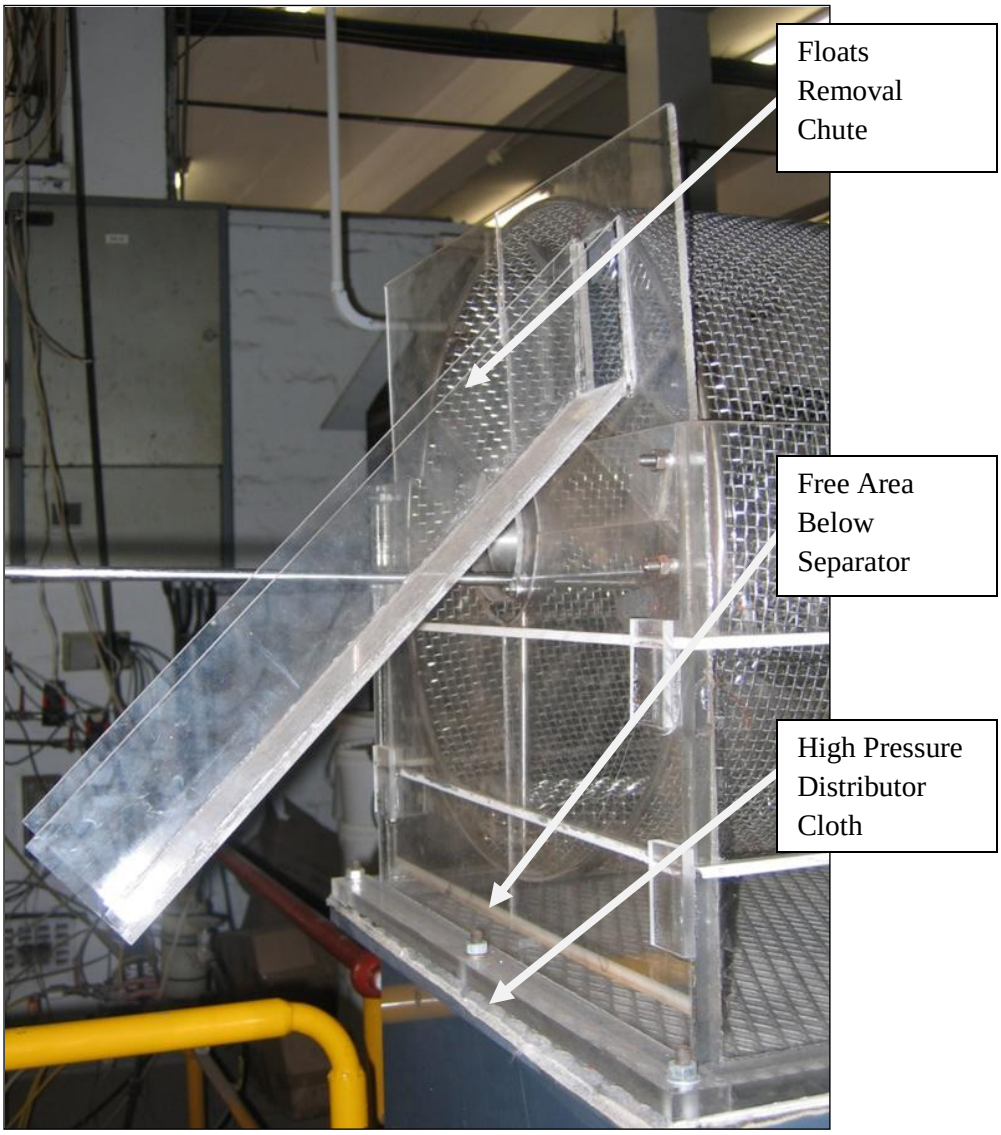


Figure 36: Back View of Separator with Floats Removal Chute in Place

### 7.4. AIR SUPPLY AND CONTROL

The air supply to the separator was provided by a high volume blower. A geared motor drove the separator. The blower settings were manipulated in the control hut (see Figure 37).

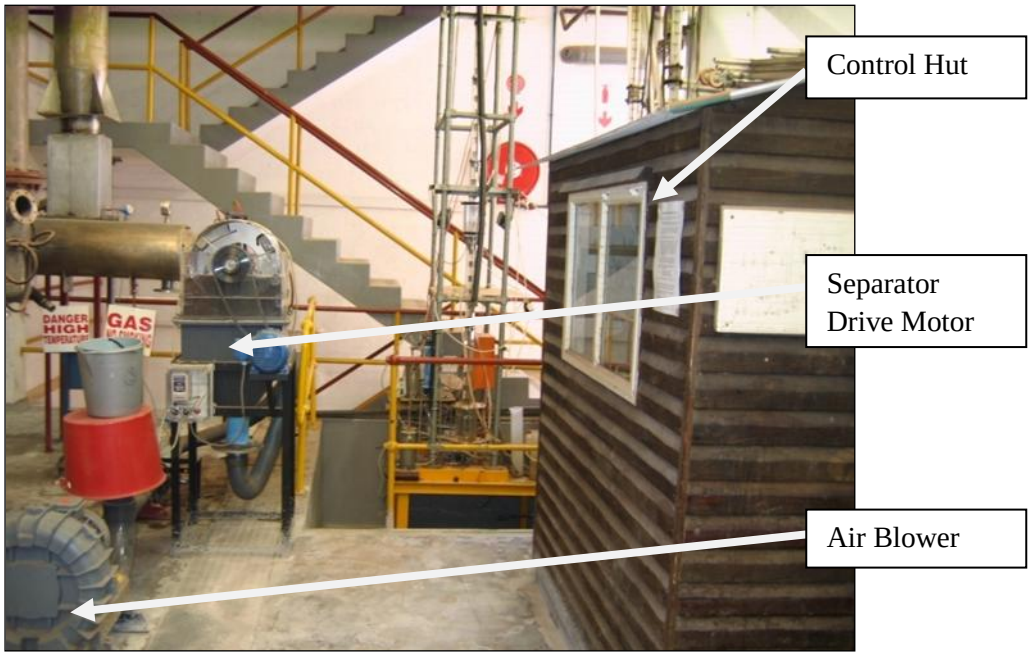


Figure 37: Overview of Pilot Plant Layout

# 8 PART 2 : OPTIMISATION AND OPERATION OF THE NOVEL SEPARATOR

With the separator constructed test work was conducted to determine its optimum operating point. From that stage the batch and continuous operating characteristics would be analysed using density tracers and coal.

## 8.1. OPTIMISATION OF THE SEPARATOR

The density tracers were again used for initial characterisation of the separator providing a feed that was both uniform in size and shape, and was easily classifiable. This allowed the number of runs undertaken to be maximised. In the optimisation tests a sample of tracers was fed into the separator. The rotational speed of the separator and the air flow rate to the bed was varied. The resultant separation inefficiency (Ep) was noted and averaged for 3 tests at each of the conditions. The optimum conditions can be observed from the bar plot Figure 38. They show a peak efficiency achieved at a superficial gas velocity of 0.13m/s and separator speed of 4rev/min.

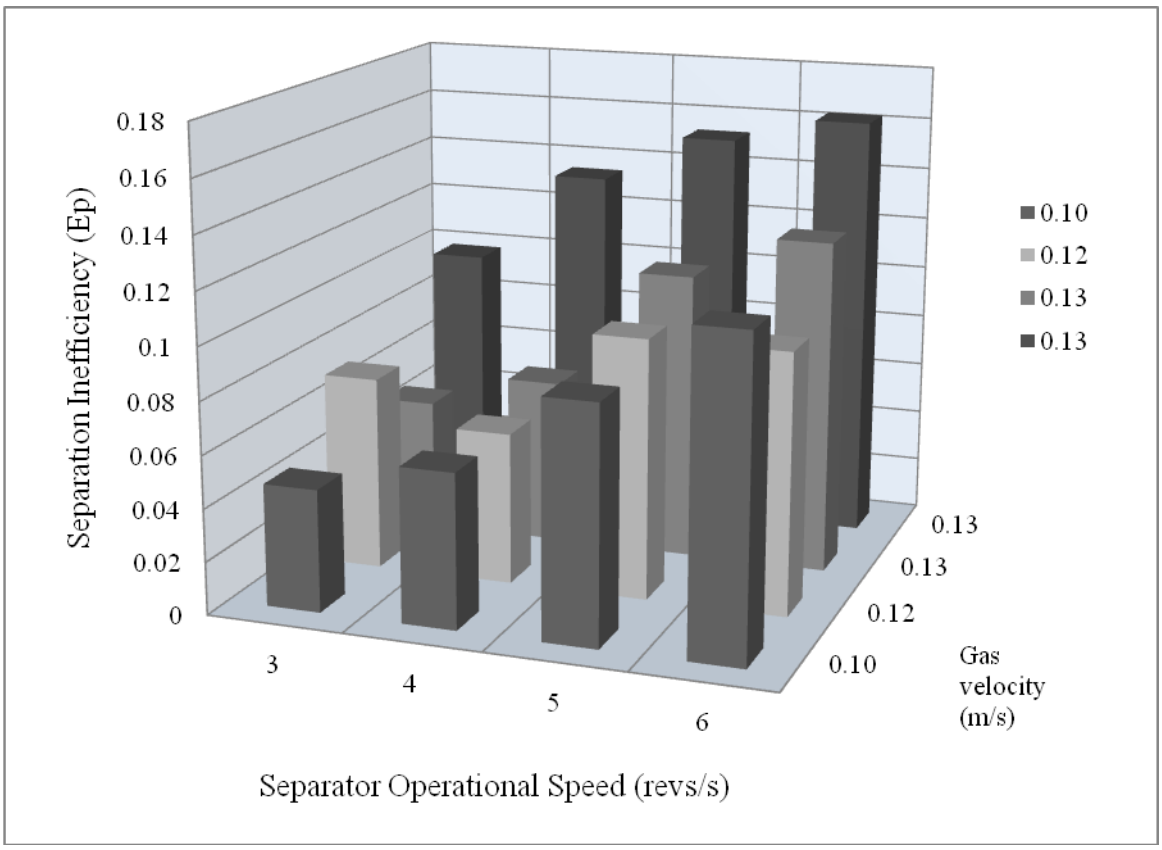


Figure 38: Composite Optimisation Graph

## 8.2. BATCH ANALYSIS OF TRACER SEPARATION

These optimum conditions allowed initial separations to be carried out on the equipment. Again density tracers were used for ease of post separation analysis. The results of this separation can be seen in Figure 39**.** These results are the combined analysis of 15 batch tests. In each batch test 2.5kg of density tracers, of an even density distribution, were fed into the separator over a period of 9 minutes and allowed to separate. An average separation inefficiency (Ep) of 0.057 was achieved at a split density of 1871kg/m$^3$.

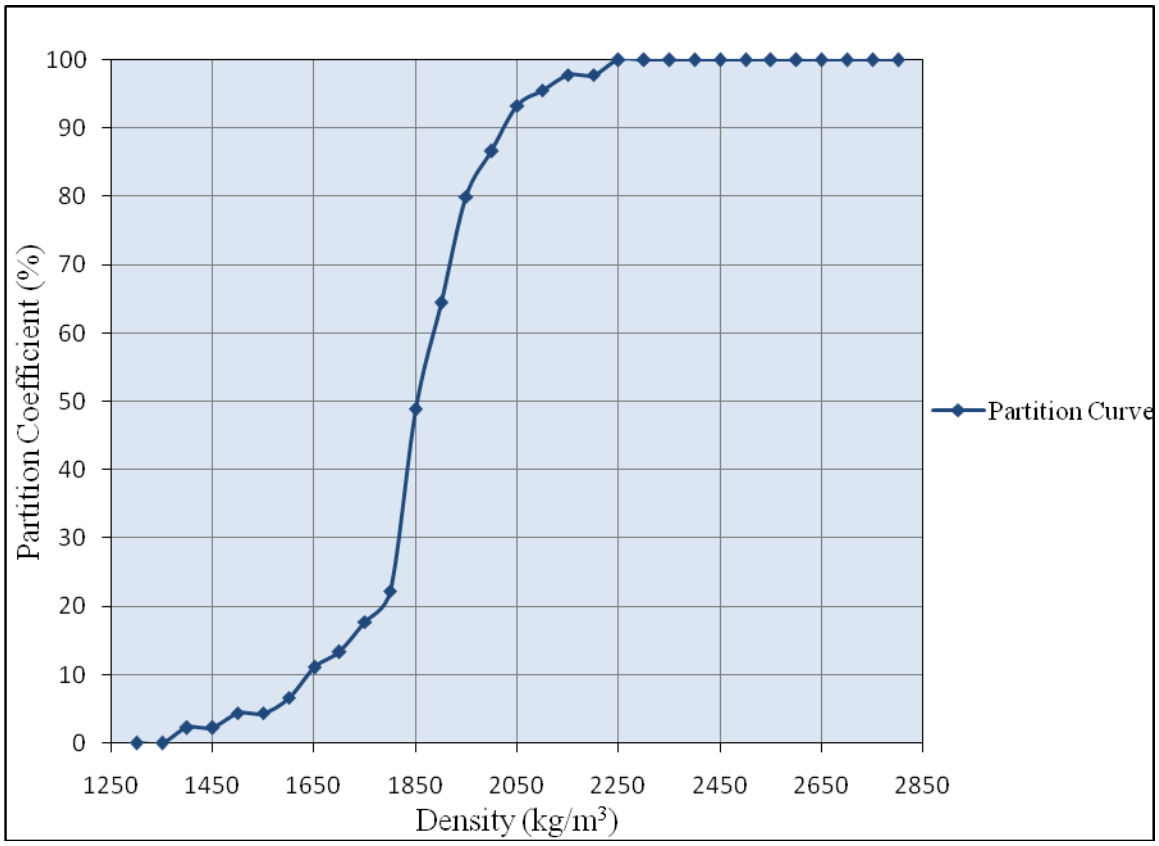


Figure 39: Best Settings Partition Curve (Density Tracers)

### 8.3. BATCH ANALYSIS OF DISCARD COAL SEPARATION

The next investigation into the efficiency of the separator was conducted using high ash Waterberg discard coal, crushed and screened to a size fraction of 1.5–3.5cm. Again the coal was fed in to the separator under the same conditions as the tracers had been in previous tests. This coal had very low free moisture content as it was dry to the touch.

After collection of the floats and sinks the samples were separated into their respective density fractions through dense liquid sorting. The separate fractions were then crushed and combusted in order to determine their ash content. The results of the separation can be seen in Table 3. The feed material, having an ash content of 60% w/w was separated into a floats fraction having an ash content of 28% and a sinks fraction having an ash content of 80% w/w. The Partition curve obtained can be seen in Figure 40. The same operating conditions were used as with the density tracers. A split was achieved at a bulk density of 1996kg/$m^3$ with a separation inefficiency of 0.046 obtained.

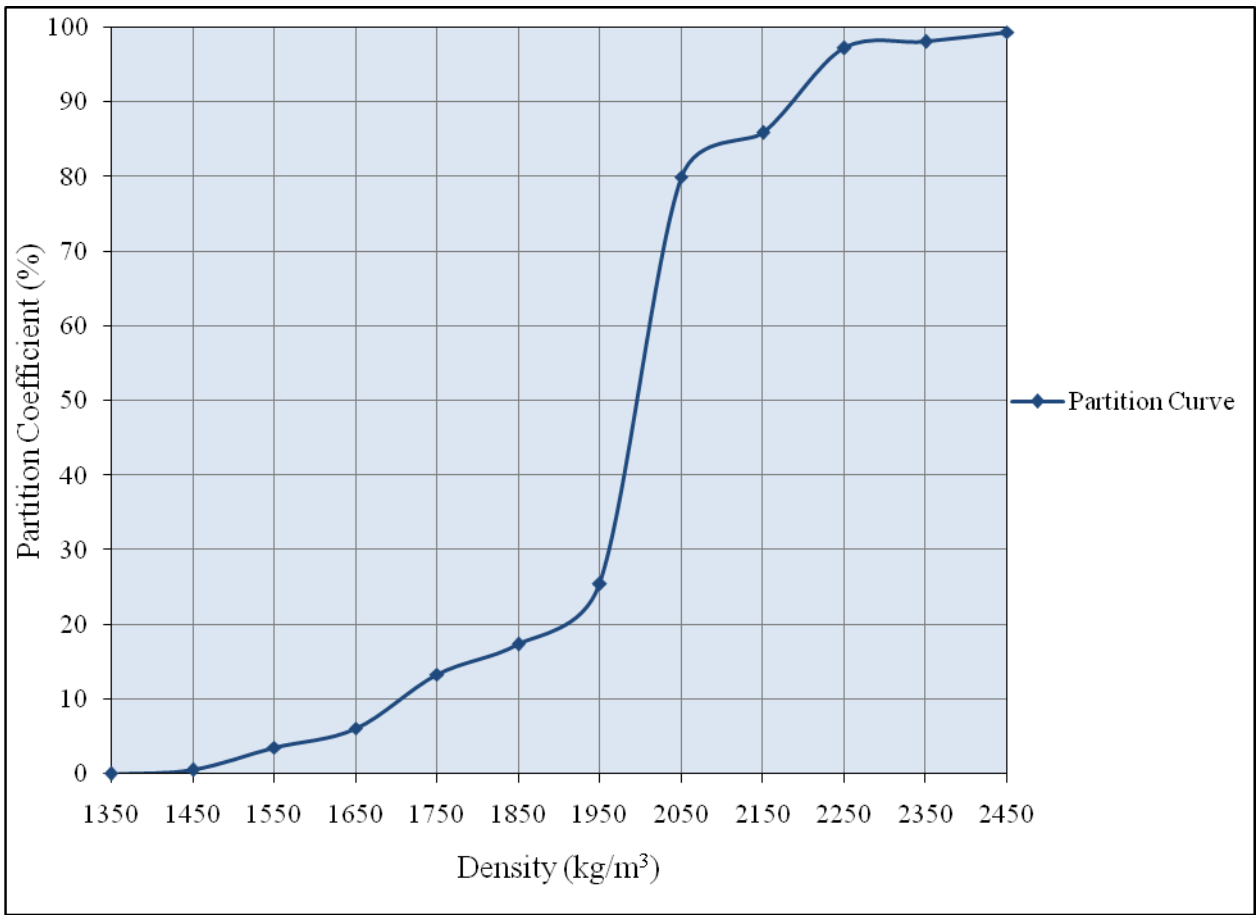


Figure 40: Partition Curve for the Batch Beneficiation of Coal

| Density Fraction ($kg/m^3$) | Floats Overflow (%) | Ash (%) | Overflow/Feed (%) | Sinks Overflow (%) | Ash (%) | Overflow/Feed (%) | Calculated Feedstock Feed (%) | Ash (%) | Partition Coefficient (%) |
|---|---|---|---|---|---|---|---|---|---|
| <1400 | 16.82 | 8.59 | 6.56 | 0.002 | 16.34 | 0.001 | 6.57 | 8.59 | 0.02 |
| 1400-1500 | 31.76 | 10.35 | 12.39 | 0.12 | 14.23 | 0.07 | 12.46 | 10.37 | 0.56 |
| 1500-1600 | 13.87 | 13.76 | 5.41 | 0.33 | 12.69 | 0.20 | 5.61 | 13.72 | 3.56 |
| 1600-1700 | 2.06 | 21.01 | 0.80 | 0.09 | 5.29 | 0.05 | 0.86 | 20.05 | 6.09 |
| 1700-1800 | 2.78 | 19.65 | 1.08 | 0.27 | 23.56 | 0.17 | 1.25 | 20.17 | 13.33 |
| 1800-1900 | 9.63 | 43.05 | 3.76 | 1.30 | 45.19 | 0.79 | 4.55 | 43.42 | 17.4 |
| 1900-2000 | 15.58 | 64.95 | 6.08 | 3.40 | 69.08 | 2.07 | 8.15 | 66.00 | 25.44 |
| 2000-2100 | 2.04 | 73.99 | 0.80 | 5.21 | 73.21 | 3.18 | 3.97 | 73.36 | 79.99 |
| 2100-2200 | 2.63 | 70.67 | 1.03 | 10.27 | 76.94 | 6.26 | 7.29 | 76.05 | 85.9 |
| 2200-2300 | 1.91 | 83.88 | 0.75 | 42.95 | 81.72 | 26.19 | 26.94 | 81.78 | 97.23 |
| 2300-2400 | 0.85 | 80.54 | 0.33 | 28.13 | 86.38 | 17.15 | 17.48 | 86.27 | 98.11 |
| >2400 | 0.08 | 89.45 | 0.03 | 7.93 | 83.80 | 4.84 | 4.87 | 83.84 | 99.34 |
| Total | 100.00 | 27.61 | 39.02 | 100.00 | 80.83 | 60.98 | 100.00 | 60.06 | |

Table 3: Coal Beneficiation Results Summary (Batch Tests)

### 8.4. CONTINUOUS ANALYSIS OF DISCARD COAL SEPARATION

A final series of tests was conducted to determine the continuous operating characteristics of the separator. The separator was run for 45 minutes with a feed flow rate of 18kg/hr. Again the split density was 1996kg/m$^3$. A separation inefficiency of 0.046 was achieved. With the separation results being seen in Table 4 and Figure 41. From the results of this test work it is clear that the separator can function continuously without detriment to the separation efficiency and with a continuous upgrading of the coal from 60% ash to 28% ash content. The clean coal product could either then be further upgraded, or is suitable for industrial use.

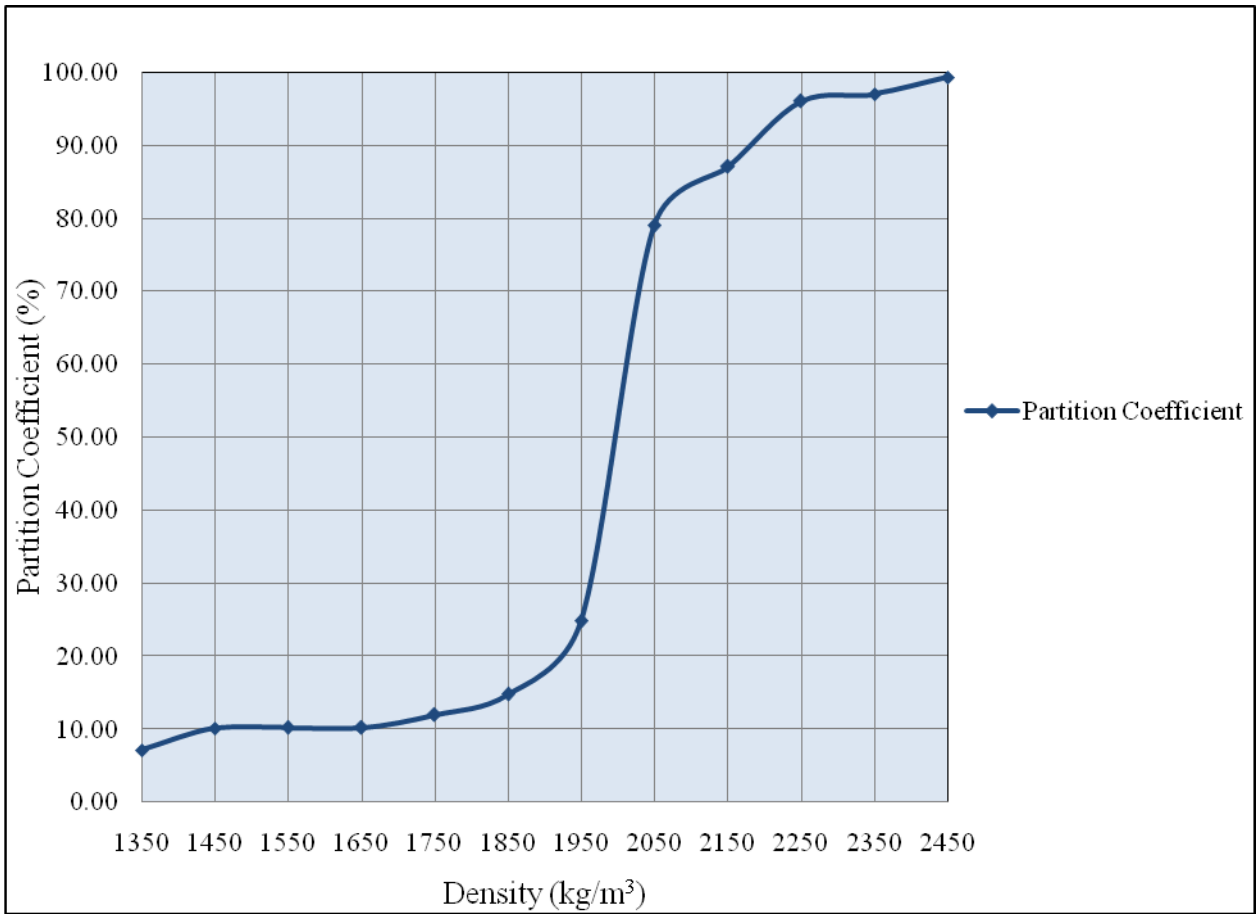


Figure 41: Partition Curve for the Continuous Beneficiation of Coal

| Density Fraction ($kg/m^3$) | Floats Overflow (%) | Ash (%) | Overflow/Feed (%) | Sinks Overflow (%) | Ash (%) | Overflow/Feed (%) | Calculated Feedstock Feed | Ash (%) | Partition Coefficient (%) |
|---|---|---|---|---|---|---|---|---|---|
| <1400 | 8.38 | 8.33 | 6.10 | 0.61 | 13.20 | 0.47 | 6.57 | 8.68 | 7.12 |
| 1400-1500 | 14.37 | 11.98 | 11.20 | 0.61 | 0.24 | 1.26 | 12.46 | 10.79 | 10.11 |
| 1500-1600 | 19.16 | 14.27 | 5.04 | 3.07 | 10.21 | 0.57 | 5.61 | 13.86 | 10.23 |
| 1600-1700 | 33.53 | 21.01 | 0.77 | 1.23 | 5.81 | 0.09 | 0.86 | 19.45 | 10.24 |
| 1700-1800 | 8.38 | 21.17 | 1.10 | 1.84 | 22.96 | 0.15 | 1.25 | 21.38 | 11.98 |
| 1800-1900 | 2.99 | 43.93 | 3.88 | 7.98 | 47.24 | 0.67 | 4.55 | 44.42 | 14.78 |
| 1900-2000 | 7.78 | 66.88 | 6.13 | 7.36 | 72.37 | 2.03 | 8.15 | 68.25 | 24.86 |
| 2000-2100 | 2.40 | 70.31 | 0.84 | 13.50 | 73.06 | 3.14 | 3.97 | 72.48 | 78.97 |
| 2100-2200 | 1.20 | 81.65 | 0.94 | 27.61 | 75.51 | 6.35 | 7.29 | 76.31 | 87.11 |
| 2200-2300 | 0.60 | 72.79 | 1.07 | 20.86 | 81.22 | 25.87 | 26.94 | 80.88 | 96.03 |
| 2300-2400 | 0.60 | 80.08 | 0.52 | 7.36 | 82.63 | 16.96 | 17.48 | 82.56 | 97.01 |
| >2400 | 0.60 | 89.09 | 0.03 | 7.98 | 84.82 | 4.84 | 4.87 | 84.84 | 99.34 |
| Total | 100.00 | 24.61 | 37.61 | 100.00 | 70.48 | 62.39 | 100.00 | 60.06 | |

Table 4: Coal Beneficiation Results Summary (Continuous Tests)

## 8.5. ACCUMULATION WITHIN THE SEPARATOR BED

Accumulation within any process is important to quantify. In the case of dense medium separation accumulation will affect not only the bulk density of the bed but may also interfere with the fluidisation. The density tracers did not pose a threat to accumulation due to their size. Coal on the other hand is brittle and regularly chips and breaks especially when in the environment of constant collisions that is usually experienced in jig separation. The fluidised separator provides an environment that produces far less attrition than traditional methods. After all the batch and test runs no coal fragments were found to have passed through the separator and into the bed. This additionally meant the bed operated with little or no coal dust formation, and important health and safety consideration.

# 9 PART 2 : CONCLUSIONS

As a result of the test work conducted on the separator from initial optimisation through batch test work and final continuous operation the following conclusions were reached.

- Magnetite powder provides an effective separation medium that can be fluidised adequately by air to create a stable separation density between 1850 and 2100kg/$m^3$. An optimum separation density was found to exist at 1996kg/$m^3$.

- The novel separator was found to operate under optimum conditions at a superficial gas velocity of 0.13m/s and a separator rotation speed of 4revs/min.

- The separation inefficiency Ep achieved was 0.057 for the runs involving the density tracers. The split density was achieved at 1996kg/$m^3$.

- The average separation inefficiency Ep achieved was 0.046 for the batch runs involving the Waterberg coal, which is comparable with traditional wet separation techniques. The 2.5kg batches of coal were fed into the separator and allowed to separate over a period of 9 minutes. The coal entered at an average ash content of 60.1%. 39.8% of the coal reported to the floats with a final average ash content of 28.5%. The remaining 60.8% of the coal reported to the sinks with a final ash content of 80.9%. The split density was achieved at 1996kg/$m^3$.

- The average separation inefficiency Ep achieved was 0.046 for the continuous runs involving the Waterberg coal, which is comparable with traditional wet separation techniques. The coal was separated at a capacity of 18kg/hr. The coal was fed into the separator at an average ash content of 60.1%. 39.7% of the coal reported to the floats with a final average ash content of 24.6%. The

remaining 60.3% of the coal reported to the sinks with a final ash content of 76.41%. The split density was achieved at 1996kg/$m^3$.

- The novel separator itself provided an effective mechanism by which the floats and sinks of the separation may be removed from the fluidised bed. This separator not only had a minimal impact on the stability of the bed, but also was highly effective preventing the accumulation of middling's and providing a mixing action within the bed to prevent the formation of dead zones.

- The scale-up potential of the bed is enormous, the advantages of dry beneficiation are clear, and the operation of this bed has proved that the disadvantages traditionally associated with dry beneficiation can be recognised and overcome.

# 10 Future Work

## 10.1. SCALE UP

The success of the lab scale separator has prompted investigation into the construction of a scaled up pilot plant. This pilot plant will correct some of the problems discovered with the operation of the laboratory scale equipment whilst allowing for large scale continuous operation. The idea was to increase the capacity of the equipment by a factor of 35 and at the same time iron out any bugs from the previous design. The final proposed future design would measure 1.5m in width by almost 6m in length. The proposed design of this separator is discussed here however the final construction and operational tests will not be considered in the scope of this dissertation.

## 10.2. ALTERATIONS TO THE SEPARATION EQUIPMENT

### 10.2.1. The Shape

The bed was lengthened in order to provide a greater residence time for the particles and thus increase efficiency by decreasing the possibility of entrainment.

### 10.2.2. The Plenum

The plenum differed from the previous design in that it was lengthened to account for the new shape and provided with four separate air supplies. These air supplies would need to provide approximately 45 times the volume of air needed to run the smaller separator. The addition of separate supplies would mean that air distribution though the length of the bed could be altered to examine the affects of fluidization quality and bulk density variation throughout the bed's length.

### 10.2.3. The Removal System

The removal system of the previous separator had been adequate but had occasionally shown itself to have several traits that could be improved upon. The angled lifters that fed the chutes at the open ends of

the separator basket did not provide as speedy a removal as was always needed there appeared to be congestion of particles at the chute entrance which occasionally caused blockage and unnecessarily increased residence time, thus reducing the capacity of the separator. The improved removal system consisted of angled lifters that dropped the floats and sinks onto outwardly moving conveyers which would ensure the rapid removal of the particles. These conveyers would be mounted above a central support plate that would run down the length of the separator.

### 10.2.4. The Scraper

The scraper for dragging the floats from the sinks removal section to the floats removal section would be replaced by a more efficient design that would be suspended from below the central support plate. This would ensure rapid transfer of the floats to the floats removal section of the bed.

### 10.2.5. The Drive Mechanism

The previous drive mechanism did place a fair degree of strain on the separator basket, and would not be an optimal choice for the scaled up bed. Rather the basket would be suspended on rollers situated just above the wall of the bed.

### 10.2.6. Materials of Construction

The materials used to construct the bed would need to be considerably more resilient than those needed for the previous design in order to cope with the substantially increased weight of the magnetite medium. Steel was recommended for the beds internals and supports and test work needs to be conducted to ensure the load bearing capacities of the support design.

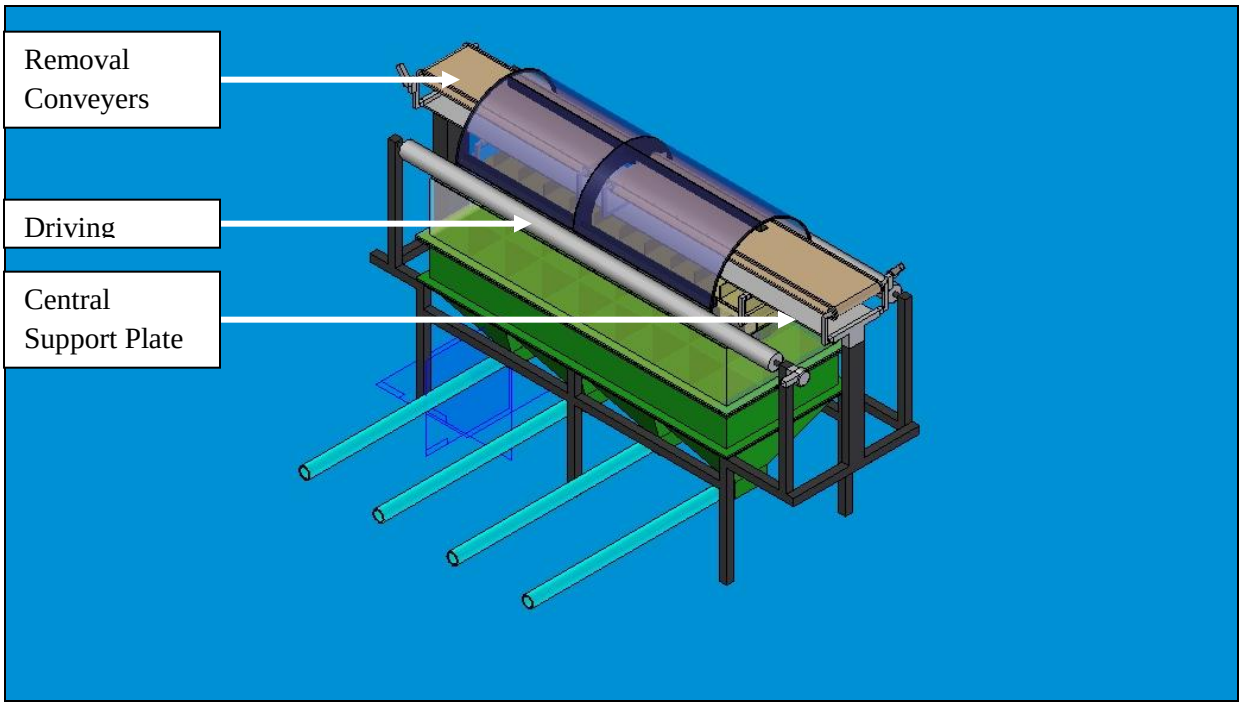


Figure 42: Isometric View of the Proposed Design for the Scaled Up Separator

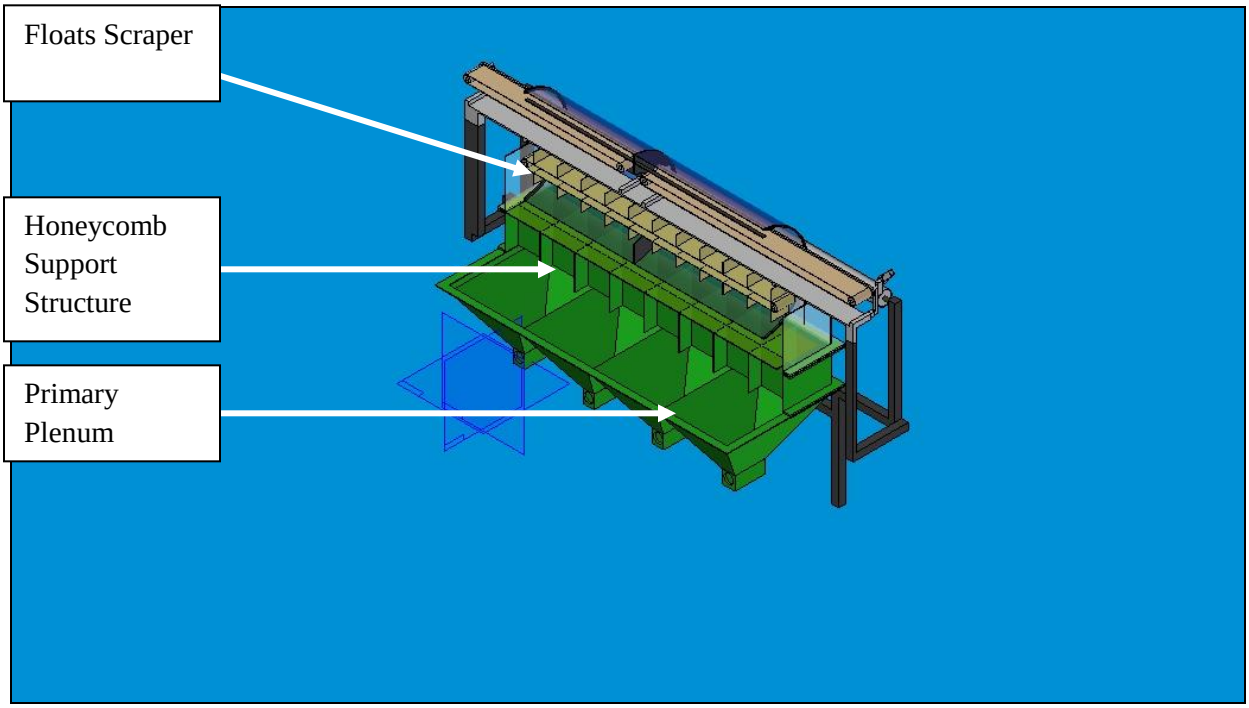


Figure 44: Sectioned Isometric View of the Proposed Design for the Scaled Up Separator

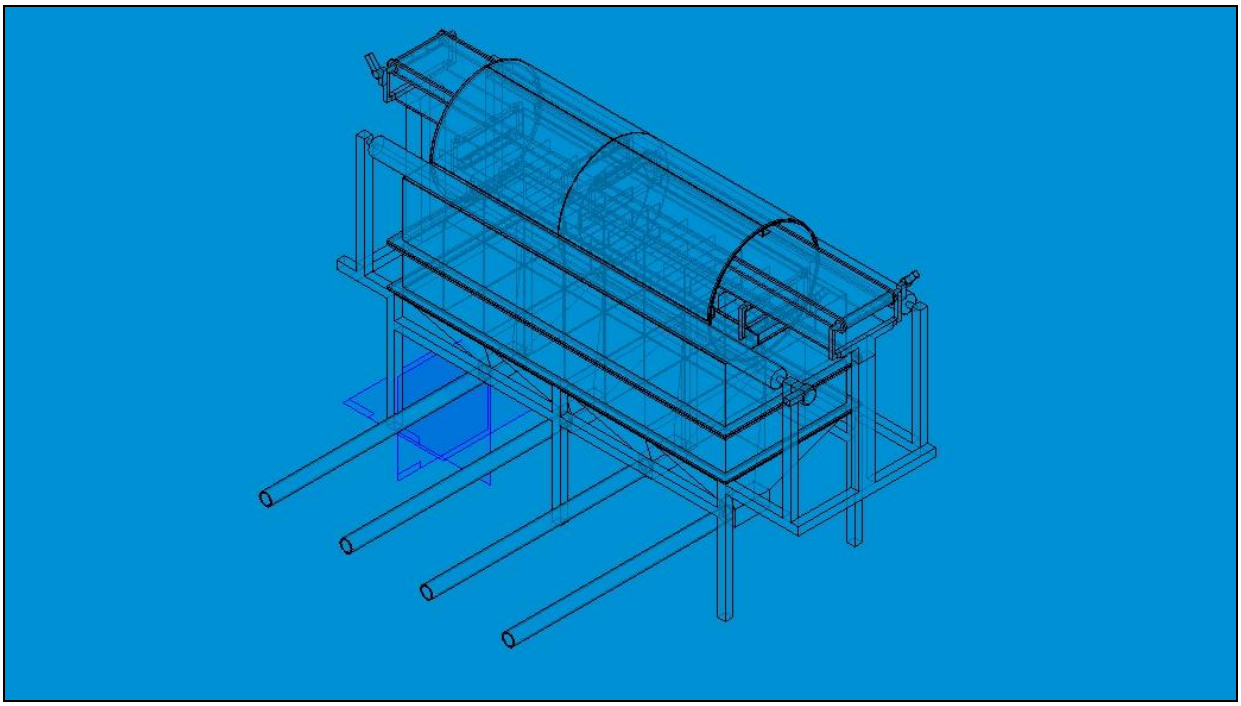

Figure 44: Construction Isometric View of the Proposed Design for the Scaled Up Separator

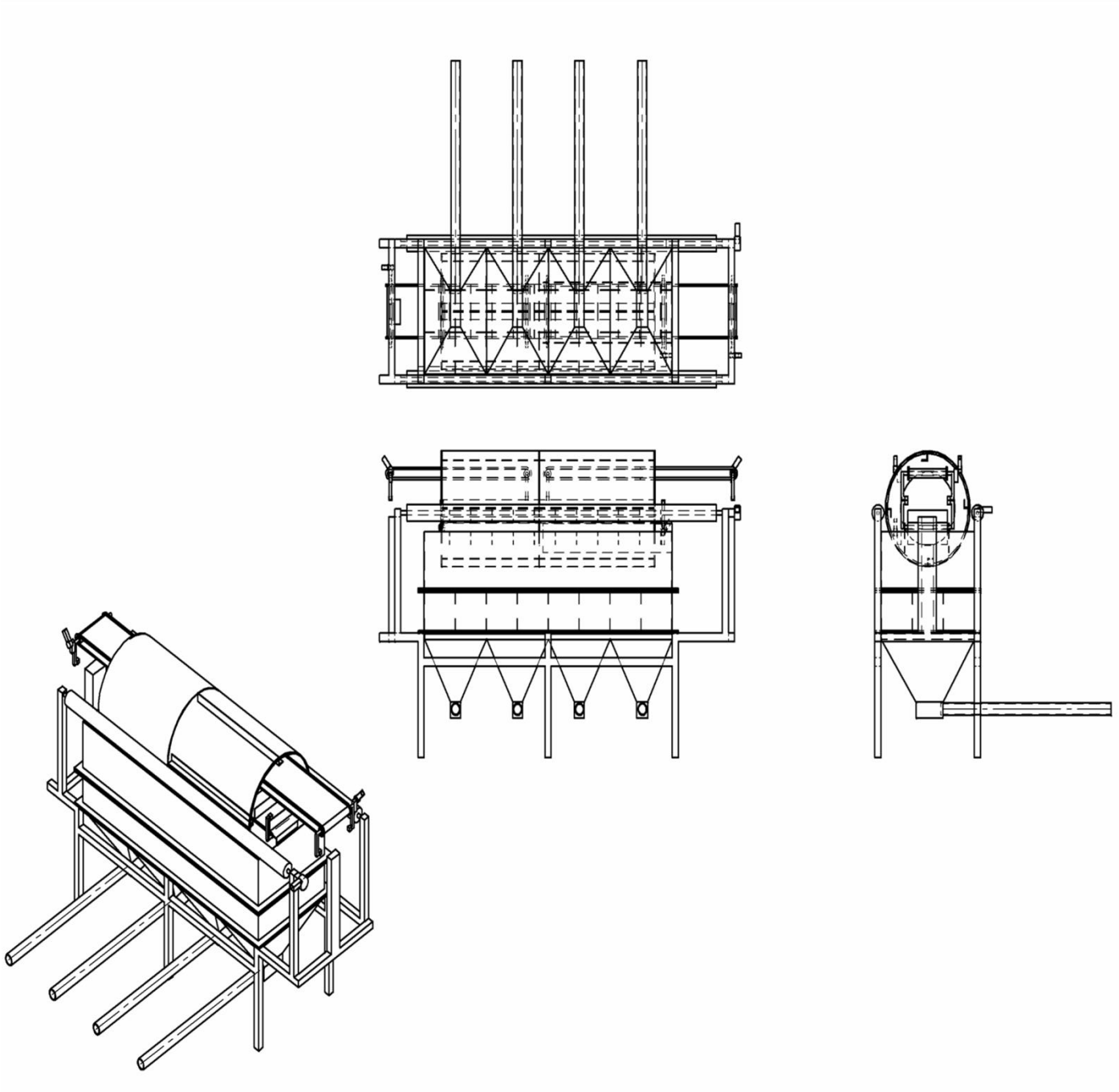

Figure 45: Isometric, Top, Front and Side Schematic Views of the Proposed Design for the Scaled Up Separator

# 11. REFERENCES


1. Chiang S.H. and Cobb J. T., 1993, *Coal Conversion Processes, Cleaning and Desulphurisation*, John Wiley & Sons

2. Clark K. 1997 , The *Business of Fine Coal Tailings Recovery*, The Australian Coal Review July 1997.

3. Cleaner Coal Technology Programme, 2001 , *Technology Status Report 015 Coal Preparation*, Department of Trade and Industry

4. Coulson J.M. and Richardson J.F., 2002, *Chemical Engineering-Volume 2: Particle Technology and Separation Processes*, 5th Ed, Butterworth-Heinemann

5. Creamer M., 2009-03-20, *Clean Coal Vital to Sustain 90%-Dependent South Africa, Says Wits Academic*, Mining Weekly

6. Davydov M. V. 2008, *Improving Coal Processing by More Effective Wastewater Regeneration*, Allerton Press

7. Donnelly J., 1999, *Potential Revival of Dry Cleaning of Coal*, The Australian Coal Review, Issue 8, 26-30

8. Geldart D., 1973, *Types of gas Fluidization*, Powder Technology 7, 285-292

9. van Houwelingen J. A. and de Jong T. P. R. 2003, *Dry Cleaning of Coal: Review, Fundamentals and Opportunities*. Geologica Belgica (2004) 7/3-4: 335 -3423

10. Industrial Technologies Program 2006, *Development of a Novel Dry Processing Technology*, U.S. Department of Energy

11. Kunii D. and Levenspiel O., 1991, *Fluidisation Engineering*, 2nd Ed, Butterworths

12. MacPerson S.A. et al, 2009, *Density Based Separations in the Reflux Classifier with an air-sand dense-medium and vibration*, Minerals Engineering 23 (2010) 74-82

13. Pell M., 1990, *Gas Fluidisation. In: Handbook of Powder Technology,* Elsevier

14. Perry R.H. and Green D., 1998, *Perry's Chemical Engineer's Handbook,* 7th Ed, McGraw-Hill

15. Qing-ru C. and Hai-feng W. 2006 , *Clean Coal Processing and Utilization of Coal*, The Chinese Journal of Process Engineering Vol 6 No. 3

16. Turton A., 2008, *Three Strategic Water Quality Challenges that Decision-Makers Need to Know About and How the CSIR Should Respond*, CSIR Report No. CSIR/NRE/WR/EXP/2008/0160/A

17. Young HD. and Freedman RA., 1996, *University Physics 9th Ed. Extended Version with Modern Physics*, Addison-Wesley

18. Zhenfu L. and Qingru C., 2001, *Dry Beneficiation Technology of Coal with an Air Dense-Medium Fluidized Bed*, International Journal of Mineral Processing 63: Issue 3, 147-175

19. Zhenfu L. and Qingru C., 2001, *Effect of fine coal accumulation on dense phase fluidized bed performance*, International Journal of Mineral Processing 63: Issue 4, 217-224

20. Bateman Engineering, , *Coal Process Plants That Work*, www.batemanengineering.com (http://www.batemanengineering.com/TECHNOLOGY/TechnologyTechnicalPapers/Coalprocess.pdf), (accessed 15/03/2009)

21. Council for Geoscience, *Coal Fields of the Republic of South Africa*, www.geoscience.org.za (http://www.geoscience.org.za/index.php?option=com_content&task=section&id=26&Itemid=441), (accessed 21/02/2008)

22. Department of Environmental Affairs and Tourism, *Mean Annual Rainfall of South Africa*, www.environment.gov.za (http://www.environment.gov.za/enviro-info/sote/nsoer/general/about.htm), (accessed 21/02/2008)

23. ESR International, *Dense Medium Separation: Coal*, http://www.esrint.com/pages/pages/coal.html , (accessed, 25/02/2010)

24. Excalibur Mineral Company, *Magnetite Mineral Data*, www.webmineral.com

(http://webmineral.com/data/Magnetite.shtml), (accessed 20/02/2008)

25. Financial Mail, Financial Mail

(http://free.financialmail.co.za/cgi-bin/pp-email.pl)
(http://free.financialmail.co.za/08/1128/cover/coverstory.html), (accessed 28/11/ 2008)

26. Keaton Energy 2003, *About SA Coal Fields*, www.keatonenergy.co.za
(http://www.keatonenergy.co.za/cm/sa_coal.asp), (accessed 21/02/2008)

27. Metso, 2009, www.metsominerals.com,
(http://www.metsominerals.com/inetMinerals/mm_home.nsf/FR?ReadForm&ATL=/inetMinerals/mm_segments.nsf/WebWID/WTB-041213-2256F-B42B4), (accessed 14/03/2009)

28. Portaclone, Coal Processing Principles, http://www.portaclone.com/pr_coalp.htm, (accessed 23/02/2010)

29. Tangshan Shenzhou Machinery Co., Ltd, FGX compound dry cleaning machine, www.tsshenzhou.com (http://www.tsshenzhou.com/eng_cpzs.cfm), (accessed 20/03/2009)

# 12 APPENDICES

## 12.1. APPENDIX 1: PART 1 RAW DATA FOR TRACER SEPARATION

| | |
|---|---|
| **RUN ID :** | 20080422 |
| **Separator Gas Velocity v (m/s)** | 0.17 |
| **Separation Inefficiency Ep** | 0.013 |
| **Separator Rotation Speed (rpm)** | 0.00 |
| **Number of Tracers Used** | 45 (3 tracers in each weight fraction) |
| **Number of Separation Runs** | 15.00 |
| **ρ75 (75% pass point)** | 2038.08 |
| **ρ25 (25% pass point)** | 2011.92 |
| **ρ50 (split density)** | 2025.00 |

| Partition Coefficient | Tracer Fraction Density ($kg/m^3$) | Number of Tracers Reporting to Underflow |
|---|---|---|
| 0.000 | 1300 | 0 |
| 0.000 | 1350 | 0 |
| 0.000 | 1400 | 0 |
| 0.000 | 1450 | 0 |
| 0.000 | 1500 | 0 |
| 0.000 | 1550 | 0 |
| 0.000 | 1600 | 0 |
| 0.000 | 1650 | 0 |
| 0.000 | 1700 | 0 |
| 0.000 | 1750 | 0 |
| 0.000 | 1800 | 0 |
| 0.000 | 1850 | 0 |
| 0.000 | 1900 | 0 |
| 0.000 | 1950 | 0 |

| | | |
|---|---|---|
| 2.222 | 2000 | 1 |
| 97.778 | 2050 | 44 |
| 100.000 | 2100 | 45 |
| 100.000 | 2150 | 45 |
| 100.000 | 2200 | 45 |
| 100.000 | 2250 | 45 |
| 100.000 | 2300 | 45 |
| 100.000 | 2350 | 45 |
| 100.000 | 2400 | 45 |
| 100.000 | 2450 | 45 |
| 100.000 | 2500 | 45 |
| 100.000 | 2550 | 45 |
| 100.000 | 2600 | 45 |
| 100.000 | 2650 | 45 |
| 100.000 | 2700 | 45 |
| 100.000 | 2750 | 45 |
| 100.000 | 2800 | 45 |

Table 5: Raw Data Obtained from Batch Test Run with Density Tracers

| Bed Y- Axis | | | | | |
|---|---|---|---|---|---|
| | 2120 | 2110 | 2110 | 2130 | 2125 |
| | 2120 | 2090 | 2090 | 2090 | 2130 |
| | 2120 | 2075 | 2075 | 2100 | 2125 |
| | 2120 | 2110 | 2110 | 2120 | 2125 |
| | 2120 | 2130 | 2130 | 2130 | 2125 |

Bed X - Axis

Table 6: Raw Data Showing the Bulk Density Variation within the Fluidised Bed in Plan View ($kg/m^3$)

## 12.2. APPENDIX 2: PART 2 RAW DATA FOR TRACER SEPARATION

| **Fluidising Gas Velocity (m/s)** | **0.10** |
|---|---|
| **Separation Inefficiency** | **Separator Rotation Speed (rev/min)** |
| 0.047 | 3 |
| 0.059 | 4 |
| 0.090 | 5 |
| 0.120 | 6 |

Table 7: Separation Inefficiencies Obtained At a Gas Velocity 0.09877m/s for Varying Rotation Speed

| **Fluidising Gas Velocity (m/s)** | **0.12** |
|---|---|
| **Separation Inefficiency** | **Separator Rotation Speed (rev/min)** |
| 0.074 | 3 |
| 0.058 | 4 |
| 0.099 | 5 |
| 0.099 | 6 |

Table 8: Separation Inefficiencies Obtained At a Gas Velocity 0.12m/s for Varying Rotation Speed

| Fluidising Gas Velocity (m/s) | 0.13 |
|---|---|
| **Separation Inefficiency** | **Separator Rotation Speed (rev/min)** |
| 0.050 | 3 |
| 0.063 | 4 |
| 0.120 | 5 |
| 0.127 | 6 |

Table 9: Separation Inefficiencies Obtained At a Gas Velocity 0.1264m/s for Varying Rotation Speed

| Fluidising Gas Velocity (m/s) | 0.13 |
|---|---|
| **Separation Inefficiency** | **Separator Rotation Speed (rev/min)** |
| 0.098 | 3 |
| 0.134 | 4 |
| 0.153 | 5 |
| 0.163 | 6 |

Table 10: Separation Inefficiencies Obtained At a Gas Velocity 0.13037m/s for Varying Rotation Speed

| RUN ID : | 20080204 |
|---|---|
| Separator Gas Velocity v (m/s) | 0.10 |
| Separation Inefficiency Ep | 0.044 |
| Separator Rotation Speed (rpm) | 3.00 |
| Number of Tracers Used | 45 (3 tracers in each weight fraction) |
| Number of Separation Runs | 15.00 |
| ρ75 (75% pass point) | 2059.72 |
| ρ25 (25% pass point) | 1970.83 |
| ρ50 (split density) | 2015.28 |

| Partition Coefficient | Tracer Fraction Density ($kg/m^3$) | Number of Tracers Reporting to Underflow |
|---|---|---|
| 0.000 | 1300 | 0 |
| 0.000 | 1350 | 0 |
| 0.000 | 1400 | 0 |
| 0.000 | 1450 | 0 |
| 0.000 | 1500 | 0 |
| 2.222 | 1550 | 1 |
| 6.667 | 1600 | 3 |
| 11.111 | 1650 | 5 |
| 13.333 | 1700 | 6 |
| 13.333 | 1750 | 6 |
| 17.778 | 1800 | 8 |
| 22.222 | 1850 | 10 |
| 28.889 | 1900 | 13 |
| 71.111 | 1950 | 32 |
| 91.111 | 2000 | 41 |
| 93.333 | 2050 | 42 |
| 97.778 | 2100 | 44 |
| 97.778 | 2150 | 44 |
| 100.000 | 2200 | 45 |
| 100.000 | 2250 | 45 |

| | | |
|---|---|---|
| 100.000 | 2300 | 45 |
| 100.000 | 2350 | 45 |
| 100.000 | 2400 | 45 |
| 100.000 | 2450 | 45 |
| 100.000 | 2500 | 45 |
| 100.000 | 2550 | 45 |
| 100.000 | 2600 | 45 |
| 100.000 | 2650 | 45 |
| 100.000 | 2700 | 45 |
| 100.000 | 2750 | 45 |
| 100.000 | 2800 | 45 |

Table 11: Raw Data Obtained From Continuous Separation of Density Tracers

| | |
|---|---|
| **RUN ID :** | 20080311 |

| | |
|---|---|
| **Separator Gas Velocity v (m/s)** | 0.10 |
| **Separation Inefficiency Ep** | 0.059 |
| **Separator Rotation Speed (rpm)** | 4.00 |
| **Number of Tracers Used** | 45 (3 tracers in each weight fraction) |
| **Number of Separation Runs** | 15.00 |
| **ρ75 (75% pass point)** | 2062.50 |
| **ρ25 (25% pass point)** | 1944.64 |
| **ρ50 (split density)** | 2003.57 |

| Partition Coefficient | Tracer Fraction Density ($kg/m^3$) | Number of Tracers Reporting to Underflow |
|---|---|---|
| 0.000 | 1300 | 0 |
| 0.000 | 1350 | 0 |
| 0.000 | 1400 | 0 |
| 0.000 | 1450 | 0 |
| 0.000 | 1500 | 0 |
| 0.000 | 1550 | 0 |
| 0.000 | 1600 | 0 |
| 2.222 | 1650 | 1 |
| 0.000 | 1700 | 0 |
| 2.222 | 1750 | 1 |
| 6.667 | 1800 | 3 |
| 8.889 | 1850 | 4 |
| 11.111 | 1900 | 5 |
| 26.667 | 1950 | 12 |
| 40.000 | 2000 | 18 |
| 75.556 | 2050 | 34 |
| 73.333 | 2100 | 33 |
| 100.000 | 2150 | 45 |
| 97.778 | 2200 | 44 |
| 97.778 | 2250 | 44 |
| 97.778 | 2300 | 44 |
| 95.556 | 2350 | 43 |

| | | |
|---|---|---|
| 100.000 | 2400 | 45 |
| 100.000 | 2450 | 45 |
| 100.000 | 2500 | 45 |
| 100.000 | 2550 | 45 |
| 100.000 | 2600 | 45 |
| 100.000 | 2650 | 45 |
| 100.000 | 2700 | 45 |
| 100.000 | 2750 | 45 |
| 100.000 | 2800 | 45 |

Table 12: Raw Data Obtained From Continuous Separation of Density Tracers

| RUN ID : | 20080314 |
|---|---|
| Separator Gas Velocity v (m/s) | 0.10 |
| Separation Inefficiency Ep | 0.080 |
| Separator Rotation Speed (rpm) | 5.00 |
| Number of Tracers Used | 45 (3 tracers in each weight fraction) |
| Number of Separation Runs | 15.00 |
| ρ75 (75% pass point) | 2014.58 |
| ρ25 (25% pass point) | 1854.17 |
| ρ50 (split density) | 1934.38 |

| Partition Coefficient | Tracer Fraction Density ($kg/m^3$) | Number of Tracers Reporting to Underflow |
|---|---|---|
| 0.000 | 1300 | 0 |
| 0.000 | 1350 | 0 |
| 0.000 | 1400 | 0 |
| 2.222 | 1450 | 1 |
| 2.222 | 1500 | 1 |
| 2.222 | 1550 | 1 |
| 2.222 | 1600 | 1 |
| 6.667 | 1650 | 3 |
| 15.556 | 1700 | 7 |
| 17.778 | 1750 | 8 |
| 22.222 | 1800 | 10 |
| 24.444 | 1850 | 11 |
| 31.111 | 1900 | 14 |
| 28.889 | 1950 | 13 |
| 71.111 | 2000 | 32 |
| 84.444 | 2050 | 38 |
| 93.333 | 2100 | 42 |
| 97.778 | 2150 | 44 |
| 100.000 | 2200 | 45 |
| 100.000 | 2250 | 45 |

| | | |
|---|---|---|
| 100.000 | 2300 | 45 |
| 100.000 | 2350 | 45 |
| 100.000 | 2400 | 45 |
| 97.778 | 2450 | 44 |
| 100.000 | 2500 | 45 |
| 100.000 | 2550 | 45 |
| 100.000 | 2600 | 45 |
| 100.000 | 2650 | 45 |
| 100.000 | 2700 | 45 |
| 100.000 | 2750 | 45 |
| 100.000 | 2800 | 45 |

Table 13: Raw Data Obtained From Continuous Separation of Density Tracers

| | |
|---|---|
| **RUN ID :** | 20080318 |
| **Separator Gas Velocity v (m/s)** | 0.10 |
| **Separation Inefficiency Ep** | 0.114 |
| **Separator Rotation Speed (rpm)** | 6.00 |
| **Number of Tracers Used** | 45 (3 tracers in each weight fraction) |
| **Number of Separation Runs** | 15.00 |
| **ρ75 (75% pass point)** | 2006.25 |
| **ρ25 (25% pass point)** | 1778.13 |
| **ρ50 (split density)** | 1892.19 |

| **Partition Coefficient** | **Tracer Fraction Density (kg/m$^3$)** | **Number of Tracers Reporting to Underflow** |
|---|---|---|
| 0.000 | 1300 | 0 |
| 0.000 | 1350 | 0 |
| 0.000 | 1400 | 0 |
| 0.000 | 1450 | 0 |
| 0.000 | 1500 | 0 |
| 2.222 | 1550 | 1 |
| 4.444 | 1600 | 2 |
| 15.556 | 1650 | 7 |
| 17.778 | 1700 | 8 |
| 20.000 | 1750 | 9 |
| 28.889 | 1800 | 13 |
| 31.111 | 1850 | 14 |
| 33.333 | 1900 | 15 |
| 71.111 | 1950 | 32 |
| 73.333 | 2000 | 33 |
| 86.667 | 2050 | 39 |
| 97.778 | 2100 | 44 |
| 97.778 | 2150 | 44 |
| 100.000 | 2200 | 45 |
| 100 | 2250 | 45 |

| | | |
|---|---|---|
| 100 | 2300 | 45 |
| 97.778 | 2350 | 44 |
| 100.000 | 2400 | 45 |
| 100.000 | 2450 | 45 |
| 100.000 | 2500 | 45 |
| 97.778 | 2550 | 44 |
| 100.000 | 2600 | 45 |
| 100.000 | 2650 | 45 |
| 100.000 | 2700 | 45 |
| 100.000 | 2750 | 45 |
| 100.000 | 2800 | 45 |

Table 14: Raw Data Obtained From Continuous Separation of Density Tracers

| RUN ID : | 20080325 |
|---|---|
| Separator Gas Velocity v (m/s) | 0.12 |
| Separation Inefficiency Ep | 0.077 |
| Separator Rotation Speed (rpm) | 3.00 |
| Number of Tracers Used | 45 (3 tracers in each weight fraction) |
| Number of Separation Runs | 15.00 |
| ρ75 (75% pass point) | 1987.50 |
| ρ25 (25% pass point) | 1737.50 |
| ρ50 (split density) | 1862.50 |

| Partition Coefficient | Tracer Fraction Density ($kg/m^3$) | Number of Tracers Reporting to Underflow |
|---|---|---|
| 0.000 | 1300 | 0 |
| 0.000 | 1350 | 0 |
| 0.000 | 1400 | 0 |
| 0.000 | 1450 | 0 |
| 0.000 | 1500 | 0 |
| 2.222 | 1550 | 1 |
| 4.444 | 1600 | 2 |
| 15.556 | 1650 | 7 |
| 17.778 | 1700 | 8 |
| 20.000 | 1750 | 9 |
| 26.667 | 1800 | 12 |
| 42.222 | 1850 | 19 |
| 44.444 | 1900 | 20 |
| 66.667 | 1950 | 30 |
| 73.333 | 2000 | 33 |
| 93.333 | 2050 | 42 |
| 97.778 | 2100 | 44 |
| 97.7778 | 2150 | 44 |
| 100.000 | 2200 | 45 |
| 100.000 | 2250 | 45 |

| | | |
|---|---|---|
| 100.000 | 2300 | 45 |
| 100.000 | 2350 | 45 |
| 100.000 | 2400 | 45 |
| 100.000 | 2450 | 45 |
| 100.000 | 2500 | 45 |
| 100.000 | 2550 | 45 |
| 100.000 | 2600 | 45 |
| 100.000 | 2650 | 45 |
| 100.000 | 2700 | 45 |
| 100.000 | 2750 | 45 |
| 100.000 | 2800 | 45 |

Table 15: Raw Data Obtained From Continuous Separation of Density Tracers

| | |
|---|---|
| **RUN ID :** | 20080401 |
| **Separator Gas Velocity v (m/s)** | 0.12 |
| **Separation Inefficiency Ep** | 0.053 |
| **Separator Rotation Speed (rpm)** | 4.00 |
| **Number of Tracers Used** | 45 (3 tracers in each weight fraction) |
| **Number of Separation Runs** | 15.00 |
| **ρ75 (75% pass point)** | 1943.75 |
| **ρ25 (25% pass point)** | 1837.50 |
| **ρ50 (split density)** | 1890.63 |

| Partition Coefficient | Tracer Fraction Density ($kg/m^3$) | Number of Tracers Reporting to Underflow |
|---|---|---|
| 0 | 1300 | 0 |
| 0 | 1350 | 0 |
| 0 | 1400 | 0 |
| 0 | 1450 | 0 |
| 0 | 1500 | 0 |
| 2.222 | 1550 | 1 |
| 2.222 | 1600 | 1 |
| 2.222 | 1650 | 1 |
| 8.889 | 1700 | 4 |
| 11.111 | 1750 | 5 |
| 13.333 | 1800 | 6 |
| 28.889 | 1850 | 13 |
| 37.778 | 1900 | 17 |
| 75.556 | 1950 | 34 |
| 80.000 | 2000 | 36 |
| 100.000 | 2050 | 45 |
| 97.778 | 2100 | 44 |
| 97.778 | 2150 | 44 |
| 100.000 | 2200 | 45 |
| 100.000 | 2250 | 45 |
| 100.000 | 2300 | 45 |

| | | |
|---|---|---|
| 100.000 | 2350 | 45 |
| 100.000 | 2400 | 45 |
| 100.000 | 2450 | 45 |
| 100.000 | 2500 | 45 |
| 100.000 | 2550 | 45 |
| 100.000 | 2600 | 45 |
| 100.000 | 2650 | 45 |
| 100.000 | 2700 | 45 |
| 100.000 | 2750 | 45 |
| 100.000 | 2800 | 45 |

Table 16: Raw Data Obtained From Continuous Separation of Density Tracers

| RUN ID : | 20080408 |
|---|---|
| Separator Gas Velocity v (m/s) | 0.12 |
| Separation Inefficiency Ep | 0.125 |
| Separator Rotation Speed (rpm) | 5.00 |
| Number of Tracers Used | 45 (3 tracers in each weight fraction) |
| Number of Separation Runs | 15.00 |
| ρ75 (75% pass point) | 1943.75 |
| ρ25 (25% pass point) | 1837.50 |
| ρ50 (split density) | 1890.63 |

| Partition Coefficient | Tracer Fraction Density (kg/m$^3$) | Number of Tracers Reporting to Underflow |
|---|---|---|
| 2.222 | 1300 | 1 |
| 4.444 | 1350 | 2 |
| 0.000 | 1400 | 0 |
| 0.000 | 1450 | 0 |
| 0.000 | 1500 | 0 |
| 2.222 | 1550 | 1 |
| 6.667 | 1600 | 3 |
| 2.222 | 1650 | 1 |
| 13.333 | 1700 | 6 |
| 33.333 | 1750 | 15 |
| 40.000 | 1800 | 18 |
| 44.444 | 1850 | 20 |
| 44.444 | 1900 | 20 |
| 73.333 | 1950 | 33 |
| 75.556 | 2000 | 34 |
| 77.778 | 2050 | 35 |
| 97.778 | 2100 | 44 |
| 97.778 | 2150 | 44 |
| 100.000 | 2200 | 45 |
| 97.778 | 2250 | 44 |
| 100.000 | 2300 | 45 |

| | | |
|---|---|---|
| 100.000 | 2350 | 45 |
| 100.000 | 2400 | 45 |
| 100.000 | 2450 | 45 |
| 100.000 | 2500 | 45 |
| 100.000 | 2550 | 45 |
| 95.556 | 2600 | 43 |
| 100.000 | 2650 | 45 |
| 100.000 | 2700 | 45 |
| 100.000 | 2750 | 45 |
| 100.000 | 2800 | 45 |

Table 17: Raw Data Obtained From Continuous Separation of Density Tracers

| RUN ID : | 20080415 |
|---|---|
| Separator Gas Velocity v (m/s) | 0.12 |
| Separation Inefficiency Ep | 0.115 |
| Separator Rotation Speed (rpm) | 6.00 |
| Number of Tracers Used | 45 (3 tracers in each weight fraction) |
| Number of Separation Runs | 15.00 |
| ρ75 (75% pass point) | 2007.50 |
| ρ25 (25% pass point) | 1778.13 |
| ρ50 (split density) | 1892.81 |

| Partition Coefficient | Tracer Fraction Density (kg/m$^3$) | Number of Tracers Reporting to Underflow |
|---|---|---|
| 0.000 | 1300 | 0 |
| 0.000 | 1350 | 0 |
| 0.000 | 1400 | 0 |
| 0.000 | 1450 | 0 |
| 0.000 | 1500 | 0 |
| 2.222 | 1550 | 1 |
| 4.444 | 1600 | 2 |
| 15.556 | 1650 | 7 |
| 17.778 | 1700 | 8 |
| 20.000 | 1750 | 9 |
| 28.889 | 1800 | 13 |
| 31.11111111 | 1850 | 14 |
| 33.333 | 1900 | 15 |
| 66.667 | 1950 | 30 |
| 73.333 | 2000 | 33 |
| 84.444 | 2050 | 38 |
| 97.778 | 2100 | 44 |
| 97.778 | 2150 | 44 |
| 100.000 | 2200 | 45 |
| 100.000 | 2250 | 45 |
| 100.000 | 2300 | 45 |

| | | |
|---|---|---|
| 100.000 | 2350 | 45 |
| 100.000 | 2400 | 45 |
| 100.000 | 2450 | 45 |
| 97.778 | 2500 | 44 |
| 100.000 | 2550 | 45 |
| 97.778 | 2600 | 44 |
| 100.000 | 2650 | 45 |
| 100.000 | 2700 | 45 |
| 100.000 | 2750 | 45 |
| 100.000 | 2800 | 45 |

Table 18: Raw Data Obtained From Continuous Separation of Density Tracers

| RUN ID : | 20080422 |
|---|---|
| Separator Gas Velocity v (m/s) | 0.13 |
| Separation Inefficiency Ep | 0.059 |
| Separator Rotation Speed (rpm) | 3.00 |
| Number of Tracers Used | 45 (3 tracers in each weight fraction) |
| Number of Separation Runs | 15.00 |
| ρ75 (75% pass point) | 2028.29 |
| ρ25 (25% pass point) | 1910.42 |
| ρ50 (split density) | 1969.35 |

| Partition Coefficient | Tracer Fraction Density (kg/m$^3$) | Number of Tracers Reporting to Underflow |
|---|---|---|
| 0.000 | 1300 | 0 |
| 0.000 | 1350 | 0 |
| 2.222 | 1400 | 1 |
| 2.222 | 1450 | 1 |
| 0.000 | 1500 | 0 |
| 2.222 | 1550 | 1 |
| 11.111 | 1600 | 5 |
| 6.667 | 1650 | 3 |
| 4.444 | 1700 | 2 |
| 11.111 | 1750 | 5 |
| 15.556 | 1800 | 7 |
| 20.000 | 1850 | 9 |
| 22.222 | 1900 | 10 |
| 35.556 | 1950 | 16 |
| 51.111 | 2000 | 23 |
| 93.333 | 2050 | 42 |
| 97.778 | 2100 | 44 |
| 97.778 | 2150 | 44 |
| 100.000 | 2200 | 45 |
| 100.000 | 2250 | 45 |
| 97.778 | 2300 | 44 |

| | | |
|---|---|---|
| 100.000 | 2350 | 45 |
| 100.000 | 2400 | 45 |
| 100.000 | 2450 | 45 |
| 97.778 | 2500 | 44 |
| 97.778 | 2550 | 44 |
| 100.000 | 2600 | 45 |
| 100.000 | 2650 | 45 |
| 100.000 | 2700 | 45 |
| 100.000 | 2750 | 45 |
| 100.000 | 2800 | 45 |

Table 19: Raw Data Obtained From Continuous Separation of Density Tracers

| RUN ID : | 20080429 |
|---|---|
| Separator Gas Velocity v (m/s) | 0.13 |
| Separation Inefficiency Ep | 0.044 |
| Separator Rotation Speed (rpm) | 4.00 |
| Number of Tracers Used | 45 (3 tracers in each weight fraction) |
| Number of Separation Runs | 15.00 |
| ρ75 (75% pass point) | 1945.83 |
| ρ25 (25% pass point) | 1857.81 |
| ρ50 (split density) | 1901.82 |

| Partition Coefficient | Tracer Fraction Density ($kg/m^3$) | Number of Tracers Reporting to Underflow |
|---|---|---|
| 0.000 | 1300 | 0 |
| 0.000 | 1350 | 0 |
| 0.000 | 1400 | 0 |
| 0.000 | 1450 | 0 |
| 0.000 | 1500 | 0 |
| 0.000 | 1550 | 0 |
| 0.000 | 1600 | 0 |
| 2.222 | 1650 | 1 |
| 6.667 | 1700 | 3 |
| 8.889 | 1750 | 4 |
| 11.111 | 1800 | 5 |
| 22.222 | 1850 | 10 |
| 40.000 | 1900 | 18 |
| 75.556 | 1950 | 34 |
| 82.222 | 2000 | 37 |
| 100.000 | 2050 | 45 |
| 97.778 | 2100 | 44 |
| 100.000 | 2150 | 45 |
| 100.000 | 2200 | 45 |
| 100.000 | 2250 | 45 |
| 100.000 | 2300 | 45 |

| | | |
|---|---|---|
| 100.000 | 2350 | 45 |
| 100.000 | 2400 | 45 |
| 97.778 | 2450 | 44 |
| 97.778 | 2500 | 44 |
| 97.778 | 2550 | 44 |
| 100.000 | 2600 | 45 |
| 97.778 | 2650 | 44 |
| 100.000 | 2700 | 45 |
| 97.778 | 2750 | 44 |
| 100.000 | 2800 | 45 |

Table 20: Raw Data Obtained From Continuous Separation of Density Tracers

| | |
|---|---|
| **RUN ID :** | 20080506 |
| **Separator Gas Velocity v (m/s)** | 0.13 |
| **Separation Inefficiency Ep** | 0.100 |
| **Separator Rotation Speed (rpm)** | 5.00 |
| **Number of Tracers Used** | 45 (3 tracers in each weight fraction) |
| **Number of Separation Runs** | 15.00 |
| **ρ75 (75% pass point)** | 1979.17 |
| **ρ25 (25% pass point)** | 1778.41 |
| **ρ50 (split density)** | 1878.79 |

| **Partition Coefficient** | **Tracer Fraction Density (kg/m$^3$)** | **Number of Tracers Reporting to Underflow** |
|---|---|---|
| 2.222 | 1300 | 1 |
| 0.000 | 1350 | 0 |
| 0.000 | 1400 | 0 |
| 0.000 | 1450 | 0 |
| 0.000 | 1500 | 0 |
| 0.000 | 1550 | 0 |
| 8.889 | 1600 | 4 |
| 8.889 | 1650 | 4 |
| 8.889 | 1700 | 4 |
| 11.111 | 1750 | 5 |
| 35.556 | 1800 | 16 |
| 35.556 | 1850 | 16 |
| 37.778 | 1900 | 17 |
| 55.556 | 1950 | 25 |
| 88.889 | 2000 | 40 |
| 93.333 | 2050 | 42 |
| 97.778 | 2100 | 44 |
| 97.778 | 2150 | 44 |
| 100.000 | 2200 | 45 |
| 100.000 | 2250 | 45 |
| 100.000 | 2300 | 45 |

| | | |
|---|---|---|
| 100.000 | 2350 | 45 |
| 97.778 | 2400 | 44 |
| 100.000 | 2450 | 45 |
| 100.000 | 2500 | 45 |
| 97.778 | 2550 | 44 |
| 100.000 | 2600 | 45 |
| 100.000 | 2650 | 45 |
| 100.000 | 2700 | 45 |
| 100.000 | 2750 | 45 |
| 100.000 | 2800 | 45 |

Table 21: Raw Data Obtained From Continuous Separation of Density Tracers

| | |
|---|---|
| **RUN ID :** | 20080513 |
| **Separator Gas Velocity v (m/s)** | 0.13 |
| **Separation Inefficiency Ep** | 0.120 |
| **Separator Rotation Speed (rpm)** | 6.00 |
| **Number of Tracers Used** | 45 (3 tracers in each weight fraction) |
| **Number of Separation Runs** | 15.00 |
| **ρ75 (75% pass point)** | 2013.75 |
| **ρ25 (25% pass point)** | 1773.21 |
| **ρ50 (split density)** | 1853.39 |

| Partition Coefficient | Tracer Fraction Density (kg/m$^3$) | Number of Tracers Reporting to Underflow |
|---|---|---|
| 0.000 | 1300 | 0 |
| 0.000 | 1350 | 0 |
| 2.222 | 1400 | 1 |
| 2.222 | 1450 | 1 |
| 4.444 | 1500 | 2 |
| 6.667 | 1550 | 3 |
| 8.889 | 1600 | 4 |
| 13.333 | 1650 | 6 |
| 17.778 | 1700 | 8 |
| 17.778 | 1750 | 8 |
| 33.333 | 1800 | 15 |
| 33.333 | 1850 | 15 |
| 35.556 | 1900 | 16 |
| 66.667 | 1950 | 30 |
| 68.889 | 2000 | 31 |
| 91.111 | 2050 | 41 |
| 97.7778 | 2100 | 44 |
| 100.000 | 2150 | 45 |
| 100.000 | 2200 | 45 |
| 100.000 | 2250 | 45 |
| 100.000 | 2300 | 45 |

| | | |
|---|---|---|
| 100.000 | 2350 | 45 |
| 100.000 | 2400 | 45 |
| 97.778 | 2450 | 44 |
| 100.000 | 2500 | 45 |
| 100.000 | 2550 | 45 |
| 100.000 | 2600 | 45 |
| 100.000 | 2650 | 45 |
| 100.000 | 2700 | 45 |
| 100.000 | 2750 | 45 |
| 100.000 | 2800 | 45 |

Table 22: Raw Data Obtained From Continuous Separation of Density Tracers

| | |
|---|---|
| **RUN ID :** | 20080520 |
| **Separator Gas Velocity v (m/s)** | 0.13 |
| **Separation Inefficiency Ep** | 0.133 |
| **Separator Rotation Speed (rpm)** | 3.00 |
| **Number of Tracers Used** | 45 (3 tracers in each weight fraction) |
| **Number of Separation Runs** | 15.00 |
| **ρ75 (75% pass point)** | 1985.94 |
| **ρ25 (25% pass point)** | 1720.83 |
| **ρ50 (split density)** | 1853.39 |

| Partition Coefficient | Tracer Fraction Density ($kg/m^3$) | Number of Tracers Reporting to Underflow |
|---|---|---|
| 2.222 | 1300 | 1 |
| 0.000 | 1350 | 0 |
| 2.222 | 1400 | 1 |
| 6.667 | 1450 | 3 |
| 0.000 | 1500 | 0 |
| 2.222 | 1550 | 1 |
| 8.889 | 1600 | 4 |
| 15.556 | 1650 | 7 |
| 20.000 | 1700 | 9 |
| 26.667 | 1750 | 12 |
| 33.333 | 1800 | 15 |
| 42.222 | 1850 | 19 |
| 48.889 | 1900 | 22 |
| 62.222 | 1950 | 28 |
| 80.000 | 2000 | 36 |
| 93.333 | 2050 | 42 |
| 97.778 | 2100 | 44 |
| 97.778 | 2150 | 44 |
| 97.778 | 2200 | 44 |
| 100.000 | 2250 | 45 |
| 95.556 | 2300 | 43 |

| | | |
|---|---|---|
| 100.000 | 2350 | 45 |
| 93.333 | 2400 | 42 |
| 95.556 | 2450 | 43 |
| 91.111 | 2500 | 41 |
| 100.000 | 2550 | 45 |
| 100.000 | 2600 | 45 |
| 100.000 | 2650 | 45 |
| 100.000 | 2700 | 45 |
| 100.000 | 2750 | 45 |
| 100.000 | 2800 | 45 |

Table 23: Raw Data Obtained From Continuous Separation of Density Tracers

| RUN ID : | 20080527 |
|---|---|
| Separator Gas Velocity v (m/s) | 0.13 |
| Separation Inefficiency Ep | 0.113 |
| Separator Rotation Speed (rpm) | 4.00 |
| Number of Tracers Used | 45 (3 tracers in each weight fraction) |
| Number of Separation Runs | 15.00 |
| ρ75 (75% pass point) | 1980.60 |
| ρ25 (25% pass point) | 1754.17 |
| ρ50 (split density) | 1867.39 |

| Partition Coefficient | Tracer Fraction Density (kg/m$^3$) | Number of Tracers Reporting to Underflow |
|---|---|---|
| 0.000 | 1300 | 0 |
| 6.667 | 1350 | 3 |
| 2.222 | 1400 | 1 |
| 2.222 | 1450 | 1 |
| 0.000 | 1500 | 0 |
| 2.222 | 1550 | 1 |
| 8.889 | 1600 | 4 |
| 6.667 | 1650 | 3 |
| 6.667 | 1700 | 3 |
| 24.444 | 1750 | 11 |
| 31.111 | 1800 | 14 |
| 31.111 | 1850 | 14 |
| 35.556 | 1900 | 16 |
| 35.556 | 1950 | 16 |
| 73.333 | 2000 | 33 |
| 100.000 | 2050 | 45 |
| 97.778 | 2100 | 44 |
| 97.778 | 2150 | 44 |
| 97.778 | 2200 | 44 |
| 95.556 | 2250 | 43 |
| 100.000 | 2300 | 45 |

| | | |
|---|---|---|
| 100.000 | 2350 | 45 |
| 100.000 | 2400 | 45 |
| 100.000 | 2450 | 45 |
| 100.000 | 2500 | 45 |
| 100.000 | 2550 | 45 |
| 100.000 | 2600 | 45 |
| 97.778 | 2650 | 44 |
| 97.7778 | 2700 | 44 |
| 100.000 | 2750 | 45 |
| 100.000 | 2800 | 45 |

Table 24: Raw Data Obtained From Continuous Separation of Density Tracers

| | |
|---|---|
| **RUN ID :** | 20080602 |
| **Separator Gas Velocity v (m/s)** | 0.13 |
| **Separation Inefficiency Ep** | 0.142 |
| **Separator Rotation Speed (rpm)** | 5.00 |
| **Number of Tracers Used** | 45 (3 tracers in each weight fraction) |
| **Number of Separation Runs** | 15.00 |
| **ρ75 (75% pass point)** | 1964.58 |
| **ρ25 (25% pass point)** | 1680.36 |
| **ρ50 (split density)** | 1822.47 |

| Partition Coefficient | Tracer Fraction Density ($kg/m^3$) | Number of Tracers Reporting to Underflow |
|---|---|---|
| 0.000 | 1300 | 0 |
| 6.667 | 1350 | 3 |
| 2.222 | 1400 | 1 |
| 4.444 | 1450 | 2 |
| 2.222 | 1500 | 1 |
| 2.222 | 1550 | 1 |
| 6.667 | 1600 | 3 |
| 15.556 | 1650 | 7 |
| 31.111 | 1700 | 14 |
| 33.333 | 1750 | 15 |
| 35.556 | 1800 | 16 |
| 31.111 | 1850 | 14 |
| 28.889 | 1900 | 13 |
| 71.111 | 1950 | 32 |
| 84.444 | 2000 | 38 |
| 93.333 | 2050 | 42 |
| 97.778 | 2100 | 44 |
| 97.778 | 2150 | 44 |
| 100.000 | 2200 | 45 |
| 100.000 | 2250 | 45 |
| 100.000 | 2300 | 45 |

| | | |
|---|---|---|
| 100.000 | 2350 | 45 |
| 100.000 | 2400 | 45 |
| 100.000 | 2450 | 45 |
| 100.000 | 2500 | 45 |
| 100.000 | 2550 | 45 |
| 100.000 | 2600 | 45 |
| 100.000 | 2650 | 45 |
| 100.000 | 2700 | 45 |
| 100.000 | 2750 | 45 |
| 100.000 | 2800 | 45 |

Table 25: Raw Data Obtained From Continuous Separation of Density Tracers

| RUN ID : | 20080609 |
|---|---|
| Separator Gas Velocity v (m/s) | 0.13 |
| Separation Inefficiency Ep | 0.114 |
| Separator Rotation Speed (rpm) | 6.00 |
| Number of Tracers Used | 45 (3 tracers in each weight fraction) |
| Number of Separation Runs | 15.00 |
| ρ75 (75% pass point) | 2006.25 |
| ρ25 (25% pass point) | 1778.13 |
| ρ50 (split density) | 1892.19 |

| Partition Coefficient | Tracer Fraction Density (kg/m$^3$) | Number of Tracers Reporting to Underflow |
|---|---|---|
| 0.000 | 1300 | 0 |
| 0.000 | 1350 | 0 |
| 0.000 | 1400 | 0 |
| 0.000 | 1450 | 0 |
| 0.000 | 1500 | 0 |
| 2.2222 | 1550 | 1 |
| 4.444 | 1600 | 2 |
| 15.556 | 1650 | 7 |
| 17.778 | 1700 | 8 |
| 20.000 | 1750 | 9 |
| 28.889 | 1800 | 13 |
| 31.111 | 1850 | 14 |
| 33.333 | 1900 | 15 |
| 71.111 | 1950 | 32 |
| 73.333 | 2000 | 33 |
| 86.667 | 2050 | 39 |
| 100.000 | 2100 | 45 |
| 97.778 | 2150 | 44 |
| 100.000 | 2200 | 45 |
| 100.000 | 2250 | 45 |
| 97.778 | 2300 | 44 |

| | | |
|---|---|---|
| 100.000 | 2350 | 45 |
| 100.000 | 2400 | 45 |
| 100.000 | 2450 | 45 |
| 100.000 | 2500 | 45 |
| 100.000 | 2550 | 45 |
| 100.000 | 2600 | 45 |
| 100.000 | 2650 | 45 |
| 100.000 | 2700 | 45 |
| 100.000 | 2750 | 45 |
| 100.000 | 2800 | 45 |

Table 26: Raw Data Obtained From Continuous Separation of Density Tracers

## 12.3. APPENDIX 3: PART 3 RAW DATA FOR COAL SEPARATION

| Density Fraction ($kg/m^3$) | Floats Overflow (%) | Ash (%) | Overflow/Feed (%) | Sinks Overflow (%) | Ash (%) | Overflow/Feed (%) | Calculated Feedstock Feed (%) | Ash (%) | Partition Coefficient (%) |
|---|---|---|---|---|---|---|---|---|---|
| <1400 | 17.18 | 9.01 | 6.65 | 0.00 | 17.03 | 0.00 | 6.66 | 9.01 | 0.02 |
| 1400-1500 | 32.57 | 11.01 | 12.61 | 0.12 | 15.07 | 0.07 | 12.69 | 11.04 | 0.57 |
| 1500-1600 | 13.83 | 13.82 | 5.36 | 0.31 | 12.74 | 0.20 | 5.55 | 13.78 | 3.52 |
| 1600-1700 | 2.00 | 21.07 | 0.78 | 0.08 | 4.69 | 0.05 | 0.82 | 20.11 | 5.86 |
| 1700-1800 | 2.90 | 19.23 | 1.12 | 0.29 | 22.90 | 0.18 | 1.30 | 19.74 | 13.88 |
| 1800-1900 | 9.68 | 39.60 | 3.75 | 1.25 | 41.58 | 0.79 | 4.54 | 39.94 | 17.36 |
| 1900-2000 | 16.22 | 64.73 | 6.28 | 3.65 | 68.64 | 2.30 | 8.58 | 65.77 | 26.77 |
| 2000-2100 | 1.99 | 72.16 | 0.77 | 5.17 | 71.41 | 3.25 | 4.02 | 71.56 | 80.85 |
| 2100-2200 | 1.57 | 69.47 | 0.61 | 11.49 | 75.20 | 7.22 | 7.83 | 74.76 | 92.24 |
| 2200-2300 | 1.53 | 83.17 | 0.59 | 42.17 | 81.05 | 26.51 | 27.10 | 81.10 | 97.82 |
| 2300-2400 | 0.43 | 77.69 | 0.17 | 27.82 | 83.27 | 17.49 | 17.65 | 83.21 | 99.06 |
| >2400 | 0.12 | 89.13 | 0.05 | 7.65 | 83.48 | 4.81 | 4.85 | 83.53 | 99.07 |
| Total | 100.00 | 26.58 | 38.74 | 100.00 | 79.22 | 62.86 | 101.59 | 60.66 | |

Table 27: Raw Data Obtained From Batch Separation of Coal

| Density Fraction ($kg/m^3$) | Floats Overflow (%) | Ash (%) | Overflow/Feed (%) | Sinks Overflow (%) | Ash (%) | Overflow/Feed (%) | Calculated Feedstock Feed (%) | Ash (%) | Partition Coefficient (%) |
|---|---|---|---|---|---|---|---|---|---|
| <1400 | 16.51 | 8.17 | 6.47 | 0.00 | 15.64 | 0.0013 | 6.48 | 8.17 | 0.02 |
| 1400-1500 | 31.03 | 9.69 | 12.17 | 0.11 | 13.39 | 0.07 | 12.24 | 9.71 | 0.55 |
| 1500-1600 | 13.93 | 13.70 | 5.46 | 0.34 | 12.65 | 0.20 | 5.67 | 13.66 | 3.60 |
| 1600-1700 | 2.12 | 20.95 | 0.83 | 0.09 | 5.83 | 0.06 | 0.89 | 19.99 | 6.32 |
| 1700-1800 | 2.67 | 20.07 | 1.05 | 0.26 | 24.24 | 0.15 | 1.20 | 20.61 | 12.78 |
| 1800-1900 | 9.59 | 46.50 | 3.76 | 1.34 | 48.81 | 0.79 | 4.56 | 46.90 | 17.44 |
| 1900-2000 | 14.95 | 65.18 | 5.86 | 3.15 | 69.55 | 1.86 | 7.73 | 66.23 | 24.11 |
| 2000-2100 | 2.09 | 75.81 | 0.82 | 5.25 | 75.01 | 3.11 | 3.93 | 75.17 | 79.13 |
| 2100-2200 | 3.52 | 71.88 | 1.38 | 9.08 | 78.76 | 5.37 | 6.75 | 77.35 | 79.56 |
| 2200-2300 | 2.29 | 84.58 | 0.90 | 43.72 | 82.39 | 25.88 | 26.78 | 82.47 | 96.64 |
| 2300-2400 | 1.25 | 83.39 | 0.49 | 28.42 | 89.49 | 16.82 | 17.31 | 89.32 | 97.16 |
| >2400 | 0.05 | 89.78 | 0.02 | 8.21 | 84.12 | 4.86 | 4.88 | 84.14 | 99.61 |
| Total | 100.00 | 28.59 | 39.22 | 100.00 | 82.44 | 59.18 | 98.41 | 64.48 | |

Table 28: Raw Data Obtained From Batch Separation of Coal

| Density Fraction ($kg/m^3$) | Floats Overflow (%) | Ash (%) | Overflow/Feed (%) | Sinks Overflow (%) | Ash (%) | Overflow/Feed (%) | Calculated Feedstock Feed (%) | Ash (%) | Partition Coefficient (%) |
|---|---|---|---|---|---|---|---|---|---|
| <1400 | 16.57 | 8.74 | 6.18 | 0.75 | 13.78 | 0.48 | 6.66 | 9.10 | 7.22 |
| 1400-1500 | 30.53 | 12.74 | 11.38 | 2.03 | 0.47 | 1.31 | 12.69 | 11.48 | 10.29 |
| 1500-1600 | 13.39 | 14.33 | 4.99 | 0.87 | 10.21 | 0.56 | 5.55 | 13.92 | 10.13 |
| 1600-1700 | 1.99 | 21.07 | 0.74 | 0.13 | 5.24 | 0.08 | 0.82 | 19.51 | 9.86 |
| 1700-1800 | 3.06 | 20.72 | 1.14 | 0.25 | 22.40 | 0.16 | 1.30 | 20.93 | 12.48 |
| 1800-1900 | 10.38 | 40.41 | 3.87 | 1.04 | 43.46 | 0.67 | 4.54 | 40.86 | 14.75 |
| 1900-2000 | 16.99 | 66.65 | 6.33 | 3.49 | 71.85 | 2.24 | 8.58 | 68.01 | 26.16 |
| 2000-2100 | 2.17 | 68.58 | 0.81 | 4.98 | 71.23 | 3.21 | 4.02 | 70.70 | 79.82 |
| 2100-2200 | 1.36 | 80.25 | 0.51 | 11.39 | 74.64 | 7.33 | 7.83 | 75.00 | 93.54 |
| 2200-2300 | 2.47 | 72.18 | 0.92 | 40.70 | 80.48 | 26.18 | 27.10 | 80.20 | 96.61 |
| 2300-2400 | 0.97 | 77.25 | 0.36 | 26.89 | 79.69 | 17.29 | 17.65 | 79.64 | 97.95 |
| >2400 | 0.12 | 88.76 | 0.05 | 7.48 | 84.50 | 4.81 | 4.85 | 84.54 | 99.07 |
| Total | 100.00 | 29.05 | 37.28 | 100.00 | 75.78 | 64.32 | 100.00 | 60.66 | |

Table 29: Raw Data Obtained From Continuous Separation of Coal

| Density Fraction ($kg/m^3$) | Floats Overflow (%) | Ash (%) | Overflow/Feed (%) | Sinks Overflow (%) | Ash (%) | Overflow/Feed (%) | Calculated Feedstock Feed (%) | Ash (%) | Partition Coefficient (%) |
|---|---|---|---|---|---|---|---|---|---|
| <1400 | 15.91 | 7.92 | 6.02 | 0.75 | 12.62 | 0.45 | 6.48 | 8.25 | 7.02 |
| 1400-1500 | 29.12 | 11.21 | 11.02 | 2.01 | 0.02 | 1.22 | 12.24 | 10.10 | 9.93 |
| 1500-1600 | 13.42 | 14.21 | 5.08 | 0.97 | 10.21 | 0.59 | 5.67 | 13.80 | 10.33 |
| 1600-1700 | 2.09 | 20.94 | 0.79 | 0.16 | 6.34 | 0.09 | 0.89 | 19.39 | 10.62 |
| 1700-1800 | 2.81 | 21.62 | 1.06 | 0.23 | 23.53 | 0.14 | 1.20 | 21.84 | 11.48 |
| 1800-1900 | 10.26 | 47.45 | 3.88 | 1.11 | 51.02 | 0.68 | 4.56 | 47.98 | 14.81 |
| 1900-2000 | 15.60 | 67.12 | 5.91 | 3.01 | 72.93 | 1.82 | 7.73 | 68.49 | 23.56 |
| 2000-2100 | 2.27 | 72.04 | 0.86 | 5.07 | 74.90 | 3.07 | 3.93 | 74.27 | 78.12 |
| 2100-2200 | 3.45 | 83.04 | 1.30 | 9.00 | 76.31 | 5.45 | 6.75 | 77.61 | 80.68 |
| 2200-2300 | 3.22 | 73.40 | 1.22 | 42.20 | 81.95 | 25.56 | 26.78 | 81.56 | 95.45 |
| 2300-2400 | 1.80 | 82.91 | 0.68 | 27.47 | 85.58 | 16.63 | 17.31 | 85.48 | 96.07 |
| >2400 | 0.05 | 89.41 | 0.02 | 8.03 | 85.14 | 4.86 | 4.88 | 85.15 | 99.61 |
| Total | 100.00 | 31.21 | 37.85 | 100.00 | 78.61 | 60.56 | 100.00 | 59.46 | |

Table 30: Raw Data Obtained From Continuous Separation of Coal

## 12.4. APPENDIX 4: DENSITY TRACER SPECTRUM

| Density (kg/m$^3$) | Tracer ID | Number of Tracers Constructed |
|---|---|---|
| 1350 | 1a | 6 |
| 1400 | 1 | 6 |
| 1450 | 2a | 6 |
| 1500 | 2 | 6 |
| 1550 | 3a | 6 |
| 1600 | 3 | 6 |
| 1650 | 4a | 6 |
| 1700 | 4 | 6 |
| 1750 | 5a | 6 |
| 1800 | 5 | 6 |
| 1850 | 6a | 6 |
| 1900 | 6 | 6 |
| 1950 | 7a | 6 |
| 2000 | 7 | 6 |
| 2050 | 8a | 6 |
| 2100 | 8 | 6 |
| 2150 | 9a | 6 |
| 2200 | 9 | 6 |
| 2250 | 10a | 6 |
| 2300 | 10 | 6 |
| 2350 | 11a | 6 |
| 2400 | 11 | 6 |
| 2450 | 12a | 6 |
| 2500 | 12 | 6 |
| 2550 | 13a | 6 |
| 2600 | 13 | 6 |
| 2650 | 14a | 6 |
| 2700 | 14 | 6 |

| | | |
|---|---|---|
| 2750 | 15a | 6 |
| 2800 | 15 | 6 |
| 2850 | 16a | 6 |

Table 31: Density Tracer Spectrum